Titre: Title:	Oxygen Reduction Reaction on Palladium-Cobalt Alloy Catalysts for Polymer Electrolyte Fuel Cells
Auteur: Author:	Kentaro Oishi
Date:	2012
Type:	Mémoire ou thèse / Dissertation or Thesis
Référence: Citation:	Oishi, K. (2012). Oxygen Reduction Reaction on Palladium-Cobalt Alloy Catalysts for Polymer Electrolyte Fuel Cells [Thèse de doctorat, École Polytechnique de Montréal]. PolyPublie. https://publications.polymtl.ca/847/

UNIVERSITÉ DE MONTRÉAL

OXYGEN REDUCTION REACTION ON PALLADIUM-COBALT ALLOY CATALYSTS FOR POLYMER ELECTROLYTE FUEL CELLS

KENTARO OISHI

DÉPARTEMENT DE GÉNIE CHIMIQUE

ÉCOLE POLYTECHNIQUE DE MONTRÉAL

THÈSE PRÉSENTÉE EN VUE DE L'OBTENTION

DU DIPLÔME DE PHILOSOPHIAE DOCTOR

(GÉNIE MÉTALLURGIQUE)

AVRIL 2012

UNIVERSITÉ DE MONTRÉAL

ÉCOLE POLYTECHNIQUE DE MONTRÉAL

Cette thèse intitulée:

OXYGEN REDUCTION REACTION ON PALLADIUM-COBALT ALLOY CATALYSTS FOR POLYMER ELECTROLYTE FUEL CELLS

présentée : OISHI Kentaro

en vue de l'obtention du diplôme de : Philosophiae Doctor

a été dûment acceptée par le jury d'examen constitué de :

M. STUART, Paul, Ph. D., président

M. SAVADOGO, Oumarou, D. d'état, membre et directeur de recherche

M.TAVARES, Jason R, Ph. D., membre

M.TERNAN, Marten, Ph. D., membre

DEDICATION

This thesis is dedicated to my spouse Akiko, to my son Waichiro Henry, to my parents Ken-ichi and Emiko, to my sister Megumi and to my grandparents Yukiyasu, Miyoko and Yoshitaka .

I also would like to dedicate this thesis to my grandmother, Sue Hori, who passed away in 2006.

ACKNOWLEDGMENTS

I wish to express my sincere gratitude to those who helped me in the completion of this thesis. First of all, I am indebted to my supervisor, Professor Oumarou Savadogo for his kind guidance, valuable support, helpful suggestions, encouragement and confidence in me.

I thank to my colleagues in Ecole Polytechnique de Montreal: Carole Massicotte, Ali Shanian, Frederic Fouda-onana, Teko W. Napporn and Eric Nguwuo Petuenju. I thank you all for working with me during my Ph.D. studies.

I also thank to Professor Professor Shigenori Mitsushima, Professor Nobuyuki Kamiya and Ken-ichiro Ota in Yokohama National University for helping me to grow as a researcher during my bachelor's thesis.

To Dr. Yuichi Suzuki, Dr. Kunchan Lee and Dr. Akimitsu Ishihara, thank you for believing in me and introducing me to the wonderful world of science.

Lastly, to all of the friends and colleagues at Ecole Polytechnique de Montreal and Yokohama National University, life has been made a much more pleasant ride with your presence.

RÉSUMÉ

L'activité de la réaction de réduction de l'oxygène (RRO) en milieu acide sur les alliages Pd-Co a été étudiée dans ce travail. Les électro-catalyseurs ont été synthétisés par deux techniques : a) La technique de dépôt physique en phase vapeur et b) la technique de réaction de pulvérisation à ultrasons qui a été développée pour la première fois dans notre laboratoire pour préparer directement des électro-catalyseurs supportés sur du tissu ou des feuilles de carbone (GDE) pour des applications de type PEMFC.

Les variations des propriétés électrochimiques telles que les quantités de charge liée à : i) l'adsorption/désorption de d'hydrogène, ii) la formation ou la réduction de la couche d'oxyde en fonction de la composition de l'alliage Pd-Co ont été mises en évidence pour la première fois dans ce travail. Les travaux ont été faits sur des couches minces de Pd-Co préparés par un procédé de pulvérisation sous vide cathodique (PVD). Même si un catalyseur à couche mince ne peut pas être utilisé directement comme électrode de PEMFC fonctionnelle parce que sa surface active est faible, le procédé de pulvérisation cathodique est très utile car la composition chimique de l'alliage et l'aire de surface de l'électrode peuvent être contrôlées avec facilité pour assurer des études fondamentales en électro-catalyse. C'est pour cela, les propriétés électrochimiques fondamentales en électro-catalyse ont été réalisées sur ces couches minces de catalyseurs à base d'alliage de Pd-Co. Ainsi, les quantités de charge des processus électrochimiques sur les alliages de Pd-Co indiqués ci-dessus ont été corrélées aux activités électro-catalytiques de la réaction de réduction de l'oxygène (RRO) en milieu acide.

Les bonnes activités électro-catalytiques de la RRO sur des alliages binaires de Pd-Co obtenues dans ce travail sont en accord avec les résultats présentés dans les études antérieures. L'activité électro-catalytique de la RRO sur ces alliages augmente dans le sens suivant : $Pd_{16}Co_{84}$ < $Pd_{42}Co_{58}$ < Pd < $Pd_{50}Co_{50}$ < $Pd_{75}Co_{25}$ < $Pd_{65}Co_{35}$. L'alliage $Pd_{65}Co_{35}$ donne l'activité de la RRO la plus élevée suivie par les alliages $Pd_{75}Co_{25}$ et $Pd_{50}Co_{50}$.

Aucunes améliorations d'activité évidentes n'ont été obtenues pour $Pd_{42}Co_{58}$ et $Pd_{16}Co_{84}$ qui ont un contenu de Co plus élevé.

Une corrélation linéaire entre les charges d'adsorption/désorption de d'hydrogène et les activités électro-catalytiques de la RRO a été obtenue sur ces alliages de Pd-Co. Les catalyseurs ayant une

teneur en Co plus élevée ont des activités en RRO plus faibles. Par contre aucune corrélation linéaire n'a été observée entre les caractéristiques de l'activité de la RRO et la quantité de charges liée à la formation ou la réduction des oxydes sur les catalyseurs. Les meilleures activités électro-catalytiques pour le RRO on été identifiées sur les alliages ayant un ratio atomique optimisé entre Pd et Co aux alentours de Pd: Co = 3:1.

La méthode de pulvérisation à ultrasons a été développée pour la première fois dans le cadre de ce travail pour la préparation de catalyseurs déposés à l'échelle nanométrique directement sur des supports de feuilles de tissus de carbone commerciaux utilisés (GDE) dans la fabrication des assemblages membranes électrodes pour les piles PEMFC dans notre laboratoire. Cette approche répond bien aux critères d'obtention de catalyseurs de fines particules ayant de grande surface sur la poudre de carbone comme matériaux de cathode pour les piles de type PEMFC. Ceci est d'autant plus pertinent qu'aucune des études réalisées avant n'a réussi à obtenir des particules fines de Pd-Co ayant des dimensions qui soient comparables à celles du catalyseur existant à base de platine à support de carbone (φ2-4 nm).

Par conséquent, la mise au point de la méthode de synthèse de catalyseur à base de particules fines de Pd-Co est nécessaire pour mieux utiliser ce catalyseur pour les applications des piles PEMFC. En utilisant cette méthode développée dans ce travail, les catalyseurs de Pt, de Pd et Pd-Co à support de carbone ont été synthétisés et caractérisés pour leur activité en RRO en milieu acide. L'imagerie TEM des échantillons préparés indiquent que la taille des particules dominante de 2,5-4,5 nm. Pour les catalyseurs obtenus. Ce qui montre que cette technique est très utile pour la préparation de catalyseurs à support de carbone à l'échelle nanométrique.

La diffraction des rayons-X (DRX) sur les échantillons fabriqués de Pt a montré que les pics de diffraction sont ceux d'une structure cubique à faces centrées (cfc) de Pt. La DRX descatalyseurs synthétisés de Pd et Pd-Co par réaction de pulvérisation ultrasonique a également indiqué des pics de diffraction d'un système cristallin cubique face centré (CFC). Tous les diffractogrammes des échantillons sont similaires à celui de Pd cfc, mais les pics d'origine Co ne peuvent être observés car le système Pd-Co est une solution solide de substitution, de sorte que certains atomes de Pd sont remplacés par des atomes de cobalt. Ce qui constitue un atout car le système de solution solide est considéré comme étant stable en milieu acide [1].

Aussi nous avons développé dans ce travail une nouvelle technique utilisant la méthode de réaction de pulvérisation à ultrasons pour réaliser dans un même processus la synthèse du catalyseur à support de carbone nanométrique qui est ensuite déposé directement sur l'électrode à diffusion de gaz (GDE) et formé ainsi un GDE catalysé. En utilisant du papier carbone comme comme support de réaction de la pulvérisation à ultrasons tel que décrit ci-dessus, le catalyseur supporté sur de la poudre de carbone à support est directement déposé sur le papier carbone et formé ainsi le GDE catalysé qui peut ainsi être utilisée dans les piles PEFC. Cette technique permet d'économiser certaines étapes importantes comme par exemple la mise en forme de la poudre de catalyseur (préparation de la pâte de catalyseur et son étalement) et de la fabrication du GDE et conduit à un moindre coût de la PEMFC.

Les améliorations obtenues sur l'activité électro-catalytique de la réaction de réduction de l'oxygène en milieu acide sur les catalyseurs de Pd-Co synthétisés par le procédé de réaction de pulvérisation à ultrasons ont été confirmées. Ce résultat est en bon accord avec l'amélioration de l'activité de la RRO de la couche mince synthétisée par PVD. Pour un potentiel donné, le courant de la RRO de Pd3Co1/C et Pd2Co1/C étaient presque les mêmes. Ensuite ce courant diminue de Pd5Co1/C, Pd1Co1/C à Pd/C.

Les résultats ont aussi montré que les catalyseurs à base de Pd ont autour de 45mV/dec de pente de Tafel et de courant d'échange normalisée à la masse de Pd qui est égale à

10^{-11} mA mg^{-1}. Il est supposé que la cinétique de RRO dans cette région de potentiel est la même pour Pd et les catalyseurs à base de Pd-Co¸ et l'ajout de Co dans le Pd a peu d'effet sur la cinétique de RRO. Nous concluons que la méthode de réaction de pulvérisation à ultrasons avec transducteur piézoélectrique est applicable pour la synthèse du catalyseur à alliage binaire de Pd-Co ou de Pt. L'effet de l'addition de Co au Pd pour former l'alliage Pd-Co sur l'amélioration de l'activité électro-catalytique de la RRO par rapport à celle de RRO sur Pd seul a été confirmé.

Cette étude contribue à l'avancement des connaissances sur les propriétés électro catalytiques fondamentales de la RRO sur les alliages de Pd-Co. En particulier la relation entre la composition de l'alliage en Co et ses activités électro-catalytiques pour la RRO a été établie et une composition optimum de l'alliage qui conduit à une meilleure activité de la RRO a été déduite. Des corrélations ont aussi étudiés réalisées entre la RRO et la quantité de charge liée à

l'adsorption/désorption de l'hydrogène et la formation et à la réduction de l'oxyde sur l'électro-catalyseur.

En outre, la méthode de réaction de pulvérisation à ultrasons, développée dans cette étude, contribue de manière significative et intéressante du point de vue industrielle à un processus intégré de préparation des catalyseurs (alliages de Pd-Co ou Pt) et de fabrication d'électrodes à diffusion de gaz (GDE) catalysées pour les piles PMFC. En plus cette méthode de synthèse mise au point dans ce travail a permis de disposer de catalyseurs ayant des particules de petite taille (φ2-4nm) en alliage Pd-Co ou de Pt qu'il n'a pas été possible d'obtenir de manière homogène et reproductible par les autres méthodes conventionnelles de préparation. Ces résultats sont d'une grade importance pour le développent commercial de la technologie des piles PEMFC parce qu'en plus de permettent l'obtention de particules de tailles optimisées, ils permettent de réduire les étapes de fabrication des assemblages membranes électrodes (MEA) comme par exemple l'étape de mise en forme du catalyseur de la poudre à la pâte et son étalement sur le GDE dans le cas des méthodes conventionnelles. Alors que dans l'approche de ce travail c'est un dépôt direct du catalyseur sur le GDE au fur et à mesure qu'il est fabriqué. En plus, notre approche permet de réduire leur coût de fabrication et augmente la fiabilité du MEA suite à la réduction des étapes de sa fabrication.

ABSTRACT

The Oxygen Reduction Reaction (ORR) activity in acid medium on Pd-Co was studied in this work. The catalysts were synthesized by two techniques; physical vapor deposition technique and ultrasonic spray reaction technique. The last technique was developed for the first time in our laboratory for the supported electro catalyst preparation and direct deposition onto the carbon paper or gas diffusion electrode the for PEMFC applications. The electrochemical properties such as the amount of hydrogen adsorption/desorption, the oxide formation/reduction of Pd-Co alloy catalyst have not been sufficiently studied before. Therefore these electrochemical properties were investigated by using the Pd-Co thin films prepared by sputtering method. A thin film catalyst cannot be directly used as an electrode of working PEMFCs, however the sputtering method is very useful since the chemical composition of alloy and surface area of the electrode can be controlled easily. Thus the fundamental electrochemical properties such as the amount of hydrogen adsorption/desorption, oxide formation/reduction and oxide reduction peak position on thin films of Pd-Co alloy, Pd and Pt catalysts were determined and their correlations to ORR catalytic activities in acid medium were studied. Enhancements of the catalytic activities for ORR by Pd-Co binary alloys were found to be in agreement with results obtained in previous studies. The electro catalytic performance of the ORR on the various electrodes studied here is: in the order $Pd_{16}Co_{84}$ < $Pd_{42}Co_{58}$ < Pd < $Pd_{50}Co_{50}$ < $Pd_{75}Co_{25}$ < $Pd_{65}Co_{35}$. This result clearly shows that alloying Pd with a specific composition of Co enhances significantly the electro-catalytic properties of the ORR on Pd-Co alloys in comparison to Pd alone. $Pd_{65}Co_{35}$ alloy exhibited the highest ORR activity followed by $Pd_{75}Co_{25}$ and $Pd_{50}Co_{50}$ alloys. No obvious activity enhancements were found for $Pd_{42}Co_{58}$ and $Pd_{16}Co_{84}$, which have higher Co content. A linear correlation between hydrogen charges and ORR catalytic activities on Pd-Co alloys was obtained. Catalysts having more Co content have lower ORR activities. With regard to the correlation between the amount of oxide formation/reduction and ORR activities, no linier correlation was found. However the results of this work indicated that the optimized atomic ratio between Pd and Co for ORR in acid medium was found to be around Pd:Co = 3:1.

Ultrasonic spray reaction method was developed for the first time in our laboratory for carbon supported nano-scale catalyst for PEMFC application. Fine catalyst particles supported on high surface area carbon powder are required to apply the catalyst as the PEMFC cathode materials for

the commercialization, but none of the studies done before were able to successfully obtain the Pd-Co fine particles which are comparable with the existing carbon supported platinum catalyst (φ2-4nm). Therefore the establishment of the catalyst synthesis method for Pd-Co fine particles are required to use the catalyst for PEMFCs. By using this method established in this study, carbon supported Pt, Pd and Pd-Co catalysts were synthesized and characterised for ORR activity. TEM images indicate that this technique is very useful for preparing carbon supported nano-scale catalysts having the dominant particle size of 2.5-4.5 nm. XRD showed diffraction peaks consistent with face-centered cubic (fcc) structure for Pt. XRD of the synthesized Pd and Pd-Co catalysts by ultrasonic spray reaction also indicated fcc crystal system. All diffractograms of the samples are similar to the structure of fcc Pd, but the Co-origin peaks cannot be found. The Pd-Co system is substitutional solid solutions where some Pd atoms are replaced by Co atoms. The solid solution system is considered to be stable in acid media [1].

We developed this new technique of the ultrasonic spray reaction method not only for nano-scale carbon supported catalyst synthesis but also fabricate directly catalyzed GDE. By using carbon paper as a filter of ultrasonic spray reaction method as described above, carbon supported catalyst are directly deposited onto the carbon paper. It directly forms catalyzed GDE. This technique saves some step of the GDE fabrication and will leads lower cost of PEMFC.

Catalytic activity enhancements of ORR for the synthesized Pd-Co catalysts by ultrasonic spray reaction method are confirmed. This result has good agreement with the ORR activity enhancement of the thin film synthesized by PVD. For a given potential, the ORR current of Pd_3Co_1/C and Pd_2Co_1/C were almost the same and show the highest values among the values of all the other alloys. After, the value of the current decreases from Pd_5Co_1/C to Pd_1Co_1/C and Pd/C. All Pd based catalysts have around 45mV/dec of tafel slope and Pd mass corrected exchange current around 10^{-11} mA mg^{-1}. It is assumed that the ORR kinetics in this potential region are the same among the Pd and Pd based catalysts and the addition of Co into Pd have small effect on the ORR kinetics. We conclude that ultrasonic spray reaction method with piezoelectric transducer is applicable for Pd-Co binary alloy catalyst synthesis and the activity enhancement effect caused by alloying with Co was confirmed on the synthesized catalyst by this technique.

This study contributes to the advancement of the knowledge of fundamental properties of Pd-Co alloy catalysts and their correlations to the oxygen reduction reaction activities. In addition, the ultrasonic spray reaction method developed for the first time in this study introduces a new easy and low cost Membrane Electrode Assembly preparation significantly to an industrial fabrication process of method of preparation of catalyzed gas diffusion electrodes for PEMFCs. The synthesis method of small particle size (φ2-4nm) Pd-Co alloy catalysts were not possible to be obtained by using the existing conventional methods. However this work has achieved the synthesis of the fine particle catalysts supported on carbons by using the ultrasonic spray reaction method. These results will contribute significantly in the development of PEMFCs based on Pd-Co alloy catalysts in the future.

TABLE OF CONTENTS

LIST OF TABLES

LIST OF FIGURES

LIST OF ABBREVIATIONS

AES	Auger Electron Spectroscopy
AFC	Alkaline Fuel Cell Fuel Cell
BE	Binding Energy
CV	Cyclic Voltammetry
DMFC	Direct Methanol Fuel Cell
EELS	Electron Energy Loss Spectroscopy
EMF	Electromotive Force
FC	Fuel Cell
FRA	Frequency Response Analyzer
GC	Glassy Carbon
GDE	Gas Diffusion Electrode
GDL	Gas Diffusion Layer
GS	Galvanostat
HOR	Hydrogen Oxidation Reaction
MCFC	Molten Carbonate Fuel Cell
MEA	Membrane and Electrode Assembly
NHE	Normal Hydrogen Electrode
ORR	Oxygen Reduction Reaction
PAFC	Phosphoric Acid Fuel Cell
PEM	Polymer Electrolyte Membrane (Proton Exchange Membrane)
PEMFC	Polymer Electrolyte Membrane Fuel Cell (Proton Electrolyte Membrane Fuel Cells
PS	Potentiostat

RHE	Reversible Hydrogen Electrode
SEM	Scanning Electron Microscope
SHE	Standard Hydrogen Electrode
SOFC	Solid Oxide Fuel Cell
SSL	Slow Scan Voltammetry
STEM	Scanning Transmission Electron Microscope
TEM	Transmission Electron Microscopy
THE	Trapped Hydrogen Electrode
USPR	Ultrasonic solution spray reaction
XPS	X-ray Photoelectron Spectroscopy
XRD	X-ray Diffraction

CHAPTER 1 INTRODUCTION

Since the time of the industrial revolution, the world's energy needs have been growing exponentially and will keep growing in the future. Fossil fuels such as coal, oil, natural gas have been used as the primary source of energy over the past 260 years, but the reserve will be depleted in the not too distant future and use of the fuels raise environmental concerns. In order to overcome the crisis by fossil fuels depletion, alternative energy resources have to found and they should be cost-effective, renewable, sustainable and environmentally friendly.

A fuel cell is a promising energy-conversion device that is more efficient and more environmentally friendly than existing combustion-based systems. Fuel cell is an electrochemical energy conversion device that converts chemical energy into electrical energy directly. Since there is no combustion or moving parts, the theoretical efficiency of fuel cells can be approximately 80% while that of combustion processes is limited to about 20% at low temperature below 100°C. Polymer electrolyte membrane fuel cells (PEMFC), which are considered in this study, usually take hydrogen, methanol or other small organic molecules as a fuel. In case of hydrogen-oxygen type fuel cells, it produces only water and heat. Therefore this system is very friendly to environment. Replacing fossil fuels with other sustainable resources plays a very important role in both environmental and economical terms. The fed hydrogen gas or small organic molecules, for example methanol and ethanol, are electrochemically oxidized at anode and the generated proton and electron react with oxygen gas fed into cathode and form water molecule (oxygen reduction reaction).

The Oxygen reduction is considered to be one of the most important electrocatalytic reactions because of its role in electrochemical energy conversion, several industrial processes, and corrosion. Consequently, for many years it has been the focus of electrochemical interest. Platinum has been the best catalyst for the ORR for over 170 years since Christian Friedrich Schoenbein and William Robert Grove reported the first study on fuel cells [2]. However, this does not mean that platinum is the optimal material for fuel cell application, because of its fundamental catalytic property limitations, very high cost, limited reserves, and political issues. Therefore a future commercialization of PEMFCs cannot be based solely on platinum-based technologies. It is essential to develop a catalyst having higher ORR catalytic activity and high cost-performance for the future.

The first study on Pd-based alloy materials was demonstrated by the research group of O. Savadogo in 2004 for PEMFC cathode catalysts [3]. The fact that palladium potentially has a high catalytic activity for ORR next to platinum and that alloying with the 3d-transition metal enhances the catalytic activity of the base element suggests that alloying can also enhance the electrocatalytic activity of palladium electrode. Palladium-Cobalt binary alloy was selected in this study, since Pd-Co exhibited the best ORR catalytic activity between Co, Cr, Ni in our previous study [3]. However since Pd-Co alloy is very new as a cathode material for PEMFCs, fundamental aspects on the Pd-alloy electro-catalysts were not deeply studied yet, so their physical, chemical and electrochemical properties were needed to be investigated. In addition, it's very important to cover from fundamental research to applications to contacts with industry. Hence not only the fundamental studies, but also catalyst synthesis process for carbon supported Pd-Co alloys which allows to use for the PEMFC cathode materials directly need to be developed.

Fine catalyst particles supported on high surface area carbon powder are essential factor to apply the catalyst as the PEMFC cathode materials for the commercialization. However I found that the conventional synthesis processes which has been used for carbon supported catalyst were not optimal methods. None of the studies done before were able to successfully obtain the Pd-Co fine particles which are comparable with the existing carbon supported platinum catalyst (φ2-4nm).

A catalyst maker with ultrasonic piezo-electric transducer was built in our laboratory to carry out an catalyst synthesis process of ultrasonic spray reaction method. This technique was firstly developed by Uematsu et al. [4-6] to prepare fine composite catalysts of Ni/TiO_2, Ni/Al_2O_3, Pd/ZrO_2, Ru/Al_2O_3, and Ru/TiO_2. The technique demonstrated excellent results for preparing multi-components composites on oxide catalyst supports. The obtained catalysts had strong interaction among the components because the composites were formed from droplets of a homogeneous solution in a quick-heating process. This technique was very unique and never been studied for PEMFCs, I've investigated the feasibilities of the technique for the catalyst synthesis process in this study.

CHAPTER 2 LITERATURE REVIEW

The anode of the fuel cell oxidizes H_2 while the cathode reduces O_2 according to Reactions Eq. 2.1 and Eq. 2.2, respectively. The overall reaction is given as Reaction Eq. 2.3.

Anode reaction

$$2H_2 \rightarrow 4H^+ + 4e^-$$

Eq. 2.1

Cathode reaction

$$O_2 + 4H^+ + 4e^- \rightarrow 2H_2O$$

Eq. 2.2

Overall reaction

$$2H_2 + O_2 \rightarrow 2H_2O$$

Eq. 2.3

Both anodic and cathodic reactions are catalyzed, typically with highly dispersed Pt on a porous carbon support. However the rate of the oxygen reduction reaction (ORR) is several orders of magnitude less than the rate of the hydrogen oxidation reaction (HOR). To counter this unavoidable constraint, the Pt loadings on the fuel cell cathode typically approach 40% or more, which dramatically increases the fabrication cost of fuel cells. Despite the high Pt loadings, the slow ORR often requires over potentials of 0.3 V – 0.4 V to achieve acceptable current densities and results in decreased efficiency.

Currently, Pt loadings for PEMFCs are between 0.6 and 0.8 mg-Pt/cm^2 (corresponding to 0.85-1.1 g-Pt/kW @ 0.65 V) which is a significant improvement achieved over the last 15 years. However, Pt loading should be reduced at least five times to meet projected requirements for large-scale commercial usage (< 0.2 g-Pt/kW @ > 0.65 V) [7]. Gasteiger *et al.* state that two strategies to meet these requirements are i) increasing MEA power densities by reducing mass-transport-limitations at high current densities and ii) reducing Pt loading in PEM electrodes to 0.15 mg-Pt/cm^2. These requirements are necessary both due to cost and Pt supply considerations.

Currently, Pt trades at well over $1,000/troy oz., and the cost is expected to increase in the next decade as demand for Pt as a catalyst, inert coating, and precious metal rises.

Decreasing Pt loadings in PEM electrodes requires both greater dispersions of Pt (the fraction of surface Pt atoms/total Pt atoms) and greater site-specific oxygen reduction activity. To distinguish these two enhancements, Gasteiger *et al.* [7] have suggested a benchmark of 0.32 to 0.64 A/mg-Pt @ 0.9 V and 400 to 800 $\mu A/cm^2$-Pt @ 0.9 V for mass and site specific activity, respectively. To reach these two goals, it is necessary to develop a new electrocatalysts and/or new synthesis techniques that provide high catalyst dispersion, ORR activity, and stability.

2.1 Fuel cells and oxygen reduction reaction

Fuel cells are expected to be one of the major clean energy sources in the near future. However, the slow kinetics of the electrocatalytic activity of the oxygen reduction reaction (ORR) and the high loading of novel metal cathode materials are the urgent issues to be addressed. This is very important because they determine the efficiency and the cost of this energy source. This study is on the material issues relating to the effect of the electrocatalyst composition on the Oxygen Reduction Reaction (ORR) in fuel cells.

2.1.1 Basic reactions

Fuel cells are electrochemical devices that convert chemical energy of fuels directly into electrical energy, thereby promising power generation with high efficiency and low environmental impact. They provide the cleanest and most efficient technologies for generating electricity. They are not limited by thermodynamic limitations such as Carnot efficiency since the system avoids the intermediate steps of producing heat and mechanical work which are typical of conventional methods of power generation. Fuel cells also avoid combustion, hence they produce power with minimal pollutants. As long as the reductant (fuel) and oxidant are provided continuously, fuel cells continue to generate electricity. Hydrogen, methanol, and hydrocarbons are various fuels commonly used in fuel cells. Oxidants used are generally air or oxygen. Several types of electrolytes can be used in fuel cells such as acids, bases, solid and polymer electrolytes, molten salt and conductive ceramics. Some typical fuel cell systems are shown in Table 2.1 Characteristics of typical fuel cell systems Characteristics of typical fuel cell systems. In addition, Table 2.2 Oxidation reactions of various fuels and their thermodynamic data at 25ºC. provides

the oxidation reactions of various fuels and their thermodynamic data which are under way in fuel cell development. This research is focused on PEM fuel cell systems with oxygen (or air). A schematic of voltage-current characteristic and thermodynamic properties of PEM fuel cell with H_2/O_2 is shown in Figure 2.1.

Table 2.1 Characteristics of typical fuel cell systems

Fuel Cell Type	Mobile Ion	Operating Temperature (°C)	Applications and Notes
Alkaline (AFC)	OH^-	20-200	Space vehicles (e.g. Apollo)
Proton Exchange Membrane (PEMFC)	H^+	30-100	Vehicles and mobile applications
Direct Methanol (DMFC)	H^+	20-90	Portable electronic systems of low power, running for long time
Phosphoric Acid (PAFC)	H^+	200	Large number of 200 kW combined heat and power system
Molten Carbonate (MCFC)	CO_3^{2-}	650	Medium to large scale heat and power combined system, up to MW capacity
Solid Oxide (SOFC)	O^{2-}	500-1000	All sizes of heat and power combined system, 2kW to multi-MW

Table 2.2 Oxidation reactions of various fuels and their thermodynamic data at 25ºC.

Fuel	Reaction	ΔH^o (kJ/mol)	ΔG^o (kJ/mol)	EMF (V)	ε (%)
Hydrogen	$H_2(g) + 1/2O_2(g) \rightarrow H_2O(l)$	-286	-237	1.23	83
Methane	$CH_4(g) + 2\ O_2(g) \rightarrow CO_2(g) + 2\ H_2O(l)$	-890	-817	1.06	92
Carbon monoxide	$CO(g) + 1/2\ O_2(g) \rightarrow CO_2(g)$	-283	-257	1.33	91
Carbon	$C(s) + O_2(g) \rightarrow CO_2(g)$	-394	-394	1.02	100
Methanol	$CH_3OH(l)+1/2O_2(g) \rightarrow CO_2(g)+2H_2O(l)$	-727	-703	1.21	97
Hydrazine	$N_2H_4(l)+O_2(g) \rightarrow N_2(g)+2H_2O(l)$	-622	-623	1.61	100
Ammonia	$NH_3(g)+4/3O_2(g) \rightarrow 3/2H_2O(l) +1/2N_2(g)$	-383	-339	1.17	89
Di-Methyl Ether	$CH_3OCH_3(g)+3O_2(g) \rightarrow 2CO_2(g)+3H_2O(l)$	-1460	-1390	1.2	95

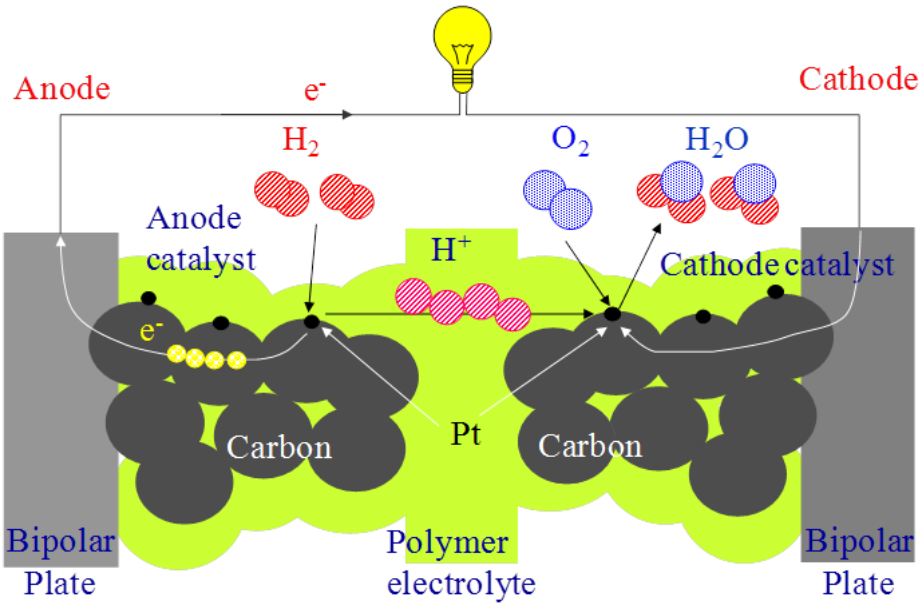

Figure 2.1 Schematic of working PEMFC

In the case of typical H_2/O_2 fuel cell system, as described in Figure 2.1, using a Polymer Electrolyte Membrane (PEM) as an electrolyte, hydrogen is continuously fed to the negative electrode (anode) and oxygen (or air) is continuously fed to the positive electrode (cathode). At the anode, hydrogen molecules diffuse through the porous pathway to encounter a catalyst which is generally platinum. At this point, anode catalysts dissociate each hydrogen molecule into two hydrogen atoms which will then be bonded to two-neighboring Pt atoms. Each of these two hydrogen atoms then releases an electron to form two H^+ ions. These H^+ ions are then conducted through the proton exchange membrane while the two electrons pass through the external circuit and reach cathode. On the cathode side oxygen gets reduced to form water, thus completing the electrochemical reactions.

Basic electrode reactions in a H_2/O_2 fuel cell system are:

Anode reaction

$$2H_2 \rightarrow 4H^+ + 4e^- \qquad \text{Eq. 2.4}$$

Cathode reaction

$$O_2+4H^++4e^-\rightarrow 2H_2O$$

Eq. 2.5

Overall reaction

$$2H_2+O_2\rightarrow 2H_2O$$

Eq. 2.6

In fuel cells, oxygen reduction at the cathode can happen either by a direct four-electron pathway where an oxygen molecule adsorbs onto the catalyst surface and gets reduced to water, or by a peroxide two-electron pathway involving the formation of hydrogen peroxide intermediate which can be further reduced to water or can chemically decompose to form water and oxygen.

Direct four-electron pathway:

Alkaline media

$$O_2+2H_2O+4e^-\rightarrow 4OH^- \qquad (E° = 0.401\ \text{V})$$

Eq. 2.7

Acid media

$$O_2+4H^++4e^-\rightarrow 2H_2O \qquad (E° = 1.229\ \text{V})$$

Eq. 2.8

Two-electron pathway:

Alkaline media

$$O_2+H_2O+2e^-\rightarrow HO_2^-+OH^- \qquad (E°=-0.065\ \text{V})$$

Eq. 2.9

followed by either the reduction of peroxide:

$$HO_2^-+H_2O+2e^-\rightarrow 3OH^- \qquad (E°=0.867\ \text{V})$$

Eq. 2.10

or by the decomposition of peroxide:

$$2HO_2^- \rightarrow 2OH^- + O_2$$

Eq. 2.11

Acid media

$$O_2 + 2H^+ + 2e^- \rightarrow H_2O_2 \qquad (E°=0.67\ V)$$

Eq. 2.12

followed by either the reduction of peroxide:

$$H_2O_2 + 2H^+ + 2e^- \rightarrow 2H_2O \qquad (E°=1.77\ V)$$

Eq. 2.13

or by the decomposition of peroxide:

$$2H_2O_2 \rightarrow 2H_2O + O_2$$

Eq. 2.14

In PEMFCs, the effective pH of the media is between 0 and 1, so the cathode reaction in the acidic media should be considered in the kinetics. It should also be noted that under these mechanisms water evolution occurs at the cathode continuously, hence the produced water should be effectively removed from the cathode side. Otherwise the product will block the gas diffusion to the electrocatalyst.

The real performance of a PEMFC can always be determined once the ideal performance and its deviation from ideal behavior are established. The losses arising from the non-ideal behavior can then be deducted from the ideal performance to express the actual performance. The ideal performance of a fuel cell depends on the electrochemical reactions that occur between different fuels and oxygen. The maximum cell voltage for a H_2/O_2 system can be calculated from the Gibbs free energy for the overall reaction as:

$$\Delta E = -\frac{\Delta G}{nF}$$

Eq. 2.15

where ΔE is the ideal cell voltage, ΔG is the Gibbs free energy change from the reaction, n is the number of electrons participating in the reaction, and F is the Faraday's constant (96,487 coulombs/mole).

ΔG can be calculated from the state function

$$\Delta G = \Delta H - T\Delta S$$

Eq. 2.16

where ΔH and ΔS are the enthalpy and entropy changes respectively.

From thermodynamic evaluations one can write the equation for Gibbs free energy change for a standard reaction $aA + bB \rightarrow cC + dD$ as

$$\Delta G = \Delta G° + RT \ln \frac{f_C^c f_D^d}{f_A^a f_B^b}$$

Eq. 2.17

where $\Delta G°$ is the Gibbs free energy change of reaction at the standard temperature and pressure (298 K and 1 atm) and f_i is the fugacity of species i. Substituting Eq. 2.17 into Eq. 2.15,

$$\Delta E = \Delta E° + \frac{RT}{nF} \ln \frac{f_C^c f_D^d}{f_A^a f_B^b}$$

Eq. 2.18

Eq. 2.18 is the general form of the Nernst equation. This gives the Nernst potential ΔE, which is the ideal open circuit cell potential. It relate $\Delta E°$, the ideal standard potential for the reaction, to ΔE, the ideal equilibrium potential.

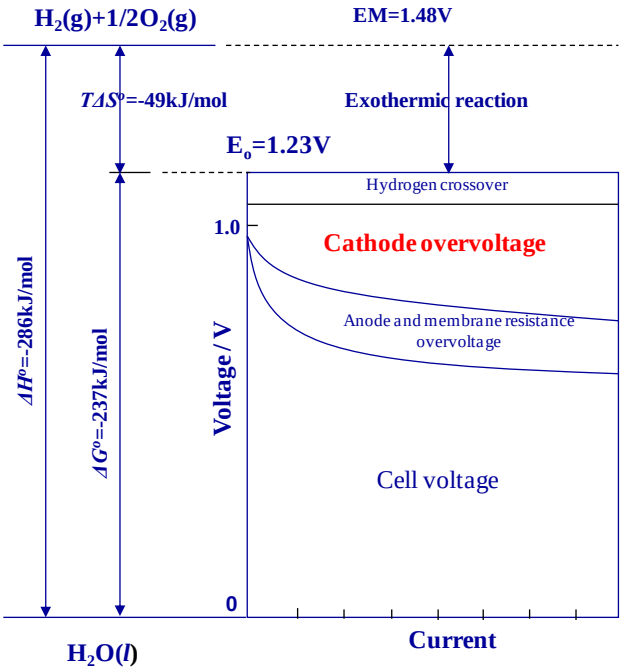

Figure 2.2 Current-Voltage characteristics and thermodynamic properties of actual PEMFC

2.2 The oxygen reduction reaction (ORR)

The cathode reaction in the current Polymer Electrolyte Fuel Cell (PEMFC) is the oxygen reduction reaction (ORR) at the catalyst (ex. platinum) surface in an acidic electrolyte. The ORR is a highly irreversible reaction even at temperatures above 100°C and at the best existing electrocatalysts - platinum [8, 9]. The overall four-electron reduction process of O_2 in acid aqueous solutions is

$$O_2+4H^++4e^-\rightarrow 2H_2O$$

Eq. 2.19

and the equilibrium potential is

$$\left(E^{\circ}_{\mathrm{NHE}}\right)_{298} = 1.229\ \mathrm{V}$$

Eq. 2.20

Since the four-electron reduction of the oxygen is highly irreversible, experimental verification of the thermodynamic reversible potential of this reaction is very difficult. The exchange current

density for the reaction is typically in the range of 10^{-8}–10^{-10} A cm^{-2} of real surface area for Pt at room temperatures. Any other side reaction, even if slow and difficult to detect, may compete with reaction Eq. 2.19 and affect the remaining potential. Indeed, unless special experimental procedures are used, the thermodynamic potential cannot be obtained at ambient temperature in aqueous electrolytes from experimental measurements. Even if the most active platinum electrodes are used in pure acid or alkaline aqueous solution under ordinary conditions, the remaining potential in the presence of oxygen at 1 atm and ambient temperature usually does not exceed 1.1 V vs. the Reversible Hydrogen Electrode (RHE) and most often has a value close to 1.0 V. These values are different from the theoretical value of 1.23 V. On the other hand, evidence showed that platinum dissolves in both acid and alkaline electrolyte at potentials of less than 1.0 V vs. RHE [10, 11]. Thus the anodic dissolution of Pt may be the steady-state complementary reaction. The dissolution may proceed through the direct dissolution of the platinum or through a Pt-OH or Pt-O intermediate. A review of the problem is offered by Norskov *et al.* [12]. The general methodology used to analyze the kinetics of the reaction is introduced here. In order to analyze the kinetics, we may use the general current-overpotential equation. For a one-step reaction $O + ne \leftrightarrow R$ taking place on a planar electrode surface, the governing equation is [13],

$$i = i_0 \left[\frac{C_O}{C_O^*} e^{+\frac{\alpha n F \eta}{RT}} - \frac{C_R}{C_R^*} e^{-\frac{\beta n F \eta}{RT}} \right]$$

Eq. 2.21

where C_O and C_R are the concentration of oxidant and reductant on the electrode surface; the superscript * indicates in bulk phase; α and β are the transfer coefficient of the anodic and cathodic reaction respectively. η in the equation is the overpotential, defined by $\eta = E - E_{eq}$, and

$$E_{eq} = E_0 + \frac{RT}{nF} \ln \frac{C_O^*}{C_R^*}$$

Eq. 2.22

where E_0 is the formal standard equilibrium potential, namely, the potential when concentrations of the reactant and product are the same. i_0 in Equation Eq. 2.21 is the exchange current density, i.e., the anodic or cathodic current of the reaction at equilibrium condition, when E=E_{eq}.

When Equation Eq. 2.21 is combined with the Rotating Disk Electrode (RDE) measurement, some kinetic parameters of the oxygen reduction reaction can be obtained. So far, it is widely accepted that in aqueous acid electrolyte, the reaction on the Pt electrode is a four-electron kinetic process, with the first charge transfer as the rate determining step [9]. A description of a detailed model for the reaction mechanism will be reviewed in the following section.

2.2.1 Electrode kinetics of the oxygen reduction reaction

The ORR is a multi-step reaction that usually can be divided into several elementary steps in the reaction mechanisms. In aqueous solutions, the ORR occurs mainly through two overall pathways: a "direct" four-electron reduction and a "peroxide" pathway, which involves H_2O_2 as the intermediate [14]. The direct four-electron pathway in an acid solution is as shown in Eq. 2.19.

The peroxide pathway is

$$O_2+2H^++2e^-\rightarrow H_2O_2 \qquad E°=0.67\ V$$

Eq. 2.23

Peroxide can undergo further reduction or decomposition in acid solutions, via the reactions:

$$H_2O_2+2e^-\rightarrow 2H_2O+O_2 \qquad E°=1.77\ V$$
$$2H_2O_2\rightarrow 2H_2O+O_2$$

Eq. 2.24

The rotating ring-disk electrode technique was the principal tool used to quantitatively determine the extent of these reactions. The oxygen reduction took place on the disk while the H_2O_2 was monitored by the ring which was maintained at a potential sufficiently positive to oxidize the peroxide back to O_2 at the diffusion limiting current.

Damjanobic *et al.* [15, 16] proposed the first O_2 reduction reaction schematics analyzed by the disk-ring current data at various rotation speeds. Later, based on the rotating disk-ring data for O_2 reduction on various electrode materials, Bagotskii *et al.* [17] proposed a more general schematics for the series-parallel reactions of O_2 and H_2O_2 as shown in Figure 2.3. In this reaction scheme, O_2, $(O_2)^*$, and $(O_2)_a$ represent molecular O_2 in the bulk solution, in the solution adjacent

to the electrode surface, and in the adsorbate state, respectively. The O_2 can be reduced either directly to water with the rate constant (k_1) without formation of intermediate H_2O_2 or through a series pathway (k_2, k_3) to water with the formation of intermediate H_2O_2. This intermediate can also desorb from the electrode surface into the bulk solution resulting in a two-electron reduction of O_2 (k_6) or be electrochemically oxidized back to O_2 (k_2'). On the other hand, heterogeneous decomposition of H_2O_2 can occur non-electrochemically through a disproportionate reaction involving a direct electron transfer between two $(H_2O_2)_a$ species and not through the electrode phase. The analysis by Bagotskii shows that the number of the rate constants involved in the reaction scheme is greater than the number of independent equations. Therefore, it is impossible to determine all the above-mentioned constants from the rotating disk-ring electrode data for the O_2 reduction alone.

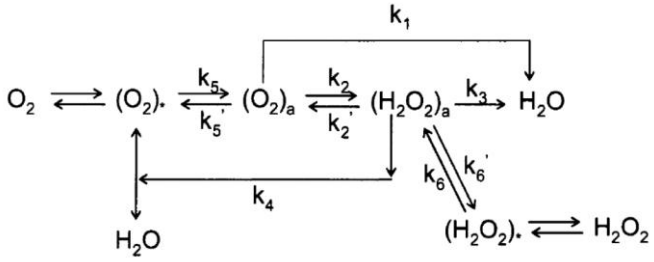

Figure 2.3 Bagotskii *et al.*'s schematic for the oxygen reduction.

Wroblowa *et al.* [18] have used a simpler scheme in which an adsorbed $(O_2)_a$ state is not considered explicitly but the desorption process of H_2O_2 is still included inside. Wroblowa *et al.*'s scheme has the same number of rate constants and independent equations, and it is most often used to analyze experimental ring-disk data. However, oversimplified schemes cannot provide enough information to determine the reaction pathway. For instance, Damjanovic *et al.* omit the (H_2O_2)* state and do not consider slow desorption of H_2O_2 which leads to insufficient diagnostic criteria regarding the series and direct paths for the O_2 reduction.

Anastasijebic [19] proposed a more comprehensive scheme that includes almost all the possible intermediates, based on the previous schemes discussed in the literature. Although, as in other previous schematics, there are more variables to be determined than the number of available equations, after carefully analyzing those equations, the authors provided some clear criteria to

determine some of the kinetic parameters of ORR. These criteria clarify some issues which were not determined well before. The general schematic is as shown in Figure 2.4.

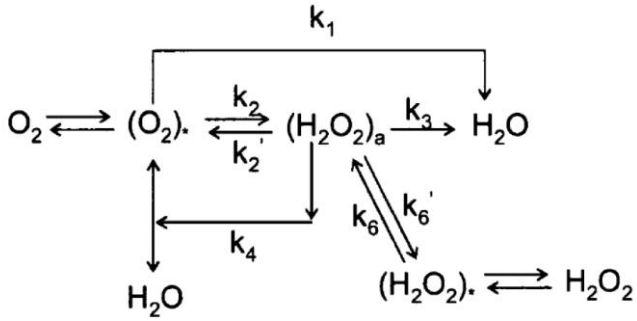

Figure 2.4 Bagotskii *et al.*'s schematic for the oxygen reduction.

The original schematic has been written for alkaline solution, but it is transformed into an analogous schematic here for acid solution, in order to maintain consistency with previous schematics discussed above. The k_i are overall rate constants for the i* step; the parameters with the subscripts a, sa, and * denote adsorbed, strongly adsorbed, and in the solution adjacent to the electrode surface, respectively; without a subscript denotes in bulk solution.

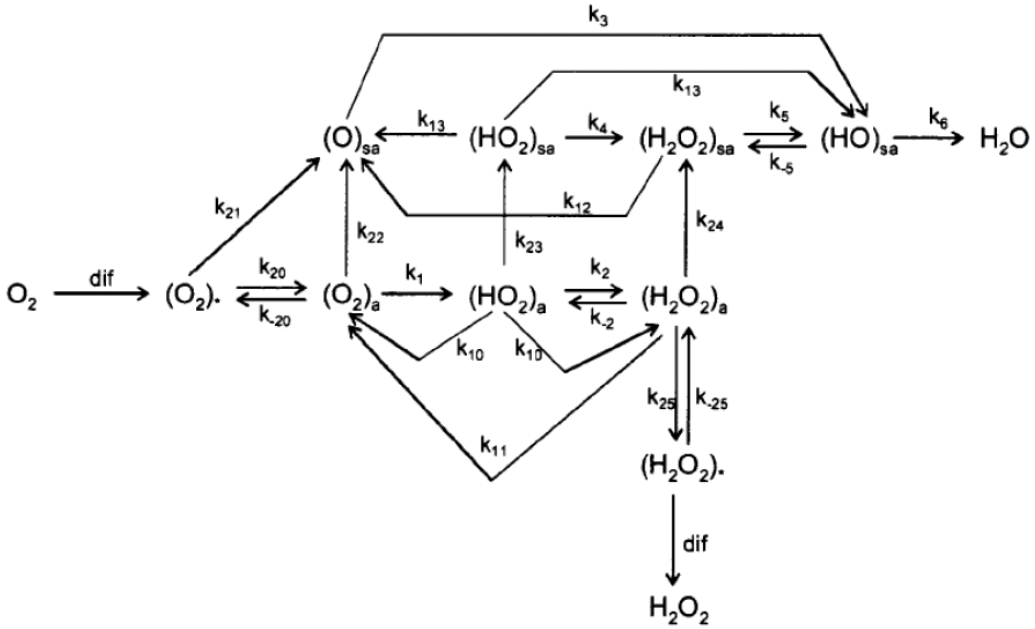

Figure 2.5 Anastasijevic *et al.*'s schematic for the oxygen reduction.

This schematic is the most comprehensive schematic proposed so far and, as before, consists of two major paths by which ORR can take place, i.e., the O_2 can be electrochemically reduced either directly to water without formation of the intermediate hydrogen peroxide or with the intermediate hydrogen peroxide. The adsorbed hydrogen peroxide can be either reduced to water, oxidized back to O_2, decomposed on the electrode surface into O_2 and H_2O, or desorbed and diffuse into the bulk of the solution. Two main features of this schematic make it distinct from previous ones indicated in reference [19] and shown in Figure 2.5: (1) the superoxide species (HO_2) can explicitly be an intermediate; and (2) weakly adsorbed intermediates from the series path can undergo surface diffusion and form their strongly bound counterparts in the direct path. The disk current I_D for this schematic is given by

$$I_D = AFk_1c_{1,a} + k_2c_{2,a} - k_{-2}c_{3,a} + k_3c_4 + k_4c_{2,sa} + k_5c_{3,5a} + (k_6 - k_{-5})c_s$$

Eq. 2.25

while the ring current is given by

$$I_R = n_R ANFZ\omega^{\frac{1}{2}}c_3$$

Eq. 2.26

where A is the area of the disk, N is the collection efficiency, ω is the rotation speed, n_R is the number of electrons exchanged on the ring electrode, and Z is a diffusion parameter for H_2O_2 (Z=0.62$D^{2/3}$/ν), with diffusion coefficient D and solution kinetic viscosity ν . The Subscripts 1, 2, 3, 4, and 5 have been used for the O_2 molecule, the hydrogen superoxide, hydrogen peroxide, the oxygen atom, hydroxyl, respectively. Although it is impossible to obtain all of the rate constants in the reaction schematic, one can draw some qualitative conclusions and obtain some information as to the pathway of the reaction by the careful examination of experimental data. The equation relating the ratio of currents at the disk (I_D) and ring (I_R) to the electrode rotation rate are as follows:

$$N\left(\frac{I_D}{I_R}\right) = 2\left(\frac{1 + A_0 + A_1k_{-25}}{Z\omega^{\frac{1}{2}}}\right)/n_R$$

Eq. 2.27

where A_0 and A_1 are dimensionless function of the rate constant. The intercepts

and slopes from the $N\left(\frac{I_D}{I_R}\right)$ vs. $\omega^{1/2}$ plots are related by the equation

$$J = 2(1 + A_3)n_R + \frac{ZS}{k_{-25}}$$

Eq. 2.28

where J and S are the ordinate intercepts and slopes at various potentials, and A_3 is a dimensionless function of rate constants. Anastasijevic *et al.* drew some conclusions after careful examinations of these equations Equation Eq. 2.25-Eq. 2.28: (1) Linearity of the $N\left(\frac{I_D}{I_R}\right)$ vs. $\omega^{1/2}$ plot is sufficient proof for a first-order reaction; (2) when the equilibrium of adsorption/desorption of H_2O_2 does not exist, S=0; (3) a non-linearity of *J*-*S* plot occurs when an interactive pathway is involved, in which diffusion of species from series path into a direct path takes place. (4) linearity of *J*-*S* plot with the J-axes intercept $J' > 2/n_R$ is a characteristic of a true parallel pathway. In such a case, the ratio of the direct pathway to the series pathway can be evaluated. These criteria provided a way to obtain the most extended information on ORR that the rotating disk ring technique can provide. Further insight into the mechanism of the ORR will depend largely on the spectroscopic methods with the ability to detect intermediates associated with the reaction.

Due to considerable non-uniformity in the terminology for the reaction schematics of the O_2 reduction, Adzid proposed a clearer standard to classify the ORR pathways. It is defined as:

1) a direct four-electron reduction to H_2O (in acid) or to OH^- (in alkaline medium) without hydrogen peroxide detected on the ring;
2) a two-electron pathway involving reduction to hydrogen peroxide;
3) a series of pathways with two- and four-electron reduction. The case of only four-electron reduction without hydrogen peroxide detected on the ring is indistinguishable from a direct four-electron reduction;
4) a parallel pathway that is a combination of 1), 2), and 3); and

an interactive pathway with diffusion of species from a series path into a direct path.

2.2.2 Electrode kinetics of ORR at platinum surface

It is widely accepted that oxygen electroreduction on platinum occurs through parallel reaction pathways with predominately direct four-electron reduction [8, 9]. However, the details of the mechanism remain elusive. The overall ORR is a multi-step process involving four-electron transfers during which bonds are broken and formed. It is still not clear whether the process starts from the oxygen molecule dissociation on the Pt electrode, which is followed by electron and proton transfer, or whether the first reduction step happens before O-O bond cleavage. To answer this question, the information about the site and the configuration of O_2 adsorbed on a Pt electrode surface is critical. Three plausible types of O_2 adsorption were proposed by earlier researchers, viz., Griffith (on-top, double bond) [20], Pauling (on-top, single bond) [21], and bridge[22] as shown in Figure 2.6.

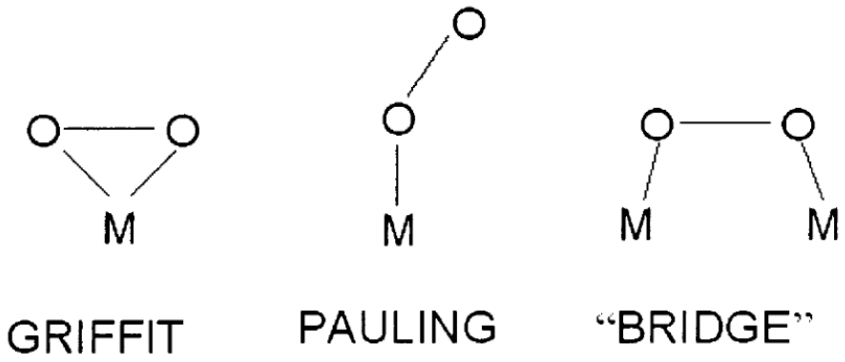

Figure 2.6 Models of O_2 adsorption on electrode surfaces.

These types of bonding are well-known in inorganic coordination chemistry. They are also expected to occur for platinum-group metals. According to these models, O_2 interacts with electrode surfaces in the following ways:

O_2 interacts with a single substrate atom (Griffith model) by forming a bond mainly between its σ orbitals and the empty d_z^2 orbitals of the metal surface atom, and by forming a σ back-bond from the partially filled d_{xy} or d_{yz} metal orbitals to the antibonding π* orbitals of O_2 [23].

End-on adsorption through a single type bond (Pauling model), in which the σ orbital of O_2 donates electron density to an acceptor d_z^2 orbital on the metal.

Bridge model, with two bonds with two sites, which was proposed by Yeager principally for the reaction on platinum-group metals.

Oxygen adsorption on clean metal surfaces at the metal-gas interface has been the subject of numerous studies in order to establish the nature of the chemisorption, the bond strength, and the structure of the absorbed layer. Oxygen adsorbs in molecular form at low temperatures, while dissociative adsorption on platinum-group metals occurs. From the experimental point of view, there is evidence of dissociative adsorption of O_2 on platinum at temperatures in the range of 150-300K [24, 25], but there is no evidence for the direct cleavage of O-O bond at the electrochemical interface.

Now, it is well established that the reaction rates of oxygen reduction on different low-index Pt surfaces are structure-sensitive, due to structure-sensitive adsorption of intermediates ($O_{2,ads}$ and OOH_{ads}) and species (OH_{ads}). From these reasons, the adsorption of OH is probably the most important in the process. In 0.05 M H_2SO_4, the ORR rate increases in the sequence Pt(111) < Pt(100) < Pt(110) [26]. An exceptionally large deactivation is observed on Pt(111) surface due to the blocking and electronic effect of strongly adsorbing (bi)sulfate anion.

In perchloric acid solution, the variation of activity at 0.8-0.9 V is relatively small between the three low-index surfaces, with the activity increasing in the order Pt(100) < Pt(110) ≈ Pt(111) [27]. A similar structural sensitivity is observed in 0.1 M KOH. In the potential range where oxygen reduction is under combined kinetic-diffusion control (E > 0.75 V), the activity increases in the sequence of Pt(100) < Pt(110) < Pt(111) [28]. The decrease of Pt(100) surface activity is related to the high affinity of (100) sites for the hydroxyl adsorption, leading to a lack of active centers for O_2 adsorption because the Pt(100) surface is highly covered by OH_{ads}. Markovic *et al.* suggested O_2 reduction should be proportional to the part of the surface not covered by hydroxyl species ($1-\Theta_{OH}$) [29].

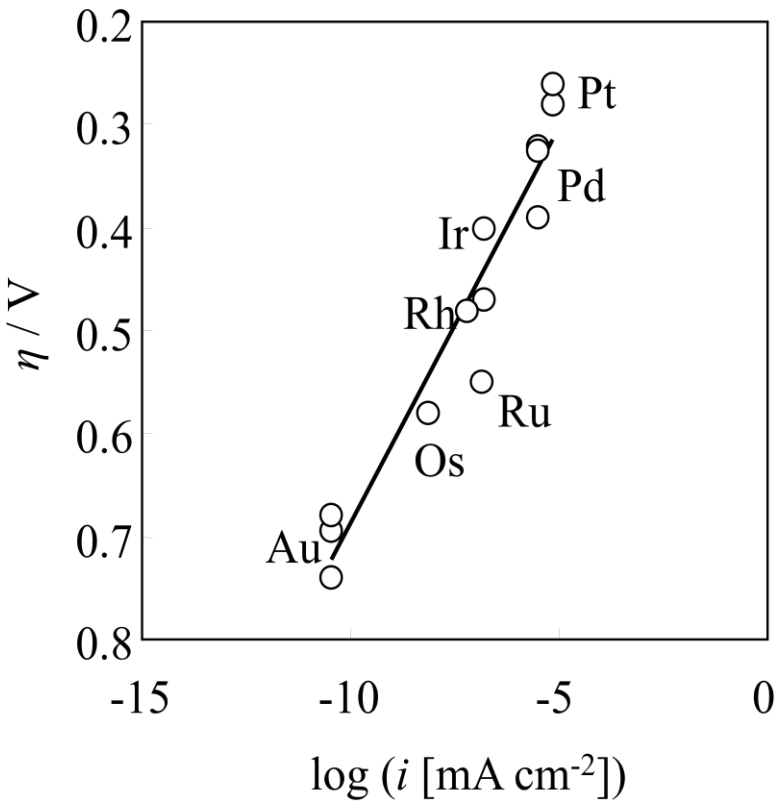

Figure 2.7 Relationship between logarithm of current density (i) [30] and overvoltage (η) [31] for ORR on various noble metal cathodes. The current density was obtained at 0.8 V vs. RHE in 85% H_3PO_4 (25°C). The overvoltage was obtained at i=10-5 A cm-2 in 0.5 M H_2SO_4 (25°C).

2.3 Catalysts materials for the ORR

2.3.1 Platinum and platinum-alloys materials

Platinum has been the best catalyst for over 170 years since Christian Friedrich Schoenbein and William Robert Grove reported the first study on fuel cells [2]. However, this does not mean that platinum is the optimal material for fuel cell application, because of its fundamental catalytic property limitations, very high cost, limited reserves, and political issues. Therefore a future commercialization of PEMFCs cannot be based solely on platinum-based technologies. It is essential to develop a catalyst having higher ORR catalytic activity and high cost-performance for the future.

Figure 2.7 summarizes the works of D.S. Gnanamuthu and A.J. Appleby, the relationship between the logarithm of current density (i) [30, 32] and overvoltage (η) [31] for ORR on various noble metal cathodes. The current density was obtained at 0.8 V vs. RHE in 85% H_3PO_4 (25°C). The overvoltage was obtained at i=10^{-5} A cm^{-2} in 0.5 M H_2SO_4 (25°C). The figure indicates that palladium has the second highest catalytic activity in the acid media after platinum. Palladium potentially has a high catalytic activity for ORR in acid media, as we can see in these studies.

Toda *et al.* have conducted studies on thin layers of sputter-deposited PtNi, PtFe, and PtCo, and reported extremely high-activity enhancement factors of 10–20 [33]. However their baseline of Pt activity is 10 times lower than what other researchers reported in their literatures. It is likely that there is significant doubt on the validity of their measurements. Paulus *et al.* have reported kinetic studies on high-surface-area Pt-based alloy catalysts such as Pt/Vulcan, PtNi/Vulcan, Pt_3Ni/Vulcan, PtCo/Vulcan, Pt_3Co/Vulcan, and $PtRh_3Fe_7$/C [34, 35]. The catalytic activity gains for ORR were compared to the activity of bulk Pt. Specific activity enhancements of a factor of 2-4 compared to bulk Pt were found in these studies. In addition to this work, E.R. Gonzalez *et al.* have reported catalytic activity enhancements by alloying with -Co, -Ni, and Fe. These studies support that alloying with 3d-transition metal such as Co, Ni, and Fe enhances the electrocatalytic activity for ORR of platinum electrode.

The fact that palladium potentially has a high catalytic activity for ORR and that alloying with the 3d-transition metal enhances the catalytic activity of the base element suggests that alloying can also enhance the electrocatalytic activity of palladium electrode. Palladium-Cobalt binary alloy was selected in this study, since Pd-Co exhibited the best ORR catalytic activity between Co, Cr, Ni in our previous study [3]. Pd-based alloy with other 3d-transition metals will be studied as my future works.

2.3.2 Palladium and palladium-alloy materials

The first Pd-based alloy catalysts for PEMFC application were presented by O. Savadogo *et al.* in 2004 [3]. Pd-Co alloy (72:28) and Pd-Cr alloy (70:30) prepared by sputtering method has shown enhanced electrocatalytic activities to Pd electrode. Following up on this work, the second paper

by O. Savadogo *et al.* presented the performance of Pd-Co alloy (78:22 and 72:28), Pd-Ni (64:36), and Pd-Cr (61:39) [36].

V. Raghuveer *et al.* prepared carbon-black-supported Pd-Co-Mo (70:20:10) catalysts by use of a conventional borohydride reduction method in 2005 [37] and carbon-supported Pd-Co-Au catalysts by use of the conventional reduction method and a reverse microemulsion method in 2006 [38]. The former showed a particle size of 15-35 nm, and the latter a size of 15-46 nm. The mean particle sizes increase by increasing the heat treatment temperature for both cases.

The work of M.H. Shao *et al.* in 2006 synthesized Pd monolayer catalysts on different single-crystal substrates; Ru(0001), Rh(111), Ir(111), Pt(111), and Au(111) [39]. The electrocatalytic activities increase in the order of Pd/Ru(0001) < Pd/Ir(111) < Pd/Rh(111) < Pd/Au(111) < Pd/Pt(111). They also prepared Pd-Co (2:1) carbon-supported catalysts having broad size distribution up to 92 nm, peaking at 18-20 nm.

L. Zhang *et al.* prepared carbon-supported Pd-Co alloy nano-particle catalysts (67:33) [40] by using the co-impregnation method with $NaBH_4$ as reducing agent, and obtained fine particles in the range of 4.8-14 nm. The catalyst with a mean particle size of 4.8 nm is relatively small – for example, the size of a commercial carbon-supported Pt catalyst widely used for fuel cell applications is in the range of 2 to 4 nm – however the particles are not well dispersed on carbon supports (as seen TEM image). More particles would be located more closely in the case of a nano-scale carbon-supported catalyst with a metal loading of 20 wt %.

One of the most interesting parts of this study was presented by K. Lee *et al.* in 2006 [41]. Pd-Co (60:40), Pd-Ni (64:36), and Pd-Cr (61:39) prepared by the sputtering method were developed for the Direct Methanol Fuel Cell (DMFC) cathode, and have the function of ORR selectivity in the presence of methanol. DMFCs have two very serious technical problems, i.e., low catalytic activity of the anode electrocatalyst and methanol crossover in which the methanol permeates from the anode compartment through the electrolyte membrane to the cathode compartment [42, 43]. The latter is concomitant with cathode performance losses due to the formation of mixed potentials on the cathode electrocatalysts as well as the decrease in the efficiency of methanol utilization. Approximately one-third of the available energy is lost at the cathode and the other one-third is lost at the anode [44]. It has been found that these kinds of Pd-based alloy catalysts

have high potential to be used as a DMFC cathode because of their very low activities for methanol oxidation.

X. Wang *et al.* managed to obtain fine Pd-Co particles on carbon support having a mean particle size in the range of 1.8 to 11.2 nm by use of a modified polyol reduction method [45]. The catalyst of Pd_2Co/C heat-treated at 500°C successfully obtained relatively smaller particles, however, the particles are non-uniformly distributed, and the presence of particles larger than 10 nm seems to be higher than the given histogram. Since 300 particles have been randomly counted for the histogram, more smaller particles may be found in another TEM images, but the TEM images of all other catalysts, especially the one for the smallest particle size of 1.8 nm, are needed to support the fact that this modified polyol reduction route makes it possible to obtain nano-scale alloy catalysts with a narrow particle size distribution and a good dispersion on a support, as the authors mentioned in the report. Yet the modified polyol method is interesting for nano-scale Pd-Co catalyst preparation, and this method was examined by H. Liu and Manthiram in 2008 [46].

L. Zhang *et al.* investigated the effects of reducing agents in the co-impregnation method following up on their previous work [47]. The method with ethylene glycol (EG) has provided the smallest mean particle sizes in the range between 4.6 and 6.6 nm, even though the catalysts were heat-treated at 700°C. The one with $NaBH_4$ yielded a mean particle size in the range of 4.6 to 13.3 nm, and the last one with HCHO was in the range of 8.8 to 22.9 nm. The catalysts prepared by EG and $NaBH_4$ with no heat treatment show well-distributed fine particles. In contrast, many aggregated particles can be seen for the one by HCHO.

J. Mathiyarasu and K.L.N. Phani studied carbon-supported Pd-Co-based ternary alloy (Au, Ag, Pt) nano-catalysts prepared by use of a reverse microemulsion method for methanol-tolerant oxygen reduction cathode materials having a mean catalyst particle size in the range of 18 to 29 nm [48]. Pd-Co-Pt ternary alloy catalyst shows the best ORR catalytic activity among them, and all of these Pd-based ternary alloys including Pd-Co binary alloy perform very low-oxidation activities for methanol.

The work on thin-layer catalysts of Pd-Co binary alloy prepared by use of electrodeposition has been reported by Tominaka *et al.* in 2008 [49] and is consistent with the work of K. Lee – the Pd-Co alloy possesses high methanol tolerance.

H. Liu and A. Manthiram prepared carbon-supported Pd-Co (7:3) alloy catalysts by use of a modified polyol reduction method, a co-impregnation method, and a reverse microemulsion method, and heat treated them at various temperatures up to 900°C [46]. The mean particle sizes of the catalysts obtained from the method are 2.4 nm (as prepared), 3.5 nm (250°C), 4.1 nm (350°C), 5.3 nm (500°C), 7.7 nm (700°C), and 12.5 nm (900°C). These values are very attractive for fuel cell applications; however, no experimental evidence such as XRD data or TEM images are provided in this report.

The work of X. Li *et al.* has, as reported in many studies above, reported the tolerance to methanol of carbon supported Pd-Co alloy catalysts [50]. The unique point of this study was to use ($NH_4F + Pd^{2+}$) complex, and they managed to obtain fine particles on carbon support in the range of 2.6 to 3.8 nm.

The deposition-precipitation (DP) method was studied by Yu-Chen Weivia *et al* [51]; various compositions of catalysts were prepared at different pH-value environments (pH 9-13) and at various temperatures (390 or 620K). They found the optimized pH value and temperature were pH=9 and T=390K, and the prepared catalyst has a particle size distribution of 3.6±0.6 nm. The mean particle sizes of the alloy were increased by increasing the pH value.

S. Zuluaga *et al.* reported density-functional-theory-based computational studies of the electronic structure of the Pd-Co alloy electrocatalysts and energetics of the oxygen reduction reaction [52]. The calculations were performed for the (111) surfaces of pure Pd, $Pd_{0.75}Co_{0.25}$ and $Pd_{0.5}Co_{0.5}$ alloys, as well as of the surface segregated $Pd/Pd_{0.75}Co_{0.25}$ alloy. They found the hybridization of dPd and dCo electronic states to be the main factor controlling the electrocatalytic properties of $Pd/Pd_{0.75}Co_{0.25}$. Namely the dPd–dCo hybridization causes a low-energy shift of the surface Pd d-band with respect to that for Pd(111). This shift weakens chemical bonds between the ORR intermediates and the $Pd/Pd_{0.75}Co_{0.25}$ surface, which is favorable for the reaction. Nonsegregated $Pd_{0.75}Co_{0.25}$ and $Pd_{0.5}Co_{0.5}$ surfaces are found to be too reactive for ORR due to bonding.

Only a few methods have so far been developed for preparing carbon-supported Pd-Co nano-scale catalysts. The ultrasonic spray reaction method for PEMFC applications was developed in our previous study [53]. It focused on the catalyzed gas diffusion electrode (GDE); a slurry consisting of platinum precursor and carbon supports was sprayed by use of an ultrasonic piezoelectric transducer. The generated mist was continuously heated at various temperatures in a

mixture of hydrogen-nitrogen gas flow through a tube reactor. The platinum precursor was reduced to solid Pt nano-particle on the carbon supports, and the synthesized catalyst was directly filtered on a gas diffusion layer.

The commercial carbon supported platinum catalysts have the optimized particle size of φ2-4nm for the best performance for the ORR. Utilization of high active surface area catalyst is an essential factor for commercialization of PEMFC with the new electro-catalyst, but none of the studies done before were able to successfully obtain the Pd-Co fine particles as comparable as the existing carbon supported Pt catalyst. The main objective of this study is to establish the method to obtain fine Pd-Co particles on carbon support.

Table 2.3 Previous work on Pd-Co electrocatalysts for ORR.

Year	Author	Synthesiz method	System	Composition atm.	Support	Heat treatment /°C	Mean particle Size /nm	Particle size definition	Reference
2011	S. Zuluaga and S.Stolbov	DFT calculation							[70]
2008	X. Li et al.								[68]
		Reduction of (NH_4F+Pd^{2+})complex with $NaBH_4$	Pd	1	XC-72	as prepared	3.9	TEM	
			Pd:Co	11:1			3.8		
				4:1			3.4		
				2:1			2.9		
				1:1			2.6		
2008	H. Liu and A. Manthiram								[69]
		modified polyol reduction	Pd:Co	7:3	Vulcan XC-72R	as prepared	2.4	TEM	
						250	3.5	XRD	
						350	4.1		
						500	5.3		
						700	7.7		
						900	12.5		
		co-impregnation with modified polyol reduction				350	7.9		
						700	7.7		
		reverse microemulsion				700	7.9		
						500	8.0		
2008	S. Tominaka et al.								[67]
		electro-deposition	Pd:Co	66:34	Au	as prepared	-	-	
				75:25					
2007	J. Mathiyarasuz and K. L. N. Phani								[66]
		reverse microemulsion	Pd:Co	89:11		500	29 ± 2	TEM	
			Pd:Co:Au	79:12:9		500	23 ± 2		
			Pd:Co:Ag	80:11:9		500	26 ± 2		
			Pd:Co:Pt	80:12:8		500	18 ± 2		
2007	L. Zhang et al.								[65]
		impregnation with $NaBH_4$	Pd	1	Vulcan XC-72R	-	6.7	XRD	
		co-impregnation with $NaBH_4$ as reducing agent	Pd:Co	67:33		as prepared	4.6		
						300	8.6		
						500	10.2		
						700	13.3		
		co-impregnation with EG as reducing agent		63:37		as prepared	N/A		
						300	4.6		
						500	6.4		
						700	6.6		
		co-impregnation with HCHO as reducing agent		73:27		as prepared	8.8		
						300	12.7		
						500	21.7		
						700	22.9		
2007	W.E. Mustain								
		electro-deposition	Pd	1	Au	as prepared	-	-	
			Pd:Co	80:20					
				75:25					
				67:23					
				50:50					
		capping polymer method	Pd:Co	1:3	unsupported	550	-	-	

Table 2.1 Previous work on Pd-Co electrocatalysts for ORR (*continued*).

2007	X. Wang et al.							[63]
	modified polyol reduction	Pd	1		as prepared	4.5	XRD	
		Pd:Co	4:1			3		
			3:1			2.8		
			2:1			2.6		
			3:2			2.2		
			1:1			1.8		
			2:1		400	6.4		
			2:1		500	7.9		
			2:1		600	9.6		
			2:1		700	11.2		
2006	K. Lee et al.							[59]
	sputtering	Pd	1	GC	as prepared	-	-	
		Pd:Co	60:40					
		Pd:Ni	64:36					
		Pd:Cr	61:39					
2006	L. Zhang et al.							[58]
	-	Pd	1	-	as prepared	6.8	XRD	
	co-impregnation with $NaBH_4$ as reducing agent	Pd:Co	67:33	Vulcan XC-72R	as prepared	4.8		
					300	9.0		
					500	10.8		
					700	14.0		
2006	M.H. Shao et al.							[57]
	commercial	-	-	Pd (111)	-	-	-	
	deposited by galvanic displacement	Pd	monolayer	Ru(0001) Ir(111) Pt(111) Au(111) Rh(111)	as prepared			
	impregnation with H_2 as reducing agent	Pd	1	Vulcan XC-72	900	-	-	
		Pd:Co	2:1			peak at 18-20 nm	TEM	
2006	V. Raghuveer							[56]
	conventional borohydride reduction	Pd:Co:Au	84:07:09	Vulcan XC-72R	as prepared	-	TEM	
			78:21:01		500	-		
			68:23:09		900	46		
	reverse microemulsion		79:14:07		500	15		
			73:17:09		650	18		
			71:21:08		750	28		
			72:20:08		900	35		
2005	V. Raghuveer et al.							[55]
	-	Pd	1	Vulcan XC-72R	-	-	-	
	co-impregnation with $NaBH_4$ as reducing agent	Pd:Co:Mo	70:20:10		500	24	XRD	
			70:20:11		700	31		
			70:20:12		900	42		
2004	O. Savadogo et al.							[9]
	Sputtering	Pd	1	GC	as prepared	-	-	
		Pd:Co	78:22					
		Pd:Co	72:28					
		Pd:Ni	64:36					
		Pd:Cr	61:39					
2004	O. Savadogo et al.							[8]
	Sputtering	Pd	1	GC	as prepared	-	-	
		Pd:Co	72:28					
		Pd:Cr	70:30					

CHAPTER 3 OBJECTIVES AND METHODOLOGY

The primary purpose of this study was to develop new cathode catalysts for polymer electrolyte membrane fuel cells for power generation system. The main objectives of the project were;

- to optimize the chemical composition of Palladium-Cobalt electro-catalysts which exhibit the highest the ORR activity,
- to investigate electrochemical properties of the Pd-Co electro-catalysts and observe their correlations to the ORR activity,
- to fabricate carbon supported Pd-Co alloy catalysts which can be directly applied for the PEMFC cathode

The first study on Pd-based alloy materials was demonstrated by the research group of O. Savadogo in 2004 for PEMFC cathode catalysts [3]. The Pd-base binary alloys with three 3d-transition metals; Pd-Co alloy (72:28) and Pd-Cr alloy (70:30) were prepared by sputtering method and all of these catalysts exhibited enhanced electrocatalytic activities to Pd electrode. Especially, Pd-Co alloy catalyst exhibited the highest catalytic activity for the ORR between these alloys. Therefore Pd-Co binary alloy catalyst was focused in this study. However since Pd-Co alloy is very new as a cathode material for PEMFCs, fundamental aspects on the Pd-alloy electro-catalysts were not deeply studied yet, so their physical, chemical and electrochemical properties were needed to be investigated. In addition, it's very important to cover from fundamental research to applications to contacts with industry. Hence not only the fundamental studies, but also catalyst synthesis process for carbon supported Pd-Co alloys which allows to use for the PEMFC cathode materials directly need to be developed.

Pd-Co thin film electrodes were fabricated by RF sputtering technique to optimize the chemical composition of the electrodes for the ORR activities. One important advantage of sputtering as a deposition technique is that the chemical composition of the multi-element thin film can be easily control, regardless of melting point or vapor pressure. In general, sputtered electrodes are not used for the PEMFC cathode or anode materials because the electrode surface area becomes much smaller than carbon supported electro-catalysts which are commonly used. However fabrication of carbon supported catalysts with new materials can be very difficult and many parameters during the catalyst synthesis process need to be optimized. To avoid time and money

consuming, various compositions of electro-catalysts were synthesized by the sputtering technique as a primary work of developing Pd-Co catalysts. This process is efficient way to develop new electrode materials for electrochemical systems. In addition, electrochemical properties of Pd-based materials were not deeply studied until now. The knowledge of studying the properties is very important for new electro-catalysts design towards the active materials of the ORR.

Fine catalyst particles supported on high surface area carbon powder are essential factor to apply the catalyst as the PEMFC cathode materials for the commercialization. However as described in the former chapter of literature review, none of the studies done before were able to successfully obtain the Pd-Co fine particles which are comparable with the existing carbon supported platinum catalyst (φ2-4nm). Therefore the establishment of the catalyst synthesis method for Pd-Co fine particles are required to use the catalyst for PEMFCs. Since most of the classical methods which have been used for carbon supported Pt catalyst synthesis have been studied for the Pd-based alloy catalyst synthesis, but none of them can be the practical method to obtain the Pd-base alloy fine particles, I've developed a completely new technique which has never been used for the carbon supported catalysts synthesis for PEMFC. A catalyst maker with ultrasonic piezo-electric transducer was built in our laboratory to carry out an catalyst synthesis process of ultrasonic spray reaction method. This technique was firstly developed by Uematsu et al. [4-6] to prepare fine composite catalysts of Ni/TiO_2, Ni/Al_2O_3, Pd/ZrO_2, Ru/Al_2O_3, and Ru/TiO_2. The technique demonstrated excellent results for preparing multi-components composites on oxide catalyst supports. The obtained catalysts had strong interaction among the components because the composites were formed from droplets of a homogeneous solution in a quick-heating process. This technique was very unique and never been studied for PEMFCs, I've investigated the feasibilities of the technique for the catalyst synthesis process in this study.

Firstly, carbon supported Pt catalysts were synthesized by using the ultrasonic spray reaction system built in our laboratory. The objective of this study is to obtain carbon supported fine Pd-Co particles, but since this is the first study of using the ultrasonic spray reaction method for carbon supported catalyst synthesis, it is very important to compare between the resulted catalysts and existing commercial catalysts and observe if fine catalyst particles can be formed on carbon catalyst support by using the new technique which is comparable to the commercial one. The optimization of parameters; heating temperature, gas flow rate, processing time, concentration of

catalyst precursors and many others for the process is also needed to obtain the catalysts which exhibit high catalytic activity for the oxygen reduction reaction. For these reasons, carbon supported Pd-Co catalysts were not firstly prepared by new spray reaction technique, but carbon supported Pt catalyst were synthesized and studied as a preliminary work towards achieving the main objective of this study.

As the final step - this is the goal of this study - the developed ultrasonic spray reaction technique for the carbon supported catalysts was applied for carbon supported Pd-Co catalysts synthesis. Fundamental electrochemical properties and optimized composition of Pd-Co electro-catalysts were obtained by using the Pd-Co thin films in the first section of this study and the new technique by using ultrasonic spray reaction was developed in the second section. These two studies were combined in the last section to achieve the goal of this study. I've tried several conventional methods to synthesize fine Pd-Co particles on carbon support in our laboratory, however obvious improvements on the resulted catalysts were not found from the catalysts presented in the literature review. The obtained catalyst particles were agglomerated and were not uniformly and highly dispersed on carbon support as same as the commercial carbon supported Pt catalyst. I found the classical methods which have been used for the synthesis of carbon supported Pt catalysts are not appropriate technique to prepare carbon supported Pd-based alloy catalysts. Therefore if an effective method of preparing nano-scale Pd-Co alloy catalyst on carbon support is able to be established in this study, it contributes significantly to an industrial fabrication process of Pd-based electro-catalysts and would be a key technology for the commercialization of PEMFCs with Pd-Co alloy catalysts in the future.

CHAPTER 4 SUMMARY OF THE WORKS

This thesis consists of the following three publications;

1. New Method of Preparation of Catalyzed Gas Diffusion Electrode for Polymer Electrolyte Fuel Cells Based on Ultrasonic Direct Solution Spray Reaction,
2. Electrochemical investigation of Pd-Co binary alloy for oxygen reduction reaction in acid medium
3. Comparison of Physico-chemical Properties of Pd-Co Alloy Catalysts for PEM Fuel Cells synthesized by Ultrasonic Spray Reaction Method.

4.1 New Method of Preparation of Catalyzed Gas Diffusion Electrode for Polymer Electrolyte Fuel Cells Based on Ultrasonic Direct Solution Spray Reaction

K. OISHI and O. Savadogo

Laboratory of New Materials for Energy and Electrochemistry

École Polytechnique de Montreal, Montreal, Quebec H3C 3A7, Canada

Published in Journal of New Materials for Electrochemical Systems, vol 11 (2008), no 4, pages 221-227

4.1.1 Introduction

The polymer electrolyte membrane fuel cell (PEMFC) is an interesting alternative power generating systems for mobile and stationary applications due to its high power density at lower temperatures [54-56]. The high cost and low reliability of PEM fuel cell are the limiting factors for their commercialization. Platinum based catalyst is one of the major contributors to the performance limitation and high cost. This same technical barrier also exists in other air-cathode fuel cells. Therefore, development of high performance, low cost catalyzed electro-catalysts is critical to fuel cell commercialization.

The membrane electrode assembly (MEA) is at the center of the PEFC that generates an electrical current from fed hydrogen, which is oxidized at the anode, and oxygen, which is reduced at the cathode, by electrochemical reactions. The MEA is typically consisted of a proton exchange membrane (PEM), an anode catalyst layer, cathode catalyst layer, and a gas diffusion layers (GDL). The PEM is sandwiched between the catalyzed anode gas diffusion electrode (GDE) and the catalyzed cathode GDE, and then pressed or not to together at high temperatures (145°C) and pressures. The catalyst layer is ether applied to the membrane or GDL before assembly. The GDL can be a porous carbon fiber paper or cloth, in the fuel cell supports that the reactant gas effectively diffuses to each catalyst particle surfaces. It has an additional function that transports the electron from and to the catalyst. The GDL also helps water management to hold an appropriate amount of the water inside and hydrate the membrane. . Efforts are made to increase the heterogeneous electron-transfer kinetics and the utilization of Pt, for example, by modification of carbon supports [54] and novel platinum deposition techniques as Impregnation method, Precipitation method, Surfactant-stabilized method and sputtering [55-58] to increase the effective catalytic area (thereby decreasing the loading of precious metal).

The classical method to prepare a GDE is shown in Figure 1and involved at least seven steps from the preparation of the mixture solution to the drying of the slurry on the GDE. This corresponds to a lot of steps and each of them must be improved if we want to get an optimized GDE. Consequently, when the number of the GDE preparation steps is reduced, its time of fabrication will be reduced and the optimization parameters will be easier to determine. On the other hands, efforts are also under way to increase the heterogeneous electron-transfer kinetics and the utilization of Pt, for example, by modification of carbon supports1 and novel platinum deposition techniques2 to increase the effective catalytic area (thereby decreasing the loading of precious metal [59-69]. For the purpose of obtaining structures which could facilitate high performance catalysis, new effective preparation methods are required. A conventional impregnation method, which is unlikely to lead to high dispersion of gold, has been reported to fail to produce active catalysts.

The spray techniques have been firstly successfully developed by Uematsu et al. [4-6] to the preparation of fine composite catalysts. They developed also a solution spray pyrolysis reaction method (SPR) [70, 71], a suspension spray reaction method (SSP) [72], and hybrid methods of spray impregnation [4]. As for metal-supported catalysts, they have prepared Ni/TiO_2, Ni/Al_2O_3,

Pd/ZrO_2, Ru/Al_2O_3, and Ru/TiO_2, and have demonstrated that the spray reaction techniques are excellent methods to prepare multi-component composites which allow strong interaction among the components because they lead to high catalytic activities due to the improved support effects and/or promoter effects [6]. The enhancement of the strong interaction between the catalyst and the support is related to the characteristic nanostructure of the fine composites being formed from droplets of a homogeneous solution in a quick-heating process. For example, for supported gold catalysts, they used USPR (Ultrasonic solution spray reaction) methods to synthesise the nano-particle catalyst for gas phase reactions. It's also called spray decomposition, mist decomposition, or spray pyrolysis [71, 73]. However until now this technique has not been used for direct fabrication of catalyzed GDE.

Very recently [74] we have shown that MEA based on catalyzed gas diffusion electrode can be fabricated using ultrasonic method. Prior to fabricating the electrodes, carbon supported catalyst is prepared by the wet impregnation method. A quantity of platinum precursor (ex. $H_2PtCl_6 \cdot 6H_2O$) is introduced in de-ionized water containing the carbon support (ex. Vulcan XC-72R). After 60 min of ultra-sonication, a reducing agent (ex. HCHO, $NaBH_4$, H_2 gas) is introduced to the suspension with vigorous stirring at room temperature or higher. The solid phase is recovered by filtration, and washed copiously with de-ionized water. The recovered solid was then dried at 40°C overnight. The carbon supported catalyst is mixed with de-ionized water and/or organic solvents. Then Nafion® solution is added to the mixture, followed by ultrasonication to form catalyst slurry. The catalyst slurry is screen-printed onto GDL to form the catalyzed GDE. The GDE is finally dried at 60°C. In this study, we develop a new technique for catalyzed GDE preparation using an ultrasonic direct solution spray reaction method. This new method has the potential to provide shorter time of catalyzed GDE manufacturing. The preparation process properties and performance of catalyzed GDE will be shown.

4.1.2 Experimental

4.1.2.1 Catalyzed GDE preparation

The outlines of the preparation of the catalyzed gas diffusion electrode using the classical method and the ultrasonic method are shown in Figure 4.1. As shown, the ultrasonic method involved less steps and preparation than the classical method. The process of the fabrication of the

catalyzed GDL is indicated in the following. A solution for the carbon supported platinum catalyst, which was sprayed on GDL, was prepared by using a hydro chloroplanic solutions ($H_2PtCl_6 \cdot 6H_2O$) (Aldrich) as a precursor and carbon support (Vulcan XC72, Cabot) as catalyst support were pre-dispersed in an aqueous solution of ultra pure water (Milli-Q, 18.2 M Ω cm) and ethanol in the ratio of 150 ml of water for 20 ml of ethanol. The solution is mixed by using the ultrasonic dispersion device for 60 minutes at 50^{o}C. The homemade catalyst fabrication system with an ultrasonic spray device was used for the catalyzed GDE fabrication as shown in Figure 4.2. The slurry containing catalyst precursor and supports was introduced into the spray chamber as shown in Figure 4.2-(2) and was sprayed with the ultrasonic unit -(1) (HM-2412, 2.4 M Hz, Honda Electronics Co., Ltd) which was placed at the bottom of the chamber. The generated mist was continuously heated in various temperatures in a reducing agent flow (3 vol.% H_2 - 97vol.% N_2 mixture gas, Air Liquide, Canada) through a quartz tube reactor -(3) (length: 1.0 m, inner diameter: 35 mm) under the suction by a vacuum pump -(10). The stream of the hydrogen gas in the mixture gas, inside of the tube reactor, chemically reduced the platinum precursor to solid platinum particles, and these particles were heat treated by a furnace which was placed around the tube reactor. The mean flux of the mist was about 0.1 m s^{-1}, the average time of the reaction and heat treatment during passing through the tube reactor was around 10 seconds. The synthesized carbon supported catalysts were directly deposited on a gas diffusion layer -(5) (Toray, Japan) which was placed on the top end of the tube.

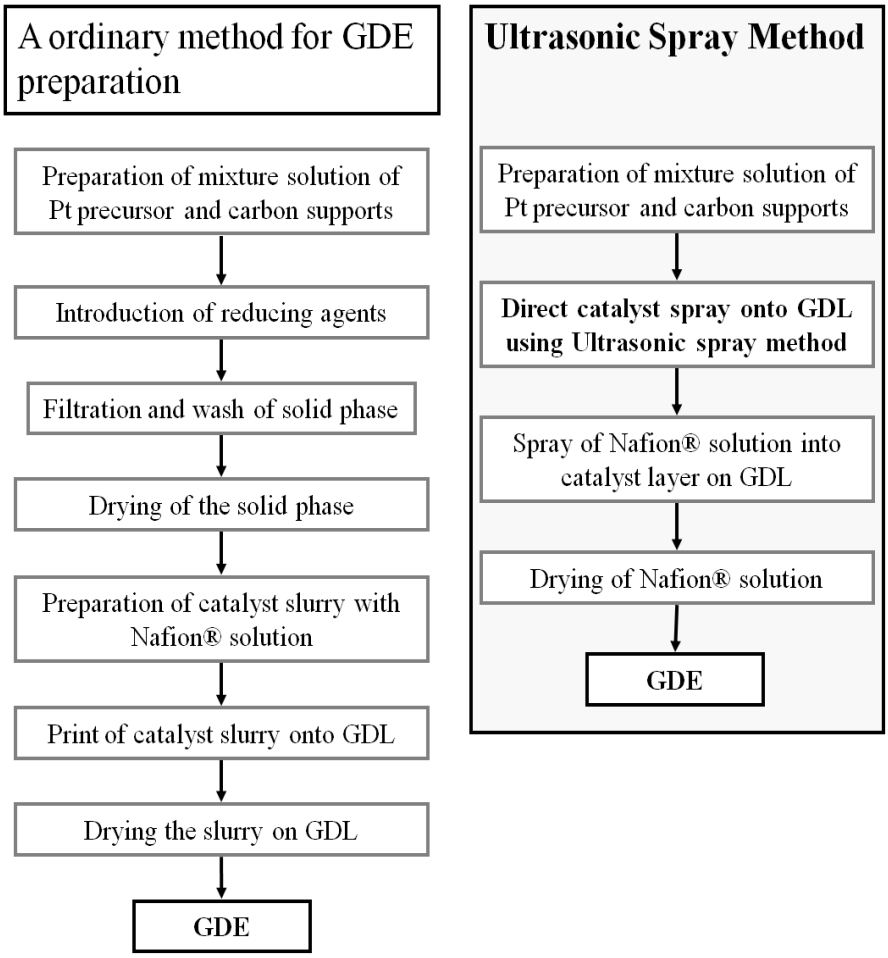

Figure 4.1 Outlines of two different techniques for the gas diffusion electrode preparation; one of the ordinary methods and the ultrasonic spray method.

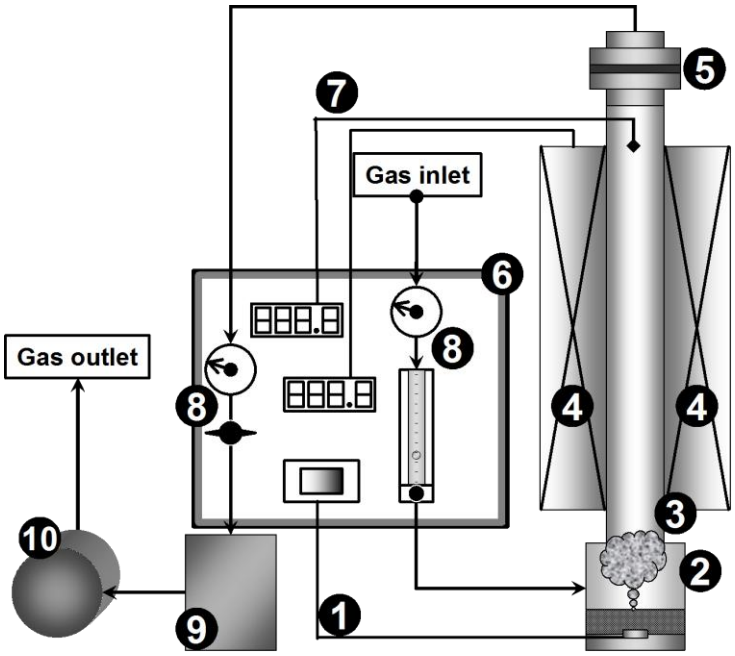

Figure 4.2 Schematic of Home made catalyst maker with ultrasonic spray device. (1)-ultrasonic spray unit and control system, (2)-solution spray chamber, (3)-quartz tube reactor, (4)-furnace, (5)-filter (gas diffusion layer), (6)-main control panel, (7)-thermocouple located at top-end of the heater, (8)-pressure gaze and control unit, (9)-cold trap system, (10)-heavy duty vacuum pump.

4.1.2.2 XRD analysis

The structural characterization of the carbon supported catalyst of prepared catalyzed GDE was determined by X-ray diffraction methods. A Philips X'Pert PRO X-ray diffractometer equipped with graphite monochromatized Cu K_α (λ=154.2 pm) as radiation source was used for this purpose. Normal diffraction patterns were obtained in the range of 10-110° with a scan speed of 0.2° min^{-1}. Slow scans were also applied to determine the angle at which maximum intensities were observed, and the accuracy in recording the angle was 0.005°. All the recorded diffractograms were compared to those of the "Standard X-ray diffraction powder patterns" [75] to identify different peaks and orientations. After identifying all the diffraction peak positions in the X-ray diffract grams obtained from normal scans, a slow scan of 0.1° min^{-1} was taken within ±2° and every peak angle. The interplanar spacing, *d*, was calculated using the peak position θ of Pt(111) peak by the use of the Bragg's relation.

$$d = \frac{\lambda}{2\sin\theta_{\mathrm{Pt(111)}}}$$

Eq. 4.1

4.1.2.3 TEM analysis

Transmitted Electron Microscopy (TEM) (JEM-2100F, JEOL) was used to obtain the morphology of the catalysts, including the particle size of the Pt nanoparticles. To prepare samples for TEM analysis, a suspension, in ethanol, of the carbon supported catalysts was transferred onto the surface of the microscope Cu grid coated with an amorphous carbon film. TEM images of the catalysts were taken at an operation voltage of 200 kV. The particle size, taken as the equivalent diameter of the measured area of the particles, was then obtained. The mean particle size $\overline{D}_{\mathrm{TEM}}$ was obtained by measuring the diameter of a sufficient number of particles to ensure a good statistic sampling and calculated according to the following equation [76].

$$\overline{D}_{\mathrm{TEM}} = \frac{\sum f_i d_i^{\,3}}{\sum f_i d_i^{\,2}}$$

Eq. 4.2

where f_i is the occurrence frequency of the particles with a diameter of d_i in the sample.

4.1.2.4 Electrochemical Measurement

The catalysts were electrochemically characterized with a common three-electrode electrochemical cell including the Platinum mesh counter electrode and RHE as a reference electrode. Each synthesized catalyzed GDE was cut into a sheet of 1 cm^2 area and used as working electrodes. Working electrodes were analyzed by slow linear potential scan voltammetry from +1100 to +400 mV at 0.5 mV s^{-1} using a PAR EG&G 273A potentiostat. The electrolyte was a 0.5 M H_2SO_4 solution prepared from concentrated sulfuric acid with deionized water. The oxygen gas (Air Liquide, Canada) was bubbled through the electrolyte for 60 minutes before the scan.

4.1.3 Results and Discussion

Figure 4.3 (a) and (b) show respectively the photos of the GDE surface after and before the preparation of the catalyzed GDE fabricated from the direct solution spray reaction method. Figure 4.4 shows the scanning electron microscopic (SEM) image of the cross section of the GDE. These figures clearly indicate that the catalyst layer is well defined on the surface of GDE. In addition, the sprayed catalyst powder including carbon supports doesn't suppress the gas flow channels of the GDE, because the catalyst layer stay just on the top surface of the GDE and was not packed into the flow channels. Since the carrier gas keeps flowing through the layer during the direct filtration process for the GDE synthesis, gas flow channels are formed in the catalyst layer. It may provide better gas flow attribute.

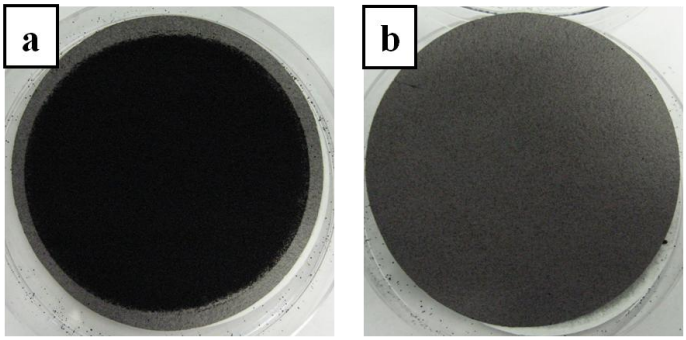

Figure 4.3 Photos of the synthesized GDE by use of the direct solution spray reaction method; a and b are after and before the synthesis, respectively.

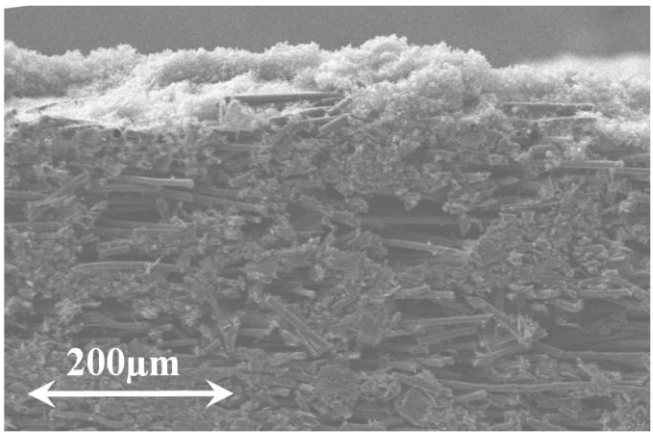

Figure 4.4 Cross section scanning electron microscopic (SEM) image of a GDE synthesized by use of the direct solution spray reaction method

The crystalline structure of the catalyst was obtained using powder XRD. Figure 4.5 shows the X-ray diffraction pattern of the catalysts on the catalyzed GDE synthesized at different temperatures between 300 and 700°C. Peak positions for the Pt metal are indicated by Miller indices. The peaks are consistent with face-centered cubic (fcc) structure for Pt, namely, the peaks at ca. 40°, 46°, 67.5°, 81.5°, and 86° were reflected from Pt(1 1 1), Pt(2 0 0), Pt(2 2 0) Pt(3 1 1), and Pt(2 2 0) planes, respectively. These diffractograms indicate that well crystallized Pt nano particles were well formed during the fabrication process. Figure 4.6 shows the variation of the *d*-spacing of Pt(111) with the synthesis temperature in the tube reactor during the catalyst preparation. The *d*-spacing of Pt(111) was calculated from the Bragg relation. It can be seen that the *d*-spacing increased with the synthesis temperature in the catalyst reactor.

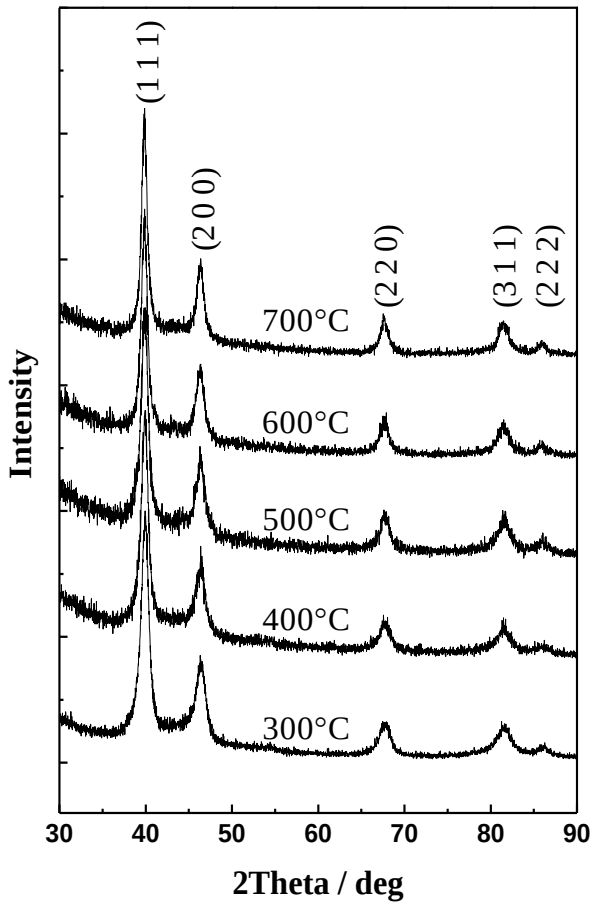

Figure 4.5 X-ray diffraction pattern of the catalysts on GDE synthesized at 300 through 700°C. Peak positions for Pt metal are indicated by Miller indices.

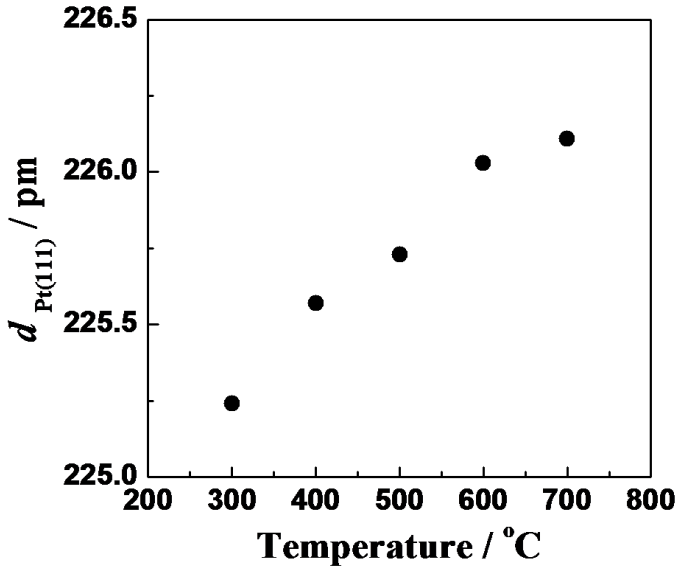

Figure 4.6 Relation between thermal treatment temperatures in the tube reactor during catalyst synthesis and d-spacing of Pt(111).

The Pt particle size and their distribution of Pt/C catalysts were characterized from TEM analysis. The TEM micrographs and the histograms of the Pt nano-particle size distributions are shown in Figure 4.7 and Figure 4.8, respectively. From the figures, the mean particle size of the Pt nano-particles increases from 3.4 nm when the catalyst reactor is at 300ºC to 4.7 nm when the reactor is at 700 ºC. From these results, it can be seen that the small Pt nano-particles are obtained if low synthesis temperatures are used for the catalyst preparation.

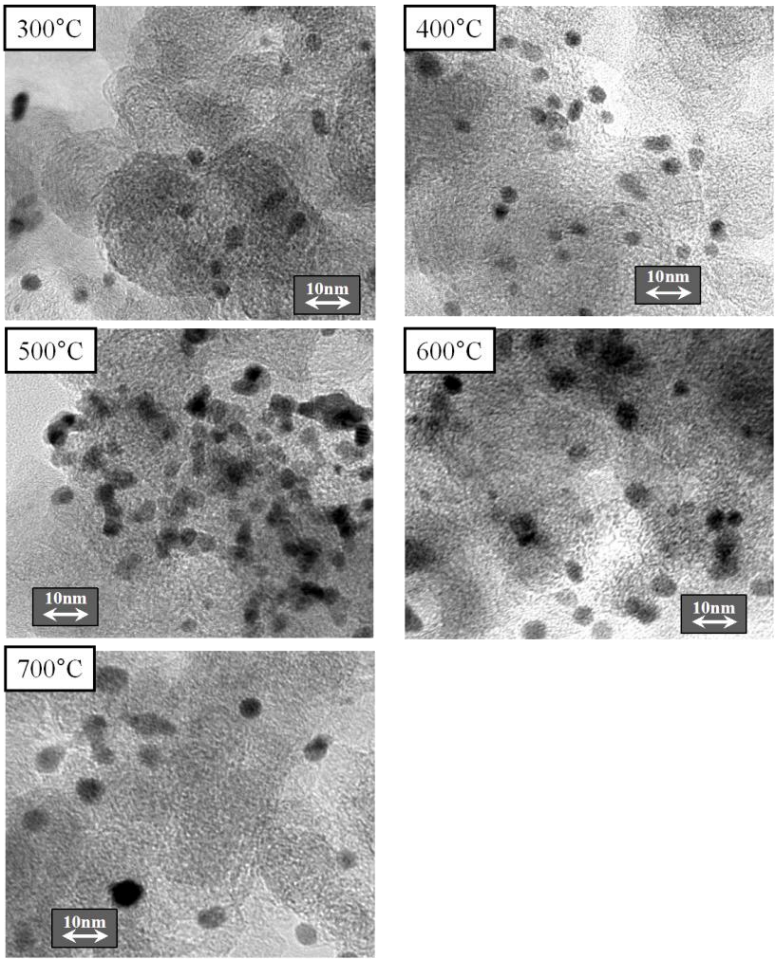

Figure 4.7 TEM micrograghs of Pt nano-particle size on carbon supports.

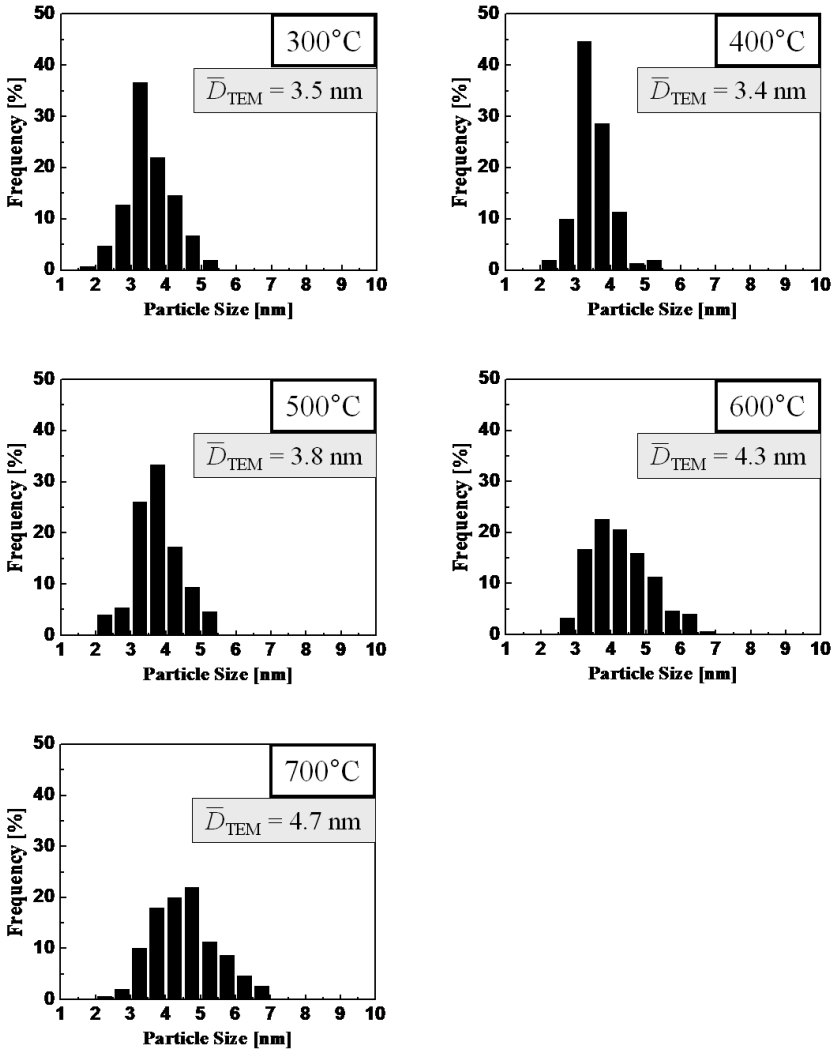

Figure 4.8 Histograms of Pt nano-particle size distributions and mean particle sizes obtained from TEM micrographs.

The oxygen electro-reduction properties of the catalyzed GDE are be obtained from Figure 4.9 The current is normalized with the unit weight of Pt which was determined by Inductively Coupled Plasma Mass Spectroscopy (ICP-MS) analysis. The electrode prepared from catalysts lower temperature exhibited higher specific current density. The variation of the current at various potentials with $\left(\overline{D}_{TEM}\right)^2$ ($\overline{D}_{TEM}$ is the mean particle diameter) are shown in Fig.10. The ---linear variation of the specific current density with $\left(\overline{D}_{TEM}\right)^2$ is shown. This is an indication that

the electrocatalysts activities of the electrodes are of course proportional to the catalysts surface area because in these potential region, the effect of the diffusion current is negligeable. Figure 4.10 shows the relation between the *d*-spacing of Pt(111) and the normalized current with Pt mass and $\left(\overline{D}_{\mathrm{TEM}}\right)^2$. This normalization was carried out to maximize the effect of *d*-spacing of Pt(111) and to minimize the particle size effect. From this figure, we can conclude that the Pt catalysts having a lower *d*-spacing can obtain a higher catalytic activity for the oxygen reduction reaction. These results are strong indications than the ORR is more related to surface properties than volume properties, accordingly the shape of the catalyst particle may have an important role on the ORR activity.

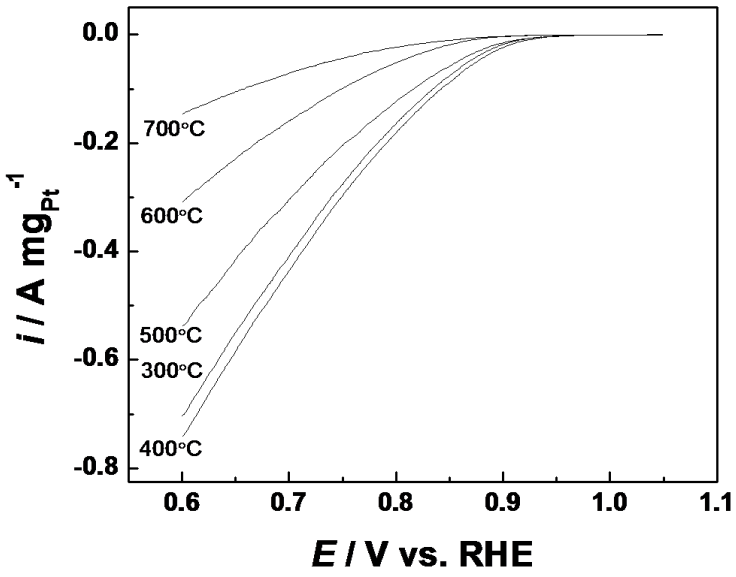

Figure 4.9 Oxygen electro-reduction properties of GDEs synthesized at different temperatures. The currents are normalized to Pt unit mass.

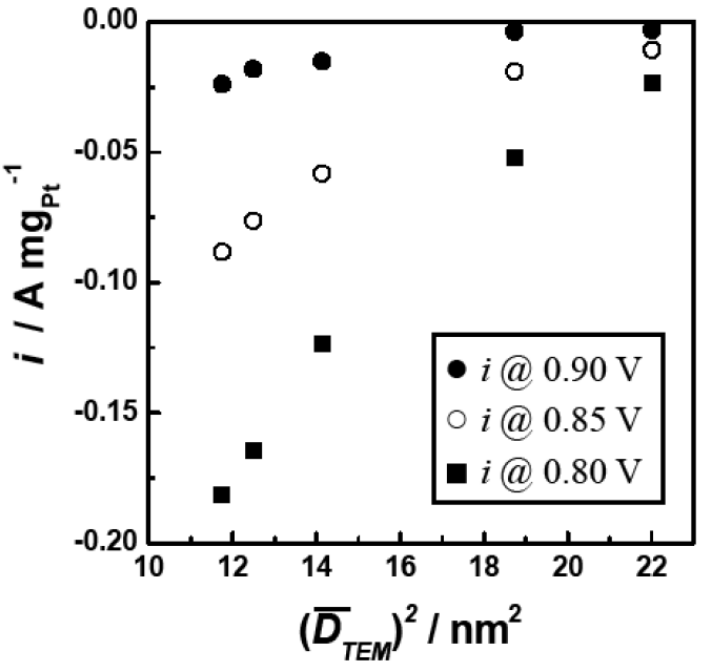

Figure 4.10 The current at various potentials and its dependence to a squaring value of the mean particle diameter.

4.1.4 Conclusions

We developed a homemade vertical furnace catalyst maker where ultrasonic spray device was used for the catalyst preparation . This allows the fabrication of carbon supported catalysts with smaller particle sizes than those of the catalyst made by the classic processes. This new method can be also used for the in-situ deposition of the catalyst on a carbon cloth or paper during the same process without altering the catalyst properties. This approach we just introduced opens the ways on in-situ catalyzed electrodes fabrication. This study showed the potential of ultrasonic solution spray reaction method for direct preparation of the gas diffusion electrode. From micrographic results, we conclude that this method is suitable for the application of catalysed GDE or carbon paper preparation and. It was shown that the properties of the catalysts changed with the synthesis temperatures. Interatomic *d*-spacing were varied on the heat treatment temperatures and it caused the differences of the electrocatalytic activity for the oxygen reduction reaction.

4.2 Electrochemical investigation of Pd-Co thin films binary alloy for oxygen reduction reaction in acid medium

K. OISHI and O. Savadogo

Laboratory of New Materials for Energy and Electrochemistry

École Polytechnique de Montreal, Montreal, Quebec H3C 3A7, Canada

Submitted to the Journal of Electroanalytical Chemistry, on April 2nd, 2012

4.2.1 Introduction

Proton Exchange Membrane Fuel Cell (PEMFC) using hydrogen or light hydrocarbons as fuels is considered as a key technology for next electric power generation system. But the high cost of the Pt catalyst involved in the core components of PEMFCs and the low content of the Pt metal reserve in the earth are most of the limitations of the mass production of this technology. Accordingly, the development of non-platinum materials with promising catalytic activity for the oxygen reduction reaction (ORR) is necessary if we want to overcome these limitations towards mass production. Current research efforts are focused on the development of catalysts to overcome this limitation through improved activities. Among various metals, nano-size palladium-alloy based catalysts have attracted particular attention.

Pd-alloys catalysts have been introduced by our group as an ORR cathode electro catalyst used in the electrochemical devices [3, 36, 77-82]. It was shown that depending on the alloying element and its composition, Pd-alloy catalysts exhibit excellent activity for the ORR in acidic media. Others groups [38, 83-85]confirmed these interesting results. We have also shown that the binary Pd-M alloys exhibited better electro catalytic activity for the ORR than pure Pd and in some cases comparable to that of Pt. The highest electro catalytic activity was observed for alloy composition *ca.* 60 -70 at% Pd in all Pd alloys [37]. These specific properties are due to their special interaction with oxygen and high selectivity for water formation in a multielectron charge transfer process [41, 86-89]. Some recent studies have reported that the combination of palladium with other metals, such as Ni [90-92], Fe [92], Sn [93], Rh [94] and Cu [92, 95-97], synthesized by different methods, i.e., co-impregnation

[92] , colloidal synthesis [96], nanotubular mesoporous PdCu by galvanic replacement [97] and electrodeposition of PdCu [49], substantially improves the activity and stability of the alloys. This is attributed to the formation of bimetallic interactions which are stronger than a single metal-oxygen (M-O) interaction, thus generating a bimetallic material with greater stability. An interesting study reported that PdCu prepared using magnetron sputtering equipment [98] also presented enhanced catalytic activity for the ORR. Therefore Pd Co based electrocatalysts as a PEMFC cathodes are one of the interesting subject in fuel cell development [3, 41, 79, 80, 99, 100]. In these various investigations, it was shown that the catalytic activity of the Pd_xCo_y PEMFC system changes, of course, with the Co content in the alloy. CoPd*x* (*x* = 1, 2, 3, 4, 5 and 9) electrocatalysts for the ORR were studied in a 5 cm^2 single cell PEMFC. The magnitude of the observed current density is nearly and order of magnitude higher for the $CoPd_3$ catalyst in the kinetic region compared to the CoPd and $CoPd_9$ and more than double at large overpotentials [101]. It was shown that, the activity of the electro catalysts changes in the following order: CoPd < $CoPd_2$ < $CoPd_3$ > $CoPd_4$ > $CoPd_5$ > $CoPd_9$. The results have shown clearly that a nominal palladium-cobalt atomic ratio of 3:1, Pd_3Co, exhibits the best performance [41, 101]. It was also shown that the Pd_3Co catalytic activity is close to the commercial Pt catalyst. On the other hands, the ORR on Pd_3Co has low activation energy, 52 kJ/mol, and a Tafel slope of approximately 60 mV/decade. Based on these kinetics parameters, it was concluded that the rate-determining step of the mechanism of the ORR on this catalyst might be a chemical step following the first electron transfer step and may involve the breaking of the oxygen bond. The electrocatalytic activity of the ORR on carbon supported Pd_4Co nano particle has been also studied and it was shown that this alloy offers higher ORR performance than Pd/C catalysts [86]. The ORR on electrodeposited Pd-Co alloys have been studied [102]. Polycrystalline electrodes were prepared by electrodeposition on a polycrystalline gold substrate using a dual ligand approach at room temperature [103]. The electrodeposits showed performance for the ORR similar to polycrystalline platinum under identical conditions, despite an observed 50 mV cathodic shift in the peak potential. Carbon supported $CoPd_3$ electrocatalysts also showed high catalytic activity for oxygen reduction in a 5 cm^2 fuel cell test.

The electro-catalytic activity of the electrodeposited $Pd_{66}Co_{34}$ and $Pd_{75}Co_{25}$ electro catalysts were investigated for the ORR [102], and it was concluded that both the Pd-Co alloys were almost the same structure, i.e. a solid solution of ca. Pd_7Co_3 with Pd-skin, and also confirmed to possess

comparable activity in oxygen reduction to Pt (potential difference at 1.0 μA cm^{-2} was 0.05 V). It was claimed that the high catalytic activity and a good selectivity for the ORR Pd-transitional metal alloys might be attributed to an electronic stabilization of the added alloy element [37, 41]. But more fundamental studies are needed to elucidate the high effect of the electrocactilytic activity of Pd-alloys for the ORR.

We developed a homemade vertical furnace catalyst maker [53, 74] where ultrasonic spray device was used for the catalyst preparation. This allows the fabrication of carbon supported catalysts on a gas diffusion layer with smaller particle sizes than those of the catalyst made by the classic processes. This new method can be also used for the in-situ deposition of the catalyst on a carbon cloth or paper during the same process without altering the catalyst properties. It was shown that the properties of the catalysts changed with the synthesis temperatures. Inter-atomic d-spacings were varied on the heat treatment temperatures and it caused the differences of the electrocatalytic activity for the oxygen reduction reaction. The effect of the heat treatment on the electro catalytic properties of the ORR on Pd-Co alloy has been studied recently [104]. The optimal heat-treatment temperature was found to be 700 °C for the lower concentration of Co in Pd–Co/C alloy, while 300°C was the best condition for the high Co content. Before heat-treatment, a Pd–Co/C alloy at room temperature showed a weak ORR activity. After heat-treatment, the Pd–Co/C alloys showed enhanced ORR activity than pure Pd/C catalyst. This is because the ORR activity is dependent on the surface composition as well as the particle size. Therefore, the heat treatment condition should be individually optimized on the alloy composition.

The high activity of Pd and Pd-Co catalysts for the ORR, as well as their high degree of tolerance to ethanol make them suitable candidates for Direct Alcohol Fuel Cell applications [41, 105-107]. Therefore their catalytic ORR activities in methanol tolerance [41, 102, 108-110], ethanol [99] and ethylene glycol [100] have been studied and it was shown that the Pd based electro catalysts can be potential candidates for cathode materials for PEMFCs. As for methanol tolerance, cell-voltage was not influenced by addition of 1 mol dm^{-3} methanol to the oxidant solution. Until now the fundamental understanding of this behaviour is not elucidated.

Based on these results on Pd-alloys for the ORR, there is a need to improve the fundamental understanding of the electro-catalytic properties of palladium alloys for the ORR in acid medium.

This will help to develop comparison tools to Pt-alloy electro catalytic properties and identify new families of electro catalysts for the ORR. Fundamental interpretations of these results will help to improve the understanding in the electro catalytic properties of these materials for the ORR and to identify new families of electrocatalysts for this reaction. In addition, the various electrochemical properties related of the electro-catalysts prepared by physical vapor deposition technique were not well examined.

In this paper, we will synthesize various compositions of Pd-Co alloys catalysts prepared by RF magnetron sputtering technique and determine their oxygen reduction reaction performance in acid medium. We will correlate these electro catalytic properties to the physicochemical and basic electrochemical properties of these interfaces. This will help to draw new understandings in fundamental electrocatalysis.

4.2.2 Experimental conditions

4.2.2.1 Chemicals

Glassy carbon (GC) rod (GC20, 5.2mm diameter) was obtained from Tokai Carbon Ltd., Japan. 4N purity of Pt, Pd and Co targets were purchased from Furuuchi Chemical Co, Japan for physical vapor deposition. Semiconductor grade acetone, semiconductor grade hydrofluoric acid and deionized water were used to clean GC substrate prior to deposition. Nitrogen and oxygen gases were purchased from Air Liquide, Canada (5N8 purity).

4.2.2.2 Electrode preparation and characterization

All electrodes, Pt, Pd and various compositions of Pd and Co alloys were synthesized by physical vapor deposition technique. GC substrates were polished using a series of silica slurries (1.0, 0.15 and 0.05 μm) in water to obtain mirror finished surface. Prior to deposition, the substrates were cleaned by acetone followed by 5% hydrofluoric acid and de-ionized water.

Pt, Pd and Pt-Co binary alloy catalyst layers were deposited using Ar plasma in a RF magnetron sputtering system equipped with 50 mm diameter targets under Ultra High Vacuum (UHV). These magnetron cathodes were driven by independent Radio-Frequency (RF) power supplies with impedance matching boxes, which permits to control ionization rate respectively. Prior to the sputtering process, RF power of 200 W was applied for 5 minutes to remove oxides and

contaminations on the top surface of targets and discharge conditioning, on the condition slide shutter is closed. The power supply connected to Pd target was set at 20W and the other connected to Co target was varied to control ionization rate and compositions of films. Prior to the condition slide shutter opens, run sputtering process for 5 minutes to stabilize the ionization state. The deposition time was 20 minutes. The temperature of the deposition substrates was controlled at 573 K. All cleaning and deposition processes were carried out in clean room to avoid contaminations.

The surface compositions of alloy samples were determined by Auger electron spectroscopy (AES). A cleaning procedure was done by repeating of Ar sputtering to obtain carbon and oxygen-free surface.

4.2.2.3 Electrochemical analysis

The electrochemical measurement was performed by using a Princeton Applied Research potentiostat 273A in a three electrodes configuration. GC substrate with deposited layer was immersed into the 0.05 M H_2SO_4 electrolyte (Fluka, TraceSELECT®, prepared with ultra pure water Milli-Q UV, 18.2 MΩ) as a working electrode. Large area platinum mesh was used as a counter electrode and a trapped hydrogen electrode (THE) [111] as a reference electrode. All potentials in this paper are quoted with respect to the reversible hydrogen electrode (RHE: ~0.00 mV vs. THE). Cyclic voltammetry (CV) was carried out under nitrogen purge at a scan rate of 50 mVs^{-1} over potential range of 0.05 to 1.2 V vs. RHE. Oxygen Reduction Reaction (ORR) activities were measured by using a conventional a rotating disk electrode (Pine Instruments) under oxygen purging at control temperature of 298.15 K at scan rate of 3 mVs^{-1} (Slow Scan Voltammetry: SSV). Rotation rate was controlled in the range of 900 – 3025 rpm.

4.2.3 Results and Discussion

Table 4.1 shows the elemental composition of the deposits measured by AES. The results show clearly that a wide range of controlled compositions (e.g. 0 to 84 atomic %) of cobalt in Pd, were obtained. The thickness of deposits was determined by mechanical profilometer and was in the range of 40-60 nm. For comparison Pt deposit was also synthesized in the same conditions and the same thickness range was obtained.

To understand the role of the possible redox reactions on the electrochemical reduction of oxygen, the cyclic voltammetric response of all the electrodes was analysed in the potential range between 0.05 and 1.2 V at 25^{o}C. Figure 4.11 shows CVs of various compositions of Pd-Co alloys, Pd and Pt electrodes, and selected CVs from Figure 4.11 are shown in Figure 4.12 The typical peaks related to hydrogen under potential deposition, oxide formation and oxide deformation were obtained on sputtered Pt electrode. Sputtered Pd electrode show a typical peak at 0.24 V which corresponds to the hydrogen under potential deposition, and also shows oxide formation and deformation peaks. The profiles for under-potential deposition and oxidation of hydrogen are very pronounced on the sputtered Pd-Co alloys a/o, indicating a strong H_{upd} region which is more visible than that even in the case of polycrystalline Pt. The behaviors of Pd-Co alloy electrodes of any compositions were totally different from the pure Pd electrode as same as described in our former study [36]. The large peaks observed in the case of the palladium alloy can be attributed to its high capability of the hydrogen adsorption and absorption properties of Pd [112]. Accordingly, these properties depend on the Pd-Co properties. In particular the large peak observed at the under deposition potential in the present work for Pd-Co alloys is due to the saturation of hydrogen in the Pd-Co films. Further, it may be considered that the addition of Co into Pd lattice is promoting the increase of the peak related to the under potential deposition of hydrogen. On the other hand as shown in Figure 4.12, the CV of sputtered Pd is completely different from both CVs of Pd-Co alloys and Pt, indicating that Pd has no significant oxide formation in the same potential range. The profiles for under-potential deposition and oxidation of hydrogen are very pronounced on the sputtered Pd_3Co a/o, indicating a strong H_{upd} region which is more visible than that even in the case of polycrystalline Pt.

Table 4.1 Chemical composition of the thin film electrode synthesized by PVD (atomic %)

Sample No.	**Composition (atomic%)**		**Label**
	Pd	Co	
Sample 1	100	0	Pd_{100}
Sample 2	75.31	24.68	$Pd_{75}Co_{25}$

Sample 3	64.90	35.10	$Pd_{65}Co_{35}$
Sample 4	50.07	49.93	$Pd_{50}Co_{50}$
Sample 5	41.75	58.25	$Pd_{42}Co_{58}$
Sample 6	16.00	84.00	$Pd_{16}Co_{84}$
Sample 7	(Pt 100%)		Pt_{100}

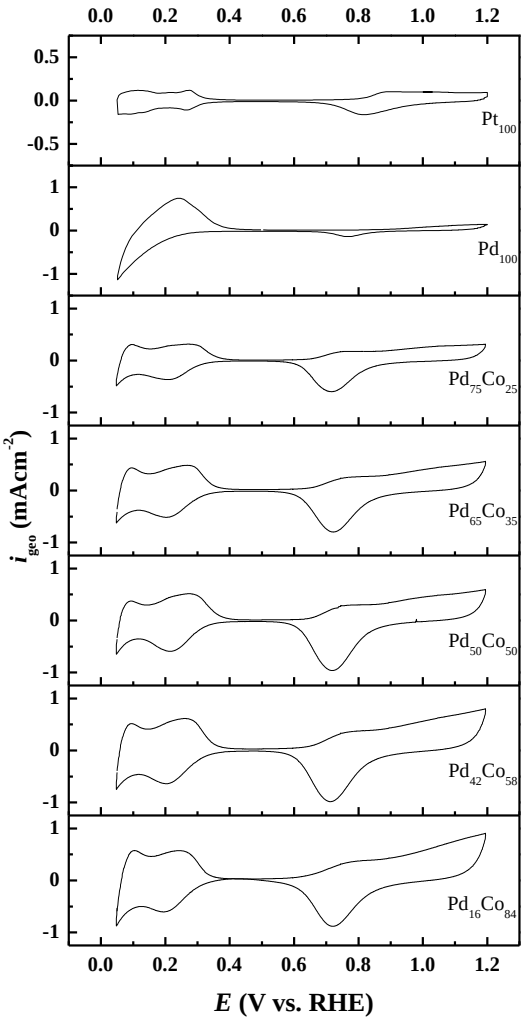

Figure 4.11 Cyclic voltammograms of Pd-Co alloy, Pd and Pt electrodes in 0.05M H_2SO_4 and nitrogen purge at 298.15K.

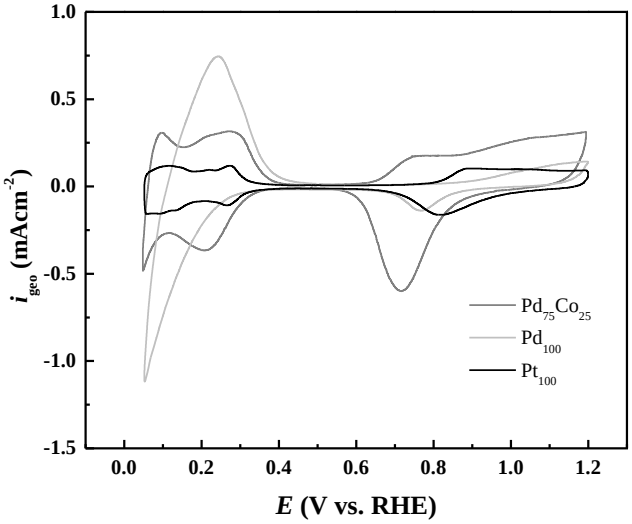

Figure 4.12 Cyclic Voltammograms of $Pd_{75}Co_{25}$, Pd_{100} and Pt_{100} electrodes in 0.05M H_2SO_4 and nitrogen purge at 298.15K.

Figure 4.12 shows that the current in the double-layer (between 0.3 and 0.8 V) is constant and the voltage of the oxide formation starts in the range of potentials (around 0.7-0.8 V) as that of polycrystalline Pt. No hysteresis was observed in the double-layer region, indicating that formation and reduction of oxides is not observed in this region. The reduction peak of the oxide observed at the CV of Pd-Co at around 0.72 V can be attributed to the alloy oxide formed at 0.8 V. This peak is not seen on the CV of Pd alone, and for the Pd-Co alloys the value of its potential is not related to the Co content. Accordingly the reason of this shift might be related to the change of the ORR activity with the presence of the cobalt in the alloy. It has also been verified experimentally that either the potential value of this peak does not change with time or the number of cycles, or both. Furthermore the sputtered Pd-Co alloy CVs are completely different from those of sputtered Pd alone. They never change and become more sputtered Pd-like. The shape of the CV of Pd-Co alloys is similar to those of Pt. Figure 4.13 shows the dependence of the hydrogen charges as a function of catalyst composition. Pd and Pd-Co alloys exhibit 3 to 5 times hydrogen charges contents when compared to those of Pt electrode. The hydrogen charges increase with the Co content in the alloy. The hydrogen charge increases from 1.5 to 2.5 mC.cm^{-2} when the cobalt content in the alloy increases from 20 to 84 atomic%. Figure 4.14 and Figure 4.15 show respectively the variations of the charges of the oxide formation and reduction with the cobalt content in the Pd-Co alloys. In both figures, the values of the charges increase with the Co

content in the Pd-Co alloy. The charge related to the oxide formation increases from 2 to 6 $mC.cm^{-2}$ when the Co content increases from 20 to 84 atomic% , and in the same range of the Co content the charge related to the oxide reduction increases from 1,75 to 3,5 $mC.cm^{-2}$. Accordingly, the most important variation of the charge with the Co content is obtained for the oxide formation. This can be attributed to cobalt presence in the alloy which may make easier the formation of the oxide when the Co content increases. The increase of the charges is an indication that respectively more hydrogen is adsorbed or more oxide is formed on the surface when the Co content increases. This will lead to an increase of the of the charges of the oxide reduction with Co content because the reduced oxide is those formed during the oxidation and which charges increases with the Co content. The increase of the Co content is more favorable for the oxide formation because the electro negativity of Co (1.9) is more favourable than Pd (2.2) for the oxide formation and the hydrogen adsorption at the Pd-Co alloys surface. The charges related to the reduction of the oxide increases with the Co content because as indicated above the oxide reduction is related to its formation. If more oxide is formed, so more will be reduced. The range or slope of the variation of the charges with the Co content for the oxide formation (from 2 to 6 $mC.cm^{-2}$) is different from those of the oxide reduction (1.75 to 3.5 $mC.cm^{-2}$.) for the same range of Co content (20 to 84%) because the oxidation-reduction process of the oxide on Pd-Co is not reversible or there are more complex processes involving the Co oxidation and its dissolution in the solution. The variation of the potential of the oxide formation peak and those of the oxide reduction will help to support this reaction.

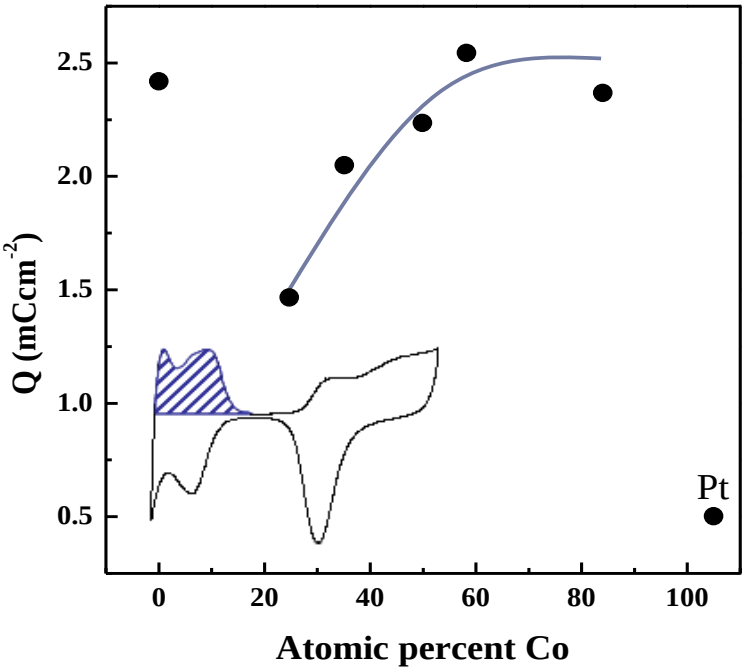

Figure 4.13 Dependence of the hydrogen charge as a function of electrode composition

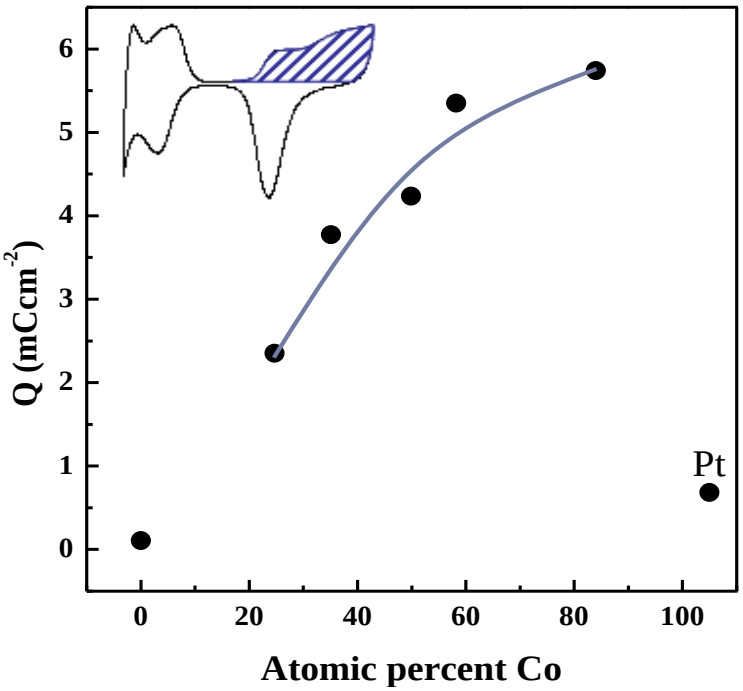

Figure 4.14 Dependence of the oxide formation charge as a function of electrode composition

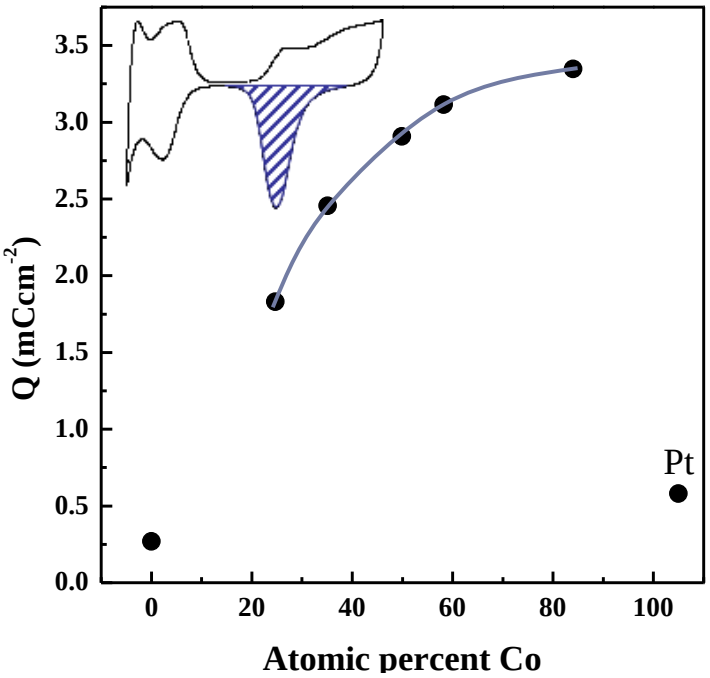

Figure 4.15 Dependence of the amount of oxide reduction as a function of electrode composition

Figure 4.16 shows the variation of the ratio of the charges of the oxide formation on those of the oxide reduction with the Co content. For comparison those of the Pd and Pt electro-catalysts, are respectively shown. The ratio of 1.1 for Pt indicates that for this electrocatalyst most of the oxide formed at higher potential range was reduced during the anodic potential sweep. On the other hand, this ratio increases with the amount of Co in Pd-Co alloy. Due to the low electro negativity of Co in comparison to Pd, Co oxide formation during its oxidation and electro oxidation might be the main factor in the increase of this ratio. Furthermore the increase of this ratio with the Co content is an indication that at high content of Co the fraction of the reduced oxide is less than those at low Co content. This is an indication that it might have two processes which is responsible of the charge formed during the cathodic sweep leading to the oxide formation current and the Co oxidation current which leads to the dissolution of the elemental Co into the electrolyte. In particular Co may play a sacrificial role by adsorbing some oxygen species which inhibit the ORR. These oxygenated species could compete with the adsorption of new oxygen molecule and gradually decrease the number of actives sites and consequently reduce the kinetics of the ORR. The ORR intermediates adsorption could be used later in this study to propose a mechanism scheme for the reaction on the Pd-Co electrode.

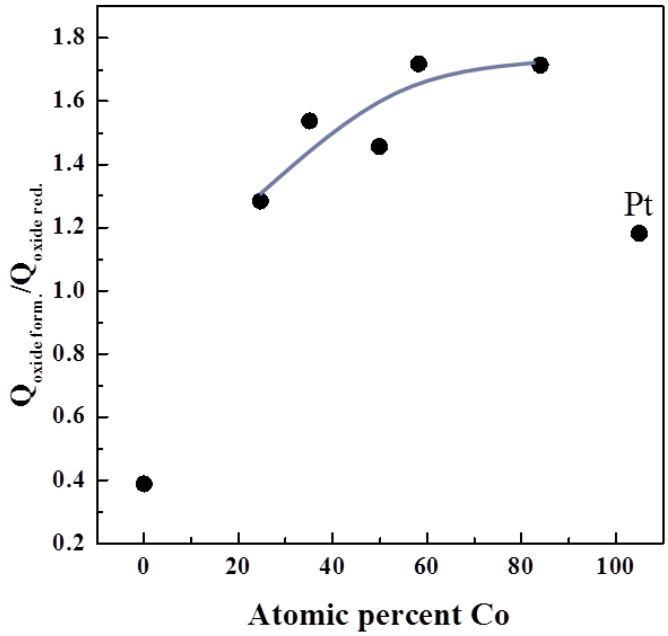

Figure 4.16 Dependence of the ratio Q (oxide formation)/(Oxide reduction) as a function of electrode composition

Figure 4.17 shows a dependence of the potential of the peak position of the oxide reduction as a function of electrode composition. The potential of the oxide reduction peak of Pd-Co alloys shifted to negative values when compared to those of Pd. The position of the oxide reduction peak does not change with the Co content (from 20 to 84%).Therefore the reduction peak can be assigned to the same oxide structure and composition for these Pd-Co alloys. In particular this behavior is related to the mixed palladium oxide and cobalt oxide formation at the surface of the Pd-Co alloy. The change in the potential of the oxide reduction peak with the Co content is not very important because as a thermodynamic parameter it may not change, of course, with the Co content but with the type of the oxide. A non perceptible variation of the potential peak might be an indication that the mixed oxide at the Pd-Co may not change significantly with the Co content.

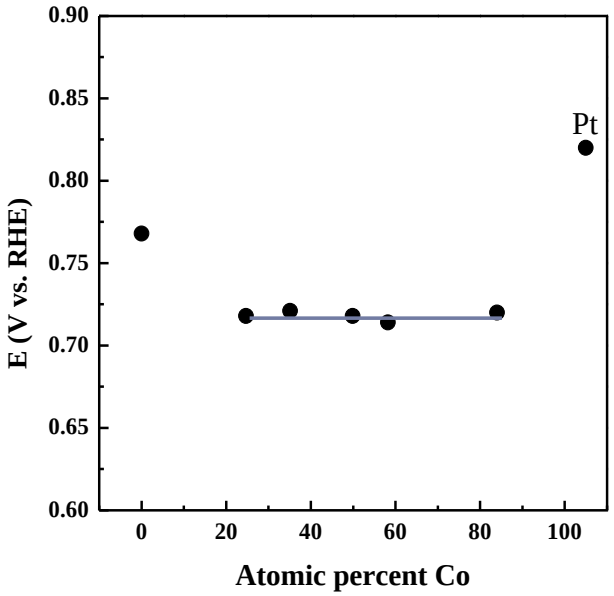

Figure 4.17 Dependence of the peak position of oxide reduction wave as a function of electrode composition

Figure 4.18 shows the slow scan (3 mV/s) polarization curves polarization curve of Pd-Co alloys, Pd and Pt electro catalysts respectively. These curves show that the Pt electro-catalyst exhibited better electro-catalyst (with higher onset potential than those of the other samples) for the ORR than the Pd and the Pd alloys electro-catalysts. The Pd electro-catalyst is less active for the ORR than all the other electro-catalyst. The activity of the Pd-Co alloys for this reaction depends, of course, of the Co content. Figure 4.18 shows that the polarization curves of $Pd_{42}Co_{58}$ and $Pd_{16}Co_{84}$ are nearly overlapped with those of Pd. In this range of the Co content in the alloy, no effects of the Co content on the ORR are seen. The polarization curves of the Pd-Co alloy with a Co content of 25% is more close to the Pt curve and exhibit the best performance for the ORR among the Pd-Co alloys electroatalysts.

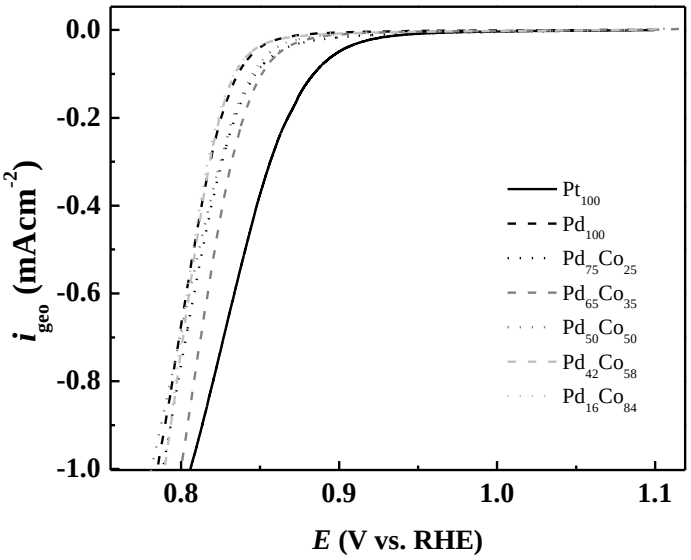

Figure 4.18 Polalization curve for ORR of Pt, Pd and various composition of Pd-Co alloy catalysts at 273.15 K.

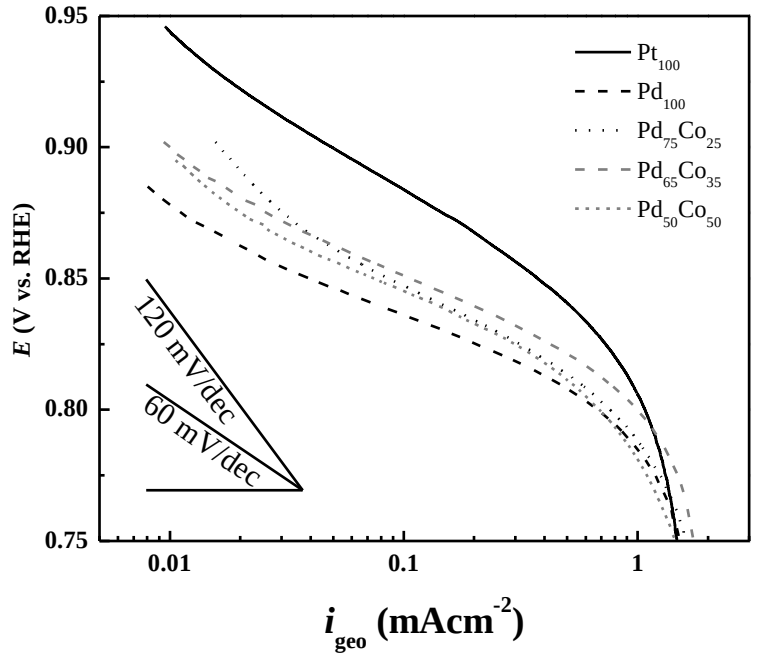

Figure 4.19 Tafel plot for the Pd-Co, Pd and Pt electrocatalysts at 273.15 K.

Table 4.2 Tafel slopes in low and high currenty density regions and calculated exchange currents densities of Pt, Pd and Pd-Co catalysts fabricated by sputtering method.

Sample	Tafel slope at low current density mV/decade	Tafel slope at high current density mV/decade	Exchange current density mA cm^{-2}
Pt	69	130	7.94×10^{-6}
Pd	47	80	3.72×10^{-9}
$Pd_{75}Co_{25}$	50	79	1.58×10^{-8}
$Pd_{65}Co_{35}$	48	80	1.10×10^{-8}
$Pd_{50}Co_{50}$	58	82	2.00×10^{-7}
$Pd_{48}Co_{58}$	38	68	3.02×10^{-11}
$Pd_{16}Co_{84}$	34	63	1.35×10^{-12}

The Tafel plots of the ORR at the high current density regions for sputtered Pd–Co alloys, Pd and Pt are shown in Figure 4.19. From these plots the values of the Tafel slopes at high current density and low current densities and the exchange current densities of the ORR on the various electro-catalysts of Pd-Co alloys including those of Pd and Pt are shown in Table 4.2. The Tafel slopes at low current and high densities of Pd and Pd-Co alloys are lower than those of Pt. The exchange current density of this reaction on Pt (7.94×10^{-6} mA cm^{-2}) is at least two orders of magnitudes higher than those on the Pd (3.72×10^{-9}ma.cm^{-2}) and Pd-Co alloys (in the range of 1.35×10^{-12} - 7.10×10^{-8} mA.cm^{-2}) which compositions are listed in Table 4.1. These values of the Tafel slopes and the exchanges current densities are in agreement with those obtained elsewhere for Pt and Pd [113] and for Pd-Co alloys [3]. As shown from Table 4.2 and Figure 4.19, the best catalyst is $Pd_{65}Co_{35}$ for which, the maximum current density is reached with 7.10×10^{-8} mA.cm^{-2}. This value remains relatively low compared to those reported for Pt (basically 7.94×10^{-6} mA cm^{-2}) [114]. We reported from Table 4.2, a 60 mV/dec for the Tafel slope for Pd-Co alloys electrodes at slightly high current densities.

The ORR kinetic process of the catalysts were also analyzed by a Koutecky-Levich plot. Figure 4.20 shows the slow scan voltammetry (3 mV/s) for ORR on $Pd_{65}Co_{35}$ at various rotating speed with RDE to determine experimental mass transfer limiting current. Figure 4.21 displays the Koutecky-Levich plot for ORR at potential of 0.4 V vs. RHE on the rotating disk electrode deposited with various composition of Pd-Co, Pt and Pd. It can be seen that the slope of all the plots are the same. The slope is directly related to the total number of electrons (*n*) involved in ORR according to the following equation:

$$\frac{1}{I} = \frac{1}{I_k} + \frac{1}{B\omega^{1/2}}$$

where I is the experimentally obserbed current, I_k is the kinetic current, B is equal to $0.62nFAC_{O_2}^{*}\left(D_{O_2}\right)^{\frac{2}{3}} v^{-\frac{1}{6}}$, ω is the rotation speed in rad s^{-1}, F is the Faraday constant 96485 $C.mol^{-1}$, A is the electrode are, $C_{O_2}^{*}$ is the concentration of oxygen at bulk (1.2×10^{-6} $mol.cm^{-3}$), D_{O_2} is the diffusion coefficient of oxygen (1.4×10^{-5} $cm^2.s^{-1}$) and v is the kinetic viscosity of the electrolyte (0.01 $cm^2.s^{-1}$) [115]. Theoretical value of four- and two- electron process are indicated in Fig 11 (straight lines) As described above, the ORR over Pt electrode surface proceeds through the four-electron pathway. The calculated value from the Koutecky-Levich plot for Pt was n=3.9, and 3.6-3.8 for the Pd and Pd-Co catalysts. Since all the plots presented the similar slopes with that of Pt, the ORR on Pd-Co/C electro-catalysts also proceeds through the four-electron pathway. This results show a good agreement with the results described above and some published elsewhere [39, 40, 116]. However considering the slightly lower value of *n* on Pd and Pd-Co electro-catalysts, it is reasonable to assume that the majority of the reaction proceeds via a four- electron pathway, however a small percentage of reaction proceeds via two-two electron pathway [34, 116, 117].

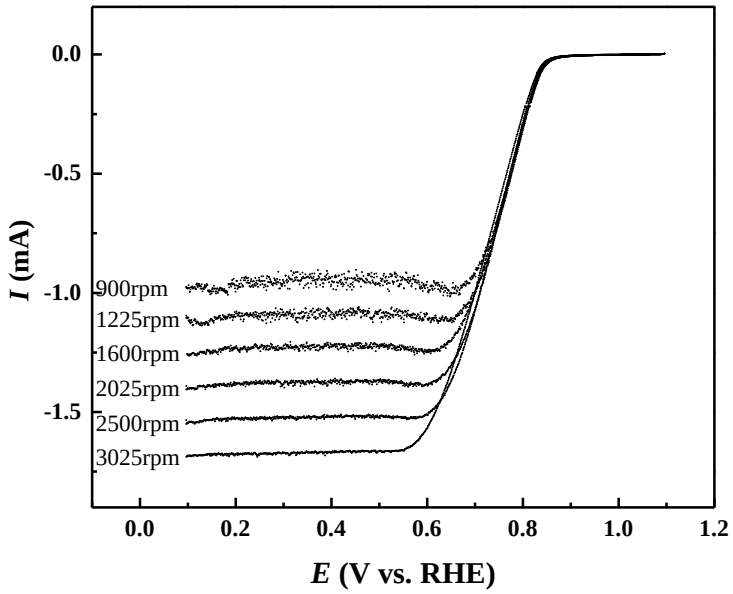

Figure 4.20 Slow scan voltammetry (3 mV/s) for the ORR on $Pd_{64}Co_{35}$ electrode at various rotation speed with RDE.

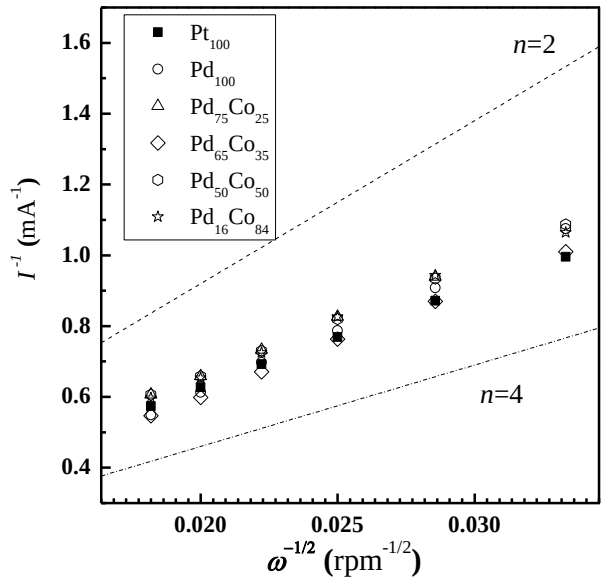

Figure 4.21 Koutecky–Levich plot of the Pd-Co, Pd and Pt electrocatalysts at 0.4V vs. RHE

Based on Tafel slope values and Koutecky-Levich plot, the possible mechanism of the ORR on Pd-Co alloys could be associative electrochemical adsorption of OOH_{ads} reaction followed by dissociative OOH recombination. Therefore, suggested mechanism for the ORRon Pd–Co we are suggesting is drawn in Figure 4.22 where the OH is sitting on Co. This is a strong indication that the RDS (Rate-Determing Step) of the reaction would be:

$$Pd\text{-}Co(OOH)_{ads} \rightarrow PdO_{ads}Co(OH)_{ads.}$$

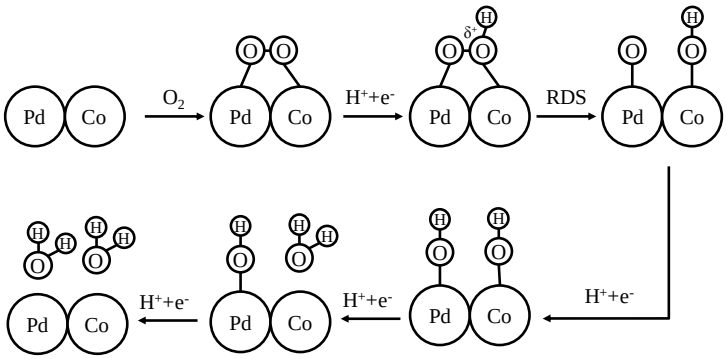

Figure 4.22 Proposed mechanism for the oxygen reduction reaction on Palladium– Cobalt electrocatalyst in acidic media.

To sustain this mechanism, we investigated the reaction order according to the pH. For three different acid solutions (0.05 M, 0.1 M and 0.2 M), we plotted the current at 0.6 V/SCE against the pH. We observed a straight line with a slope (~0.89) which was very close to the theoretical value of 1 for a Langmuir adsorption isotherm estimated by Bockris [118]. Damjanovic found the value of 1.5 for a Temkin adsorption isotherm [16]. From Figure 4.17 we justify the Langmuir isotherm adsorption. The potential oxide reduction peak on Pt is higher than those on Palladium alloys. This shows that oxides have more affinity with Palladium alloys than Platinum. In addition, with the curve in Figure 4.15, we clearly see that Pt needs less charge than the Pd-Co alloys to reduce or to desorb the oxide. Therefore, from these results, we propose the above mechanism scheme based to large oxide coverage on Palladium –cobalt alloys surfaces that justify the Langmuir type adsorption isotherm and a chemical reaction as the rate determining step. The practical evaluation of the performance of an electro catalyst for the ORR for PEM Fuel Cell application is determined through the current density of this reaction at potential close to the onset potential. Accordingly, the variation of the current densities with the Co atomic content are

shown in Figure 4.23 for the potentials 0.80, 0.825 and 0.850 V A Volcano behavior of the curves is obtained for each potential. The optimum cathodic current density for the ORR is obtained for $Pd_{65}Co_{35}$ alloy. This indicates that among the series of Pd-Co alloys studied here, this alloy ($Pd_{65}Co_{35}$) exhibits the best performance for the ORR in acid medium. This is, of course in agreement with the above results obtained from the Tafel plots. These results are supported by the variations of the ORR current densities at 0.800, 0.825 and 0.850 V as a function of hydrogen charge (Figure 4.24), the charge of the oxide formation (Figure 4.25), and the charge of the oxide reduction (Figure 4.26) respectively where the optimum current density is obtained for $Pd_{65}Co_{35}$. The enhancement of the electro catalytic activity is attributed to an optimal d band property that makes easier the OOH dissociative adsorption which is considered as chemical rate determining step (RDS) for the ORR. This mechanism is in agreement on the previous results of our group on the OOR on Pd-Cu alloys [98].

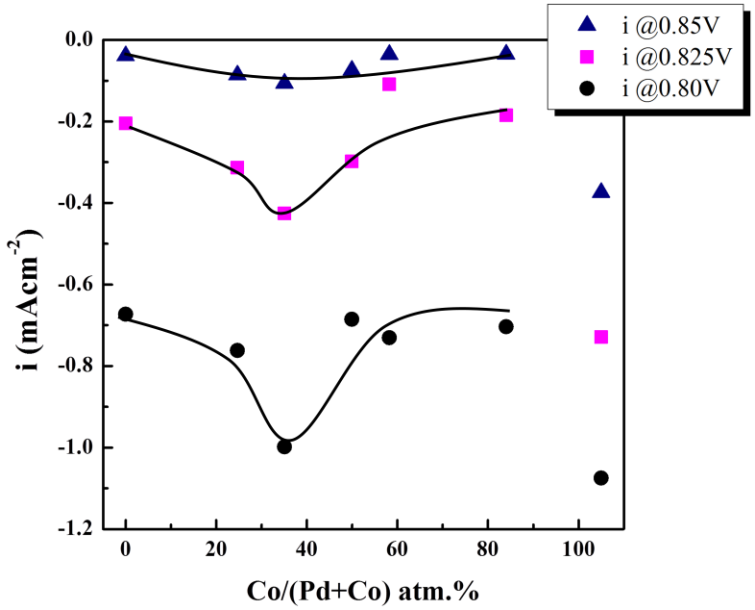

Figure 4.23 Dependences of the ORR currents at0.800, 0.825 and 0.850 V as a function of electrode composition

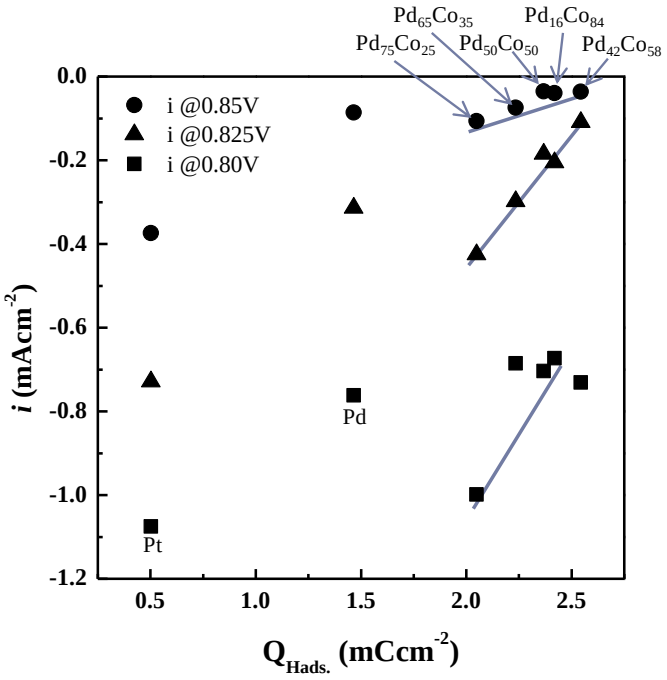

Figure 4.24 Dependence of the ORR currents at 0.800, 0.825, 0.850 V as a function of hydrogen charge

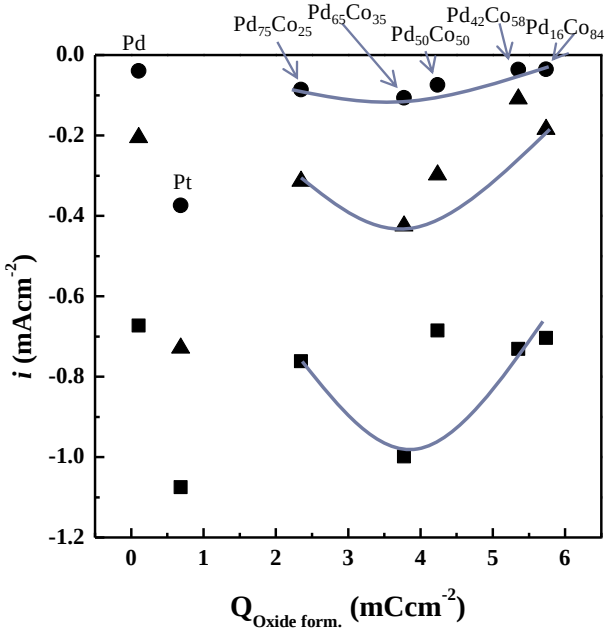

Figure 4.25 Dependence of the ORR currents at 0.800, 0.825, 0.850 V as a function of oxide formation charge

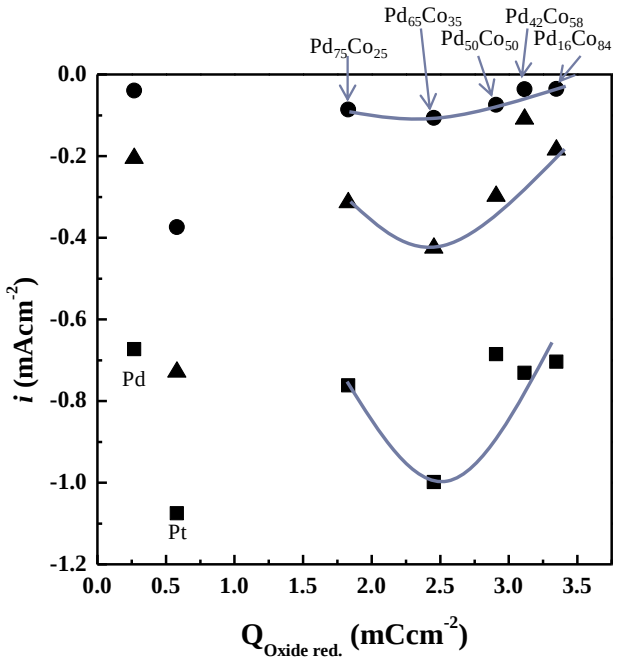

Figure 4.26 Dependence of the ORR currents at 0.800, 0.825, 0.850 V as a function of the amount of oxide reduction

From these results the following classification on the electro catalytic performance of the ORR on the various electrodes studies here is: $Pd_{16}Co_{84}$ < $Pd_{42}Co_{58}$ < Pd < Pd < $Pd_{50}Co_{50}$ < $Pd_{75}Co_{25}$ < $Pd_{65}Co_{35}$ < Pt. This result also clearly shows that alloying Pd with a specific composition of Co enhances significantly the electro-catalytic properties of the ORR on Pd-Co alloys in comparison to Co alone. Since the Pd-Co compositions studied here exhibit less activity for the ORR than Pt, there is room for improvement in the elctrocatalyst performance of these family of alloys by developing: new alloy composition, method of preparation of Pd-Co or other Pd-alloys.

4.2.4 Conclusion

Based on the results published here it may be concluded that:

1) The oxygen reduction reaction (ORR) on Pd–Co electro-catalyst has been studied in acidic media. The palladium alloys were prepared by coating glassy (GC) carbon substrates using a R-F magnetron sputtering equipment with a palladium and cobalt wafers as targets. Thin films of 40-60 nm thick films were obtained.

2) The ORR kinetics was studied on these catalysts in 0.05 M H_2SO_4. An increase in the hydrogen adsorption charge, the oxide formation and the oxide reduction or desorption was studied with the Co content in the alloy.

3) The mechanism of the ORR on the Pd–Co alloys was found to proceed through a four transferred electrons mechanism and a Tafel slope of 60 mV/dec.

4) The electro catalytic performance of the ORR on the various electrodes studied here is: in the order $Pd_{16}Co_{84} < Pd_{42}Co_{58} < Pd < Pd_{50}Co_{50} < Pd_{75}Co_{25} < Pd_{65}Co_{35} < Pt$.

5) The enhancement of the electro catalytic activity is attributed to an optimal d band property that makes easier the OOH dissociative adsorption which is considered as chemical rate-determining step (RDS) for the ORR.

4.3 Correlation between the Physico-chemical Properties and the oxygen reduction reaction electro catalytic activity in acid medium of Pd-Co alloys synthesized by Ultrasonic Spray Method

K. OISHI and O. Savadogo

Laboratory of New Materials for Energy and Electrochemistry

École Polytechnique de Montreal, Montreal, Quebec H3C 3A7, Canada

Submitted to Electrochimica Acta, on April 2nd, 2012

4.3.1 Introduction

Our group introduced the first work on Pd based alloy base on Pd-Co alloy (78:22 and 72:28), Pd-Ni (64:36), and Pd-Cr (61:39) as the electro-catalyst for the Oxygen Reduction Reaction(ORR) for PMEFC applications [3]. Furthermore we indicated aspects related to the tolerance to methanol of the electro catalyst cathode for the ORR for direct alcohol PEM Fuel Cell based on Pd-Co alloy (72:28) and Pd-Cr alloy (70:30) [41]. These electrodes prepared by sputtering method have shown enhanced electro-catalytic activities to Pd electrode. It was found that these electrodes are very tolerant to methanol because their ORR parameters are not affected by the presence of methanol. This may solve the problem of the luck of Direct Methanol Fuel cell (DMFC) cathodes performance to the fuel crossover. Effectively it is well established that DMFCs have two very serious technical problems, i.e., low catalytic activity of the anode electrocatalyst and methanol crossover in which the methanol permeates from the anode compartment through the electrolyte membrane to the cathode compartment [42, 43]. The latter is concomitant with cathode performance losses due to the formation of mixed potentials on the cathode electro-catalysts as well as the decrease in the efficiency of the methanol utilization. Approximately one-third of the available energy is lost at the cathode and the other one-third is lost at the anode [44]. Accordingly, the necessity to look for new electro-catalyst cathode for the ORR in direct alcohol fuel cell, we determined the effect of the type of the electro-catalyst and its

composition on its tolerance to the methanol crossover in DMFC cathode performance by studying systematically the electro-catalytic performances of the ORR on Pd-aloys (Pd-Co, Pd-Ni and Pd-Cr) prepared by sputtering method and their performance and selectivity as DMFC cathodes [41]. Their electrochemical characteristics for the oxygen reduction reaction (ORR) were determined in sulfuric acid solution with and without methanol at 30°C. The Pd alloys showed a higher ORR electro-catalytic activity than Pd, although lower than Pt. The Pd alloys also had no electro-catalytic activity for methanol oxidation. The maximum electro-catalytic activities for ORR were observed for the alloy composition of ca. 60 atom % Pd in all the Pd alloys. While the Pd–Cr alloy showed the highest ORR activity in the absence of methanol, the Pd–Ni alloy had a better ORR activity in the presence of methanol. The various Pd-alloys exhibited high tolerance for methanol. It has been found that these kinds of Pd based alloy catalysts have high potential to be used as a DMFC cathode because of its very low activities for methanol oxidation. Based on the XPS analysis, it was found that the electronic Density of State (DOS) at the Fermi level decreased by filling of the Pd d-band upon alloying Pd with 3d-transition metals. The decrease in the DOS inhibited the formation of Pd oxide and should contribute to the improvement of the ORR activity. Based on the X-ray photoelectron surface analysis, it was confirmed that the filling of the Pd d-band by alloying element decreased the DOS at the Fermi level. The decreased of DOS inhibited the formation of Pd oxide on the surface of the electro-catalyst.

Carbon black supported Pd-Co-Mo (70:20:10) electro-catalysts was prepared for the ORR by using a conventional borohydride reduction method [83]. The particle size is in the range of 15-35 nm. The mean particle sizes increase with increasing heat treatment temperature. Investigation of the electro-catalytic activity of the Pd-Co-Mo system with varying composition and heat treatment temperature reveals that a Pd:Co:Mo atomic ratio of 70:20:10 with a heat treatment temperature of 500 °C exhibits the highest eletro-catalytic activity. Although the degree of alloying increases with increasing temperature from 500 to 900 °C as indicated by the X-ray diffraction data, the electro-catalytic activity decreases due to an increase in particle size and a decrease in surface area. The electro-catalytic properties of carbon supported Pd-Co-Au catalysts prepared by the conventional reduction method and a reverse micro emulsion method was also studied [48]. The size of the particles is in the range 15-46 nm. As for Pd-Co-Mo, the mean particle sizes also increase with increasing heat treatment temperature. The samples

prepared by the micro emulsion method show better electro-catalytic activity for the ORR when compared to those prepared by the conventional borohydride method due to a higher degree of alloying at lower temperatures while keeping the particle size small and the surface area high. The activity for the ORR of the samples prepared by the micro emulsion method is comparable or slightly better than that of commercial Pt/C catalyst at 60^{o}C. The former has shown particle sizes in the range of 15-35 nm, and the latter has given the particle sizes in the range of 15-46 nm. The mean particle sizes increase with increasing heat treatment temperature for both cases. These ternary alloy electro-catalysts are not more effective than the binary Pd-alloys because their electro-catalytic activity for the ORR is not significantly higher than the Pd-Co based electro-catalyst and ternary based electro-catalyst are more expensive than binary based materials.

The Pd electro-catalyst monolayer was synthesized on different single crystal substrates; Ru(0001), Rh(111), Ir(111), Pt(111), and Au(111) [39]. It was found that the electro-catalytic activities increase in the order of Pd/Ru(0001) < Pd/Ir(111) < Pd/Rh(111) < Pd/Au(111) < Pd/Pt(111). The Pd-Co (2:1) carbon supported catalysts having broad size distribution up to 92 nm, peaking at 18-20 nm was also prepared in the same work. The results showed a volcano-type dependence of the ORR electro-catalytic activity on the energy of the d-band center of Pd monolayer's, with Pd/Pt(111) at the top of the curve. The activity of the non-Pt Pd_2Co/C alloy electro-catalyst nano particles was comparable to that of commercial Pt-containing catalysts. The kinetics of the ORR on this electro catalyst predominantly involves a four-electron step reduction with the first electron transfer being the rate-determining step. The downshift of the d-band center of the Pd "skin", which constitutes the alloy surface due to the strong surface segregation of Pd at elevated temperatures, determined its high ORR activity. Additionally, it showed very high methanol tolerance with a very high catalytic activity for the ORR at high concentrations of methanol. It was indicated that due to its relative good stability, this catalyst could possibly replace Pt in fuel-cell cathodes, especially those of direct methanol oxidation fuel cells (DMFCs).

The effect of heat treatment on nano particle size and ORR activity for carbon-supported Pd–Co alloy electro catalysts has been studied [40]. Accordingly the impregnation method was employed for the synthesis, in which sodium borohydride was used as a reducing agent. Surface cyclic voltammetry was used to confirm the formation of the Pd–Co alloy. In order to improve activity and stability, the catalysts were heat-treated in the temperature range of 300 ˚C to 700˚C. The optimal heat-treatment temperature was found to be 300 ◦C, where the average particle size

of 8.9 nm, and the highest ORR catalytic activity, was obtained. The ORR kinetics on these electro-catalysts were also studied using the rotating disk electrode (RDE) method. These particle sizes are lower than those of Pt widely used for fuel cell applications and which are in the range of 2 to 50 nm. Electro catalytic ORR activity was also examined in an acidic solution containing methanol. The results showed that the synthesized Pd–Co/C catalyst has methanol tolerant capabilities. These results confirm the high tolerance of the Pd-alloy cathode for the ORR in Direct alcohol PEM Fuel cell we have previously indicated [41].

Carbon-supported Pd-Co bimetallic nanoparticle electro-catalysts of different Pd/Co atomic ratios were prepared by a modified polyol reduction [45]. Their electro-catalytic activities for the oxygen reduction reaction (ORR) have been investigated using porous rotating disk and disk-ring electrode techniques. It was shown that the mean particles of the as-prepared Pd-Co bimetallic nano particles size decreases with an increase in Co content. A typical TEM image of the best electr-catalyst was the Pd2Co/C electrode, heat-treated at 500^{o}C which revealed a mean particle diameter of 8.3 nm with a relatively narrow size distribution and a Pd-Pd mean inter-atomic distance of 0.273 nm.. Kinetic analysis based on the rotating disk and disk-ring electrode measurements reveals that the ORR on Pd-Co/C catalysts undergoes a four-electron process in forming water. Based on the TEM image of the electro-catalyst of Pd_2Co/C heat treated at 500°C showed that the particles are not uniformly distributed and the particles larger than 10 nm seems to be in higher quantity than those indicated in the given histogram. From these results it is claimed that the modified polyol reduction route which was used could allow obtaining nano-scale alloy electro-catalysts with a narrow particle size distribution and a good dispersion on a support.

Carbon supported Pd-Co (7:3) alloy catalyst was prepared by a modified polyol reduction method, a co-impregnation method, and a reverse micro emulsion method, and heat treated at various temperatures up to 900°C [46]. It was claimed that the mean particle sizes of the catalysts obtained from the modified polyol reduction method are 2.4 nm (as prepared), 3.5 nm (250°C), 4.1 nm (350°C), 5.3 nm (500°C), 7.7 nm (700°C), and 12.5 nm (900°C). These values are very attractive for the fuel cell applications but they were not supported by XRD experiments or TEM images which may help to determine correct particle size and their distribution onto the support.

The Effect of the synthetic reducing agents based on co-impregnation on morphology and ORR activity of

carbon-supported nano-Pd–Co alloy electro-catalysts has been investigated [47]. Three different reducing agents, ethylene glycol (EG), formaldehyde (HCHO), and sodium borohydrate (NaBH4) were used. The method with ethylene glycol (EG) has provided the smallest mean particle sizes in the range between 4.6 and 6.6 nm even though the catalysts were heat treated at 700°C. The electro-catalyst based on $NaBH_4$ provided the mean particle size in the range of 4.6-13.3 nm, and those based on HCHO has exhibited a mean particle size in the range of 8.8-22.9 nm. The catalysts prepared by EG and $NaBH_4$ with no-heat treatment show well distributed fine particles from their TEM images.

The carbon-supported nano particles of Pd–Co–M (M = Pt, Au, Ag) catalysts for DMFC in a ratio of 70:20:10 were prepared through reverse micro emulsion method [38]. The X-ray diffraction XRD analysis showed well-defined reflections corresponding to a face centered cubic phase of palladium. From transmission electron microscopy analysis, the particle size after heat-treatment at 500°C was found to be approximately 20 nm, which was also confirmed by XRD analysis. Voltage versus current polarization curves indicated that Pd–Co–Pt exhibited better oxygen reduction reaction (ORR) activity than the other combinations with Ag and Au, in terms of shift in onset potential to a positive value of more than 100 mV and increase in reduction current. The ORR kinetics on Pd–Co–Pt was analyzed by using rotating disk electrode to follow a 4 electron pathway. An additional advantage observed with Pd–Co–Pt was its high methanol tolerance and ORR activity very close to that of Pt.

Synthesis of nanoporous PdCo Catalyst by electro-deposition and electrochemical dealloying for Microfuel Cells PdCo electro-catalyst synthesized by electrodeposition and electrochemical de-alloying for direct methanol microfuel cells [49, 119] . It was found that the electro-deposition technique can be successfully synthesized selective Pd-Co alloys onto conductive Au substrates, and by changing the potential applied, morphologies of the deposits were tuned into thin films or dendrites. The electrochemical de-alloying technique successfully increased the electrochemically active surface area by roughly ten times. Thus, such combination of electro-deposition and de-alloying was proved effective for synthesizing high performance electrodes for micro-fuel cell packaging. In terms of fuel cell catalyst, the PdCo nanostructures exhibited better

activity for oxygen reduction reaction than Pt catalyst in direct methanol micro fuel cells, especially in the potential range of interest for actual fuel cell operation (0.8V versus NHE). This is because of the smaller Tafel slope value (similar to those obtained in [3]) of the PdCo catalysts. It was concluded that detailed analyses on the results indicated that getting very low Tafel slope is of course quite important for developing effective fuel cell catalysts.

Carbon-supported Pd Co alloy electro catalysts of different Pd/Co atomic ratios were prepared in an aqueous solution at room temperature with NH_4F as a complexing agent for Pd^{2+} and H_3BO_3 as a buffer, followed by NaBH4 reduction [50]. As-prepared Pd Co bimetallic nano-particles showed a single-phase face-centered-cubic (fcc) disordered structure, and the mean particle size is found to decrease with an increase in Co content. TEM images demonstrated that the as-prepared Pd Co alloy nana particles are well dispersed on the surface of the carbon support with a small particle size and a relatively narrow particle size distribution. It was claimed that the average particle size of a Pd_2Co_1/C catalyst is ca. 3.0 nm. It was also indicated that the maximum ORR mass activity was observed for a Pd:Co atomic ratio of 4:1, but the highest specific activity was found on a Pd:Co atomic ratio of 2:1. Kinetic analysis reveals that the ORR on Pd Co/C catalysts follows a four-electron process leading to water. Moreover, the Pd Co/C catalyst exhibited much higher methanol tolerance during the ORR than the Pt/C electro-catalysts [50]. The unique point of this study was the utilisation of (NH_4F + Pd^{2+}) complex, and they obtainend fine particles on carbon support in the range between 2.6 and 3.8 nm.

Based on the above results, it may be concluded that only few methods (impregnation, micro emulsion, electro-deposition, electrochemical de alloying) have been developed for carbon supported Pd-Co nano-scale catalysts preparation so far. They are based on classical methods which involve a lot of steps which involve the reduction from the electro-catalyst salt to the preparation the catalyst powder and its coating on the Gas Diffusion Electrode (GDE) support.

Ultrasonic Direct Solution Spray Reaction method for PEMFC applications has been developed for the first time in our previous studies [53, 74]. In these works, we focused on the preparation of Pt-electro-catalyzed gas diffusion electrode (GDE). Slurry consists of platinum catalyst precursor and carbon catalyst supports were sprayed by use of ultrasonic spray device. The generated mist was continuously heated in various temperatures in a mixture of hydrogen-nitrogen gas flow through a tube reactor. The platinum precursor was reduced to solid Pt nano-

particle on the carbon supports, and the synthesized catalyst was directly filtered on a gas diffusion layer. This method is less expensive, less consuming time and provides optimized electro-catalyst particle sizes (~ 2-3 nanometers) for PEM Fuel cells applications.

This work is on the development of a new method of preparation of Pd-Co electro-catalyst for the ORR for PEM Fuel Cell applications based on Ultrasonic Spray Method. It is the first time this method is used to prepare directly the Pd-alloys electro-catalyst layer on the gas diffusion electrode from the salts of the active materials. Correlation between the preparation parameters and the properties of the ORR of these electro-catalysts in acid medium for PEM Fuel Cell applications will be determined. The particles size obtained from this method will be compared to those of the electro-catalysts obtained by the other methods. The advantage of this method is to obtain smaller scale catalysts than the other methods. A feasibility of the new technique for a carbon supported nano-scale palladium-cobalt alloy catalyst was also studied. Since only a few techniques have achieved vary small nano-scale catalyst particles having the diameter of less than 10 nm.

4.3.2 Experimental

4.3.2.1 Catalyst synthesis

The details of this technique are described in our previous study [53]. The procedure of catalyst fabrication by ultrasonic spray reaction method for carbon supported palladium and palladium-cobalt alloy catalyst is as follows (Figure 4.27). arbon support (Vulcan XC-72R) was dispersed into (Milli-Q, 18.2 MΩcm). Palladium precursor using palladium(II) nitrate dehydrate ($Pd(NO_3)_2 \cdot 2H_2O$, Fluka) and cobalt precursor using cobalt(II) nitrate hexahydrate ($Co(NO_3)_2 \cdot 6H_2O$, Aldrich) were dissolved into ultra pure water, and added into the carbon suspension after which it was ultrasonificated for 60 minutes at 50^{o}C. The homemade system with an ultrasonic piezoelectric transducer (Figure 4.2) was developed. The slurry containing catalyst precursors and carbon support was introduced into a spray chamber (2) and sprayed by the ultrasonic piezo transducer (1) (HM-2412, 2.4 M Hz, Honda Electronics Co., Ltd) which was placed at the bottom of the spray chamber. The transducer continuously generated mist. It was carried into a quarts tube reactor (3) (length: 1.0 m, inner diameter: 35 mm) in a stream of reducing agent gas flow (3 vol.% H_2 - 97vol.% N_2 mixture gas, Air Liquide, Canada) under

suction by a vacuum pump (10). A thermocouple was placed at the upper end center of the reactor, and the heater was controlled to achieve the measured temperature at 400 ^{o}C. The stream of the hydrogen gas in the mixture gas, inside of the tube reactor, chemically reduced the precursors to solid metal particles on the carbon support, and it was heat treated simultaneously. The synthesized carbon supported palladium and palladium-cobalt catalysts were collected by a filter which was placed on the top end of the tube (5).

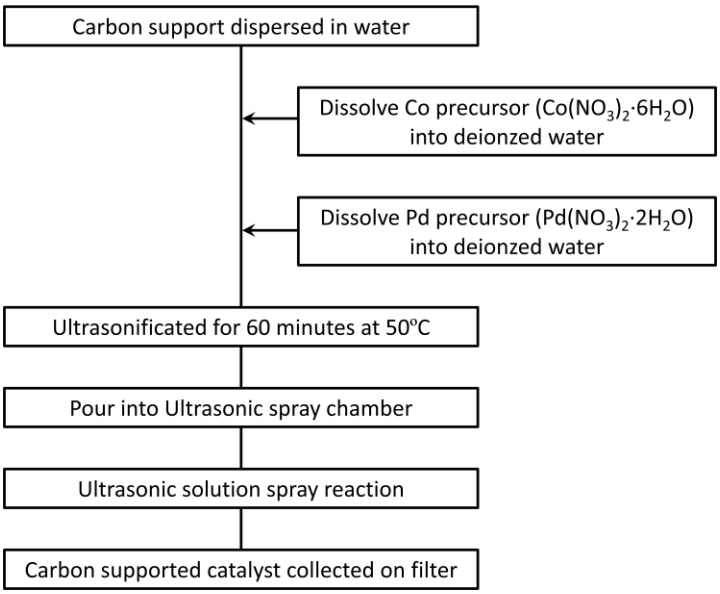

Figure 4.27 Catalyst synthesis procedure by ultrasonic spray reaction method

4.3.2.2 Electrode preparation

Glassy carbon (GC) rod (GC20, 5.2mm diameter) was purchased from Tokai Carbon Ltd., Japan. A surface of GC was polished with 1, 0.3 and 0.05 μm aluminum slurries on a polishing cloth, respectively, until a mirror-like surface was obtained. Afterwards, rinsed in in acetone, 5% nitric acid and deionized water thoroughly. The polished GC was then allowed to dry at room temperature. 7 mg of synthesized catalyst in 5 mL of de-ionized water was ultra-sonificated and dispersed, and afterwards 30 μL of the slurry was pipetted onto the GC mirror-like surface and dried at room temperature. Then diluted Nafion® solution was drew off on the catalyst layer and dried at 323K.

4.3.2.3 XRD analysis

The structural characterization of the synthesized carbon supported catalysts was determined by X-ray diffraction methods (XRD). A Philips X'Pert PRO X-ray diffractometer equipped with graphite monochromatized Cu Kα (λ=154.2 pm) as radiation source was used for this purpose. Normal diffraction patterns were obtained in the range of 10-110° with a scan speed of 1° min-1. All the recorded diffractograms were compared to those of the Standard X-ray diffraction powder patterns to identify different peaks and orientations. After identifying the entire diffraction peak positions in the X-ray diffract grams obtained from normal scans, slow scans were also applied to determine the angle at which maximum intensities were observed, and the accuracy in recording the angle was 0.005°. The average catalyst particle was determined from the full width at half maximum (FWHM) of the x-ray diffraction peak using Scherrer's equation.

$$\overline{D}_{\mathrm{XRD}} = \frac{K\lambda}{B\cos\theta}$$

Eq. 4.3

where $\overline{D}_{\mathrm{XRD}}$ is the particle diameter defined from the Scherrer's equation, λ the X-ray radiation of Cu K_α (λ=154.2 pm), *B* the FWHM of a diffraction peak at (111), *K* the Scherrer's constant of the order of unity for usual crystals (*K*=0.9), and θ the diffraction angle of the peak (111).

4.3.2.4 TEM analysis

Transmitted Electron Microscopy (TEM) (JEM-2100F, JEOL) was used to obtain the morphology of the catalysts, including the particle size and distributions of the synthesized Pd and Pd-Co nano-particles on carbon supports. To prepare samples for TEM analysis, a suspension, in ethanol, of the carbon supported catalysts was transferred onto the surface of the microscope Cu grid coated with an amorphous carbon film. TEM images of the catalysts were taken at an operation voltage of 200 kV. The particle size, taken as the equivalent diameter of the measured area of the particles, was then obtained. The mean particle size $\overline{D}_{\mathrm{TEM}}$ was obtained by measuring the diameter of a sufficient number of particles (more than 500 particles) to ensure a good statistic sampling and calculated according to the following equation.

$$\overline{D}_{\mathrm{TEM}} = \frac{\sum f_i d_i^{\,3}}{\sum f_i d_i^{\,2}}$$

Eq. 4.4

where f_i is the occurrence frequency of the particles with a diameter of d_i in the sample.

4.3.2.5 XPS analysis

X-ray photoelectron spectroscopy (XPS) analysis was conducted on a VG ESCALAB 3 Mark II spectrometer using an Al Kα- ray source. Avantage data acuision and processing software (Thermo Fisher) was used to analyze the valence state of Pd3d in synthesized catalysts.

4.3.2.6 Electrochemical measurement

All electrochemical analysis was performed using PAR 273A potentiostat (Princeton Applied Research, Oak Ridge, TN) in acid medium (0.05 mol dm^{-3} H_2SO_4, 298K) with a conventional three-electrode cell equipped with a rotating disk electrode (Pine Instruments), reversible hydrogen electrode (RHE) and platinum mesh counter electrode. Cyclic voltammetry (CV, 50 mV s^{-1}, 0.1-1.1 V vs. RHE) with nitrogen purge and slow scan voltammetry (SSV, 3 mV s^{-1}) with oxygen purge (ca. 1 hour) were carried out to evaluate electrochemical properties and electro-catalytic activity for oxygen reduction reaction (ORR). The both gases were 5N8 purity and supplied by Air Liquide, Canada.

4.3.3 Results and Discussion

Table 4.3 shows the chemical compositions and related parameters of five electro-catalysts based on Pd-Co alloys which have been synthesized by using the Ultrasonic Direct Solution Spray Reaction method. The chemical composition, the electro-catalyst net loadings, the atomic ratio between palladium and cobalt, the weight % of palladium and cobalt respectively were determined by Inductively Coupled Plasma Mass Spectrometry (ICP-MS). During the sample preparation, the chemical composition of palladium and cobalt in the electro-catalyst alloys were varied by changing the concentration in a large range of the cobalt precursor in the slurry for the synthesis process, in contrast the concentration of the palladium precursor were added in the slurry in a restricted range of concentration. Palladium loading of all the samples from sample 1 to 5 are in the small range between 13.5 and 17.8 wt.% and cobalt loadings are controlled in the

large range between 0 and 10.3 wt.%. Based on the atomic ratio between palladium and cobalt shown in Table 1, Sample 1 is noted as Pd/C, Sample 2 Pd_5Co_1/C, Sample 3 Pd_3Co_1/C, Sample 4 Pd_2Co_1/C, and Sample 5 Pd_1Co_1/C. These notifications will be used in the following.

Table 4.3 Mean particle size of the catalysts synthesized by ultrasonic spray reaction method analyzed by XRD and TEM

Sample	Approximate Composition (Pd:Co, atmic)	Mean particle size nm (XRD)	dominant particle size nm (TEM)
Sample 1	1:0 (Pd)	3.38	4.15
Sample 2	5:1	3.94	4.29
Sample 3	3:1	3.55	4.31
Sample 4	2:1	2.61	4.36
Sample 5	1:1	4.61	4.29

The XRD spectra recorded of the carbon supported Pd and Pd-Co catalysts are shown in Figure 4.28. According to the reference (ASTM 05-0681), all the samples predominately exhibit the characteristics of a single-phase face-centered cubic (FCC) crystalline structure. The lines of the Pd/C are the standard values corresponding to the 2 θ of (111), (200), (220) reflections for pure Pd respectively. The diffraction peak at around θ =25◦ corresponds to the (002) plane diffraction of the hexagonal structure of the Vulcan-XC-72R carbon support. The mean particle sizes were calculated from the (111) diffraction line using the Scherrer equation show reflections that are characteristic of a single phase fcc lattice unlike the samples all exhibit the characteristics of a single-phase, fcc disordered structure, indicating that the method of preparation has strong reduction capabilities as the classical methods. Although cobalt can take two different crystal systems; Hexagonal (P63/mmc, ASTM 05-0727) and FCC (Fm3m, ASTM 15-0806), all spectra of the samples shown in Figure 4.28 are similar to those of fcc Pd and the Co-origin peaks can't be found. This indicates that all the samples Pd-Co alloys prepared here are substitution solid solutions (Figure 4.29) where some atoms of Pd are replaced by Co atoms. The phase diagram was obtained from Fact Sage software [120]. As we have shown experimentally [3], some of the

solid solution systems might be stable in acid medium. This is in agreement with other results [1] which have considered that the Pd-Co solid solution system might be stable in acid med. This alloy system mainly forms solid solution phase, but in some composition range, ordered phases of inter metallic compounds such as L12 phase (i.e., Pd_3Co_1) and L10 phase (i.e., Pd_1Co_1) can be formed [1, 121] . Accordingly this difference in phase between Pd_3Co and PdCo may indicate that the electro-catalytic properties of PdCo for the ORR may differ from those of Pd_3Co.

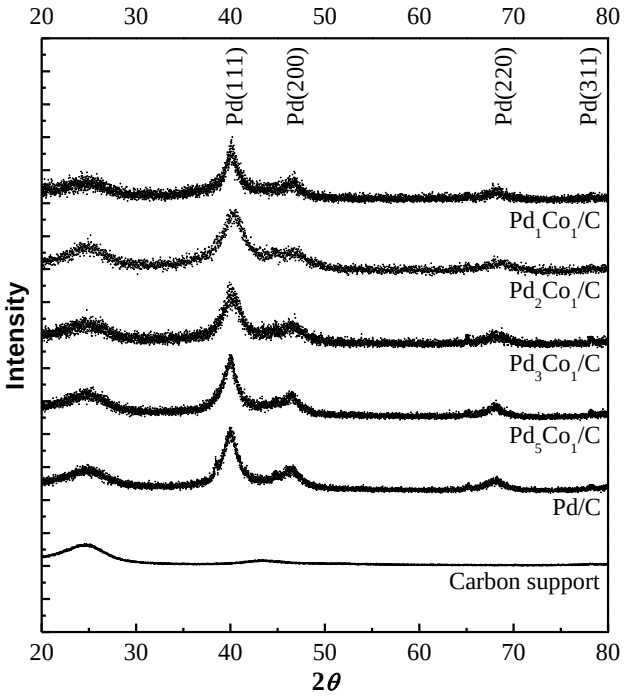

Figure 4.28 XRD patterns of the carbon support, Pd and Pd-Co alloys synthesized by ultrasonic spray method at various compositions.

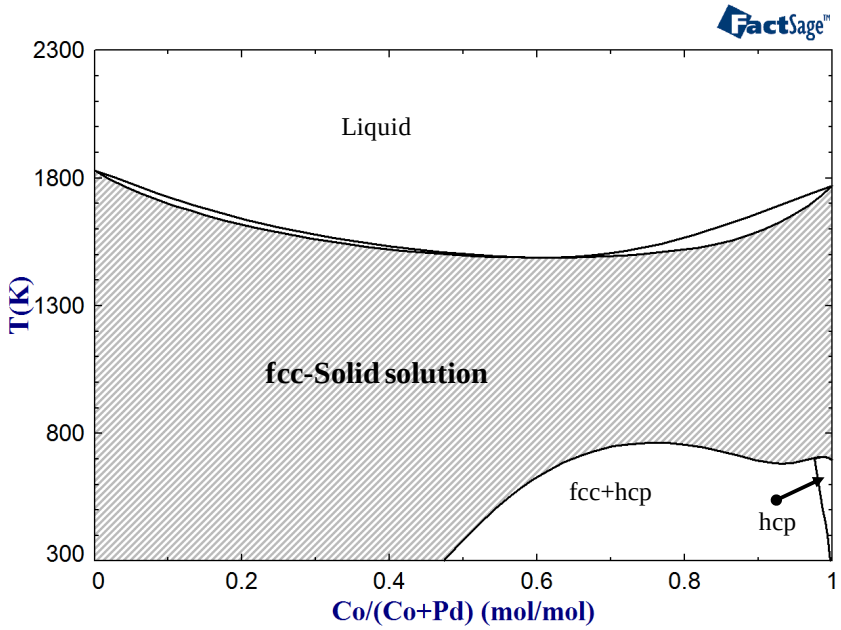

Figure 4.29 Phase diagram of Pd-Co system obtained from FactSage software.

Transmission Electron Microscopy (TEM) images, Selected Area Electron Diffraction (SAED) patterns and the corresponding particle size distribution histograms are shown in Figure 4.30, Figure 4.31 and Figure 4.32 respectively. The TEM images show clearly that the electro-catalyst particles for all the samples are highly dispersed on the carbon support. Aggregated particles can be rarely found. Their dispersion attributes are relatively fine when we compare to those of other results of previous work by other groups [47, 50]. Box-and-whisker diagram indicating sample minimum, lower quartile (25%), median (50%), upper quartile (75%), and sample maximum for the five different samples are shown in Figure 4.33. The × mark indicates the mean particle size calculated from Figure 4.30. The range of the highest and the smallest particle size in the histogram depend on the alloy composition. The highest range which is between 10.3 and 2.5 nanometers is obtained for Pd/Co and the lowest range is obtained with the Pd_5Co/C alloy and is between 6 and 2.5 nanometers. The dominant particle sizes are between 2.5 and 6.5 nm for all samples. The catalyst particle sizes are controlled in very narrow distribution range. This high distribution and the small size of the nano particles obtained in this work is attributed to the method of the electro-catalyst preparation. In particular, the method allows the stream of the hydrogen gas in the mixture gas to go inside of the tube reactor and chemically reduced the platinum precursor to solid platinum particles on carbon supports, and these particles were heat

treated by a furnace which was placed around the tube reactor. This enhances the strong interaction between the catalyst and the support due to the characteristic nanostructure of the fine composites being formed from droplets of a homogeneous solution in a quick-heating process. Such interaction is not possible with the electro-catalyst fabricated with the classical methods shown in the introduction.

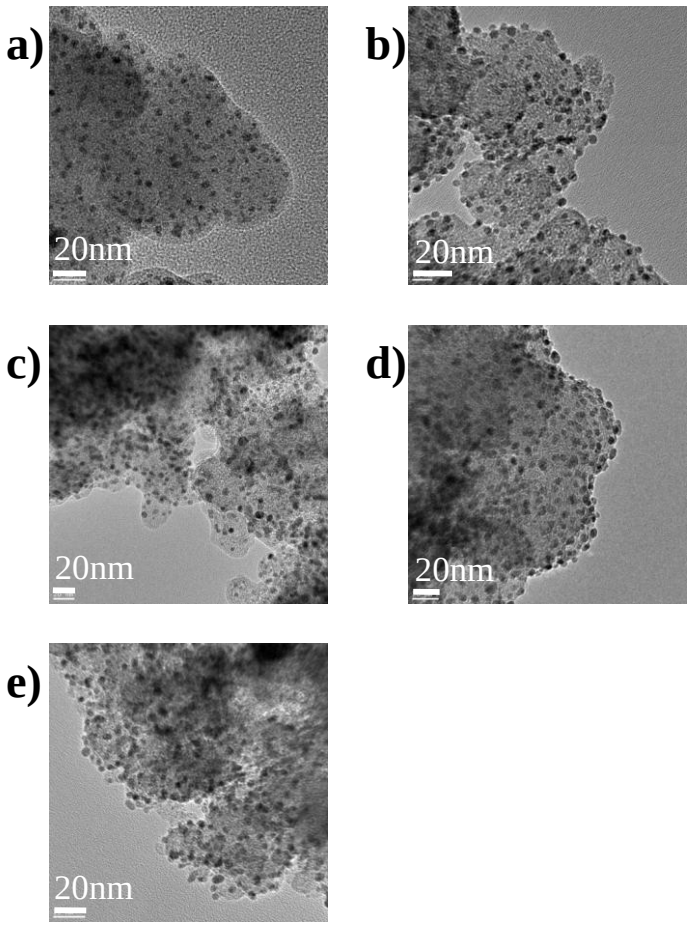

Figure 4.30 TEM images of synthesized catalysts; a) Pd/C, b) Pd_5Co_1/C, c) Pd_3Co_1/C, d) Pd_2Co_1/C, e) Pd_1Co_1/C.

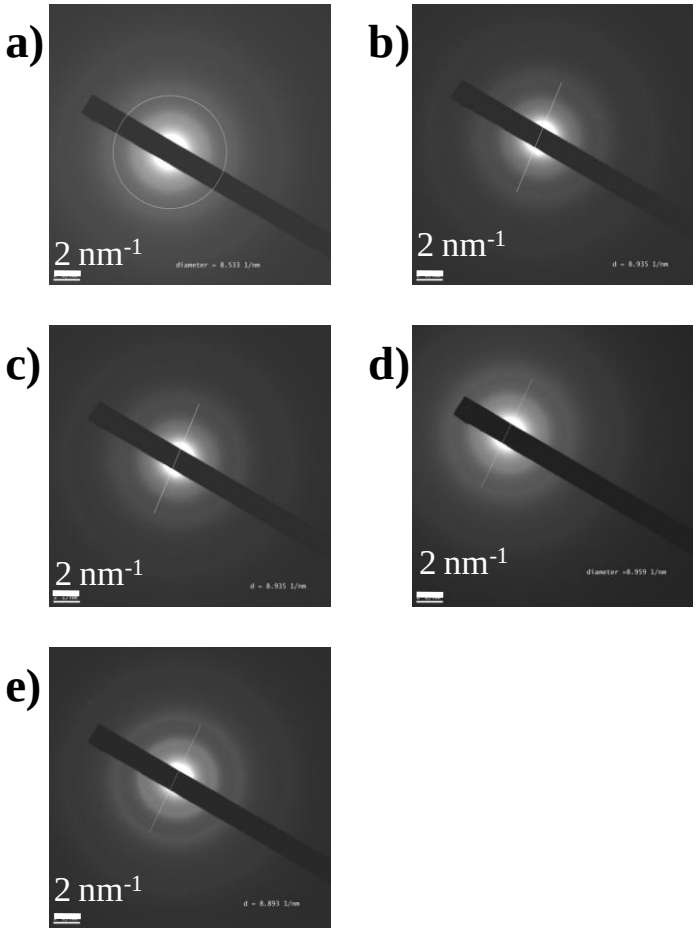

Figure 4.31 TEM Selected Area Electron Diffraction (SAED) pattern taken from synthesized catalysts; a) Pd/C, b) Pd_5Co_1/C, c) Pd_3Co_1/C, d) Pd_2Co_1/C, e) Pd_1Co_1/C.

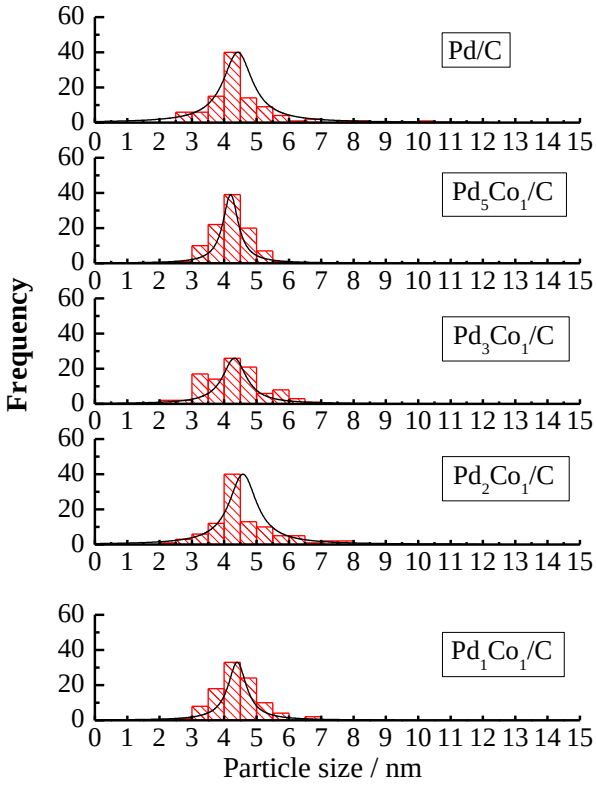

Figure 4.32 Particle Size Distribution Histogram of Palladium-Cobalt alloy catalysts obtained from TEM images.

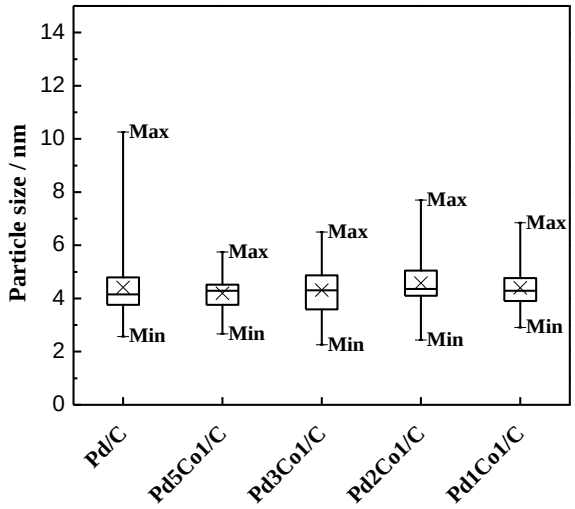

Figure 4.33 Box-and-whisker diagram indicating sample minimum, lower quartile (25%), median (50%), upper quartile (75%), and sample maximum for the five different samples. The × mark indicates the mean particle size calculated.

The comparison of the particle Pd-Co particle sizes obtained from different literature results to those in the present work are shown in Figure 4.34. The cross mark indicates the average particle sizes which are given in these literatures and the bar indicates the range of particle size distributions between maximum and minimum which are obtained from the particle size distribution histograms or TEM images in these literature data. A significant difference in particle sizes is observed from these data. The maximum size of the particles changes from 90 nanometers in [39] to 3 nanometers for this work. The electro-catalysts obtained with the ultrasonic method we developed here have very narrow range of the particle size distributions and small average particle size when compared to those obtained with the classical method from the literature. This difference might be related to the method of preparation, the reduction agent and the annealing temperature. For example in [47] the range of the particle size varies from 4.6 to 22.9 nanometers when the classical reduction process was used for the Pd-alloys preparation based on three reducing agents(ethylene glycol (EG), formaldehyde (HCHO), and sodium borohydrate ($NaBH_4$)). The biggest particle sizes were obtained with $NaBH_4$ and the smallest particle sizes were obtained with ethylene-glycol. This is not the case of the result obtained in this work with this new method of preparation where the same particle sizes are obtained when ethylene-glycol, sodium borate or hydrogen are used as reducing agent. It has been verified experimentally that when we use the classical method to synthesize the Pd-Co alloys, a change in particular size with the type of the reducing agent was also obtained. This support well the results obtained in [47]. Accordingly the non variation of the particle size of the synthesized Pd-Co alloys in this work for various reducing agents is a strong indication that the ultrasonic method may allow to get smaller particle size than the classical method for various reducing agents. Thus the experimental conditions of the ultrasonic method we used here to prepare the Pd-Co are appropriate to get very small particles. The small particle size of the electro catalyst would improve the catalyst utilization and specific surface area toward low catalyst loadings.

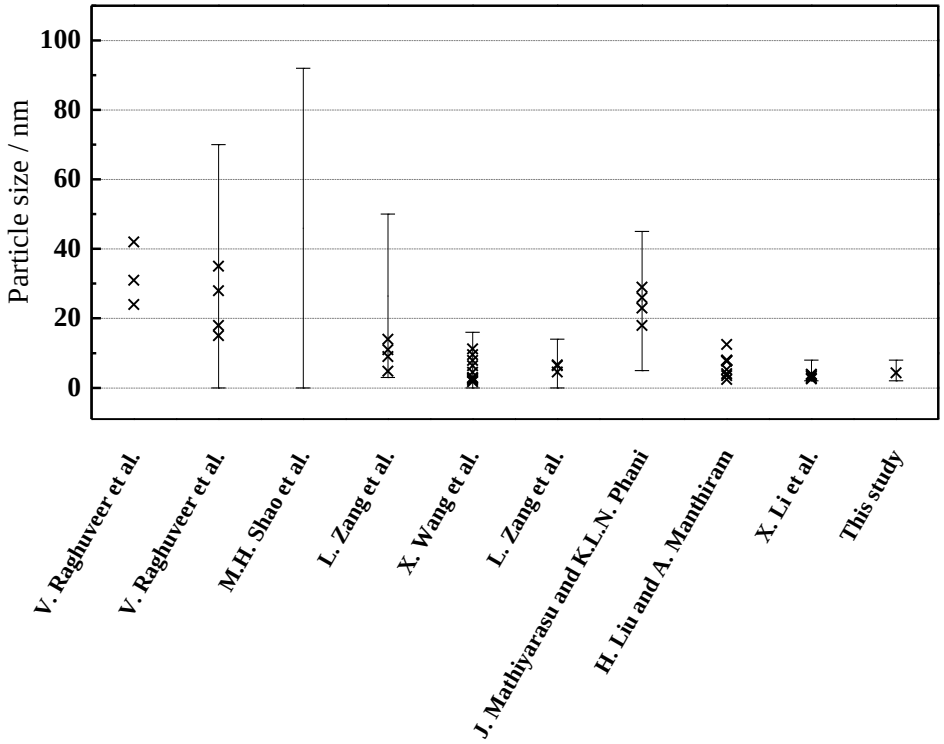

Figure 4.34 Particle size comparisons between this study and literatures

XPS of Pd-Co alloys are shown in Figure 4.35 (a) and (b) (XPS spectra of the various Pd-Co alloys were almost the same). The peak area of Pd is clearly larger than that of Co, that is, the surface is considered to be Pd rich even taking sensitivity factors into consideration (the sensitivity factor of Pd-3d is 2–3 times higher than that of Co-2p [122]). This result probably indicates the formation of Pd-skin [123, 124]. The Pd skin is probably rationalized in terms of thermodynamics with the alloy segregation theory [125] or replacement of surface Co by Pd in the bath after electrodeposition. The surface Pd and Co are found to be metallic, not oxide, by comparing experimental binding energies (Pd-$3d_{5/2}$: 334.7 eV, Co-$2p_{3/2}$: 777.4 eV) to those of a literature (Pd-$3d_{5/2}$: 334.4 eV, Co-$2p_{3/2}$: 781.5 eV) [126]. As for the binding energy of Co, the shift of $2p_{3/2}$ peak to lower energy suggests alloying of Co with Pd [126]. These are in agreement with the other published data. This is also supported by the XPS spectra shown in Figure 4.35. No specific oxide is expected because PdO and PdO_2 is not matching well with th Pd-Co alloys. The spectra of Pd-$3d_{5/2}$ shows clearly that PdO nor PdO_2 peaks is not formed on PdCo(even it is closed) nor on Pd_2Co, Pd_3Co and Pd_5Co.

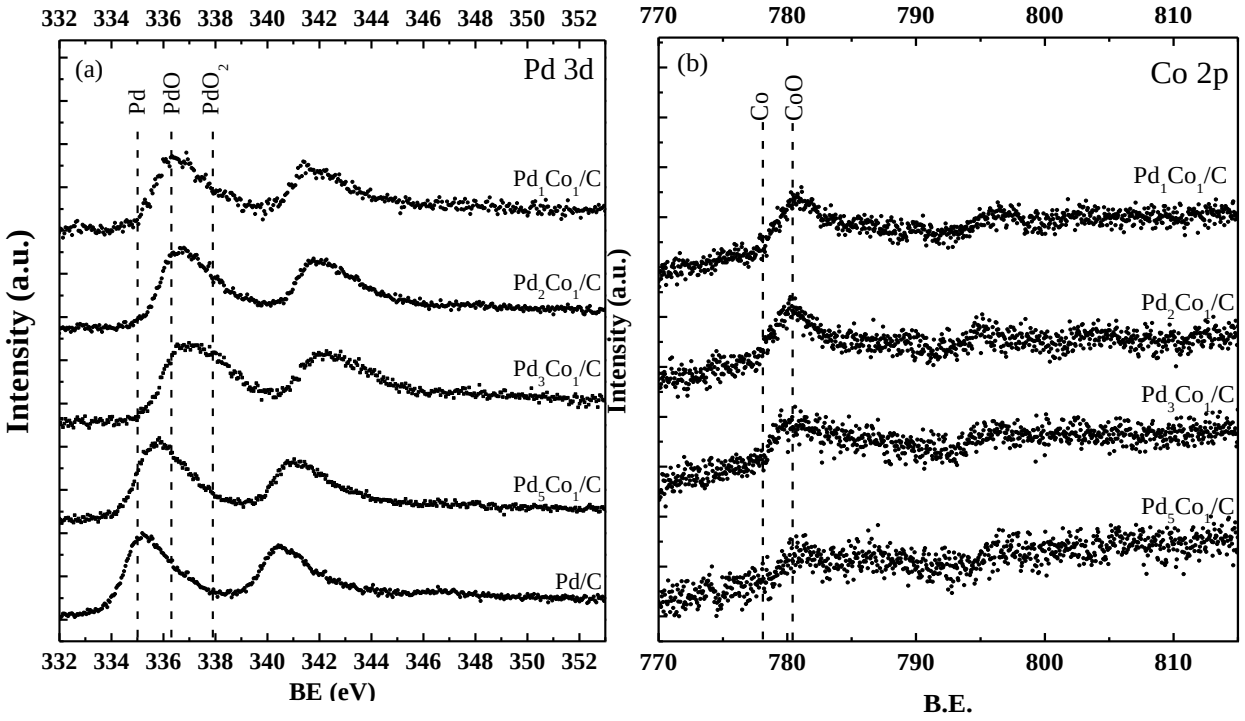

Figure 4.35 XPS spectra obtained from synthesized Pd/C and Pd-Co/C catalysts for Pd 3d core level and Co 2p core level.

Figure 4.36 shows the cyclic voltammograms (CVs) of commercial Pt/C and Pd/C electro catalysts and those of the various Pd-alloy electro catalysts coated on glassy carbon disk electrode in 0.05 M H_2SO_4 electrolyte under N_2 atmosphere at 298 K. The first five cycles are given respectively. The scan range of potentials was between 0.1 and 1.1 V vs. RHE because of under potential deposition of hydrogen on Pd electrode. An under potential deposition of hydrogen on Pd electrode is well known and the generation of hydrogen gas would cause falling the catalyst thin films off from the GC substrate surface. The CVs of the synthesized Pd/C and Pd-Co/C electro-catalysts show peaks in the potential range of 0.1 to 0.3V versus RHE, which correspond to the hydrogen adsorption/desorption processes [112]. However no well-defined peaks were observed for all the commercial and synthesized electro-catalysts because of the narrow scan range. In addition, oxide formation/reduction or desorption currents were clearly seen and obvious decreasing of hydrogen adsorption/desorption and oxide formation/reduction or desorption charges were not seen during the first five cycles. Although the synthesized Pd-Co catalysts were relatively stable during the electrochemical cycles in the potential range of 0.1-1.1

V vs. RHE, further studies are required to fully demonstrate the long-term stability of the electro-catalysts for PEM Fuel Cell applications.

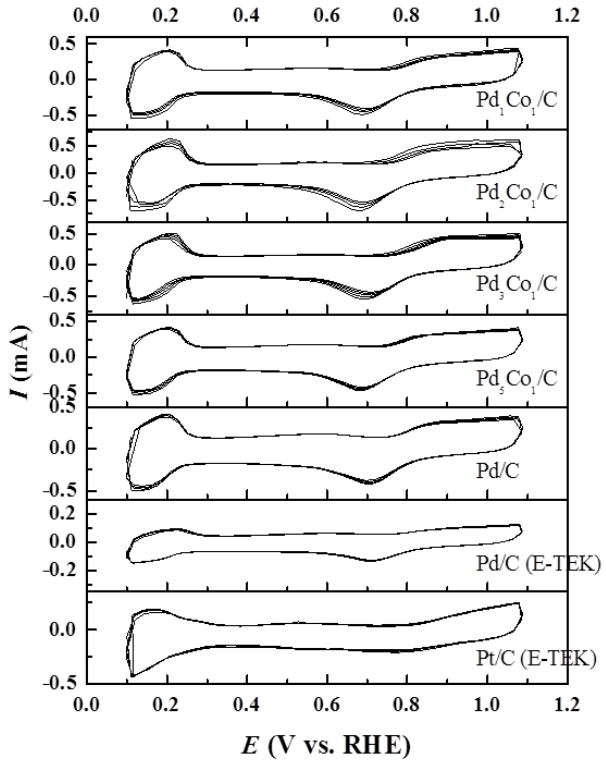

Figure 4.36 Cyclic voltammograms of commercial catalysts (E-TEK) and various compositions of carbon supported Pd-Co catalyst synthesized by ultrasonic spray reaction method in nitrogen purged 0.05 mol.dm^{-3} H_2SO_4 at 298K

Figure 4.37 shows the slow scan voltammograms of the ORR on commercial catalysts (E-TEK) and various compositions of carbon supported Pd-Co catalyst synthesized by ultrasonic spray reaction method in oxygen purged 0.05 mol dm^{-3} H_2SO_4 at 298K.The curves are plotted according to the variation of the electro-catalytic activity for the ORR of the electro catalyst expressed in mAmg^{-1} (Pt or Pd) on the electrode potential. From this graph the potential at 0.015mA/mg (Pt or Pd) which is almost the onset potential changes with, of course, the type of the sample. The values of this potential are shown in table 3(first column) for various electro catalysts. Pt exhibited of course the highest value for this potential because it is the best electro-catalyst for this reaction. Based on the values of this potential, the Pd-Co alloy electro catalysts obtained in this work exhibited less activity for the ORR than Pt electro catalyst. The results also

show that the ORR activity on these Pd-Co alloys is higher than those on Pd. These results might be correlated to kinetics parameters deduced from the Tafel slopes.

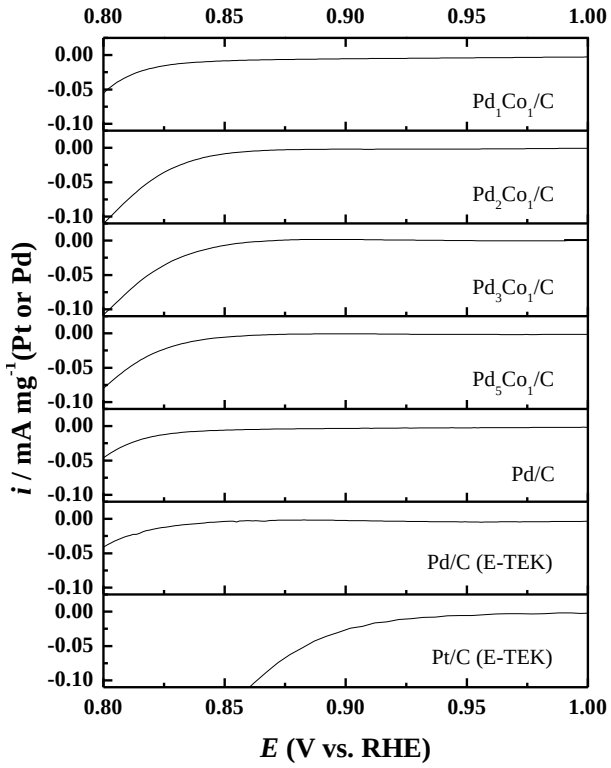

Figure 4.37 Slow scan voltammograms of commercial catalysts (E-TEK) and various compositions of carbon supported Pd-Co catalyst synthesized by ultrasonic spray reaction method in oxygen purged 0.05 mol.dm^{-3} H_2SO_4 at 298K.

Figure 4.38 shows the mass activities of the various electro-catalysts for three different potentials. Pt electro catalyst exhibits, of course the best mass activity for the different potentials. The mass activity of Pt/C (0.15 mA.mg^{-1} Pt vs. 0.85V vs RHE) obtained here and in our previous work [53] is slightly higher, but in the same agreement to those obtained recently in the literature (0.05-0.12 mAmg^{-1} Pt at 0.93 V vs. RHE) [127]. On the other hands the mass activity of the commercial Pd/C electro-catalyst is slightly smaller than those of the Pd/C prepared in this work. This indicates that when good electro catalysts are prepared with the method of this work, it might exhibit better electro catalytic properties than the same electro catalyst prepared by the classical method. Fig 14 shows the variation of the mass activity with the Pd content. This Figure exhibits

Volcano behaviour and the optimum value of the mass activity is obtained for the Pd_3Co sample which is the best electro catalyst for this reaction. This is in agreement with a lot of results in the literature which show clearly that Pd_3Co is the best electro catalyst for the ORR toward the Pd-Co alloys [3, 36, 41, 50].

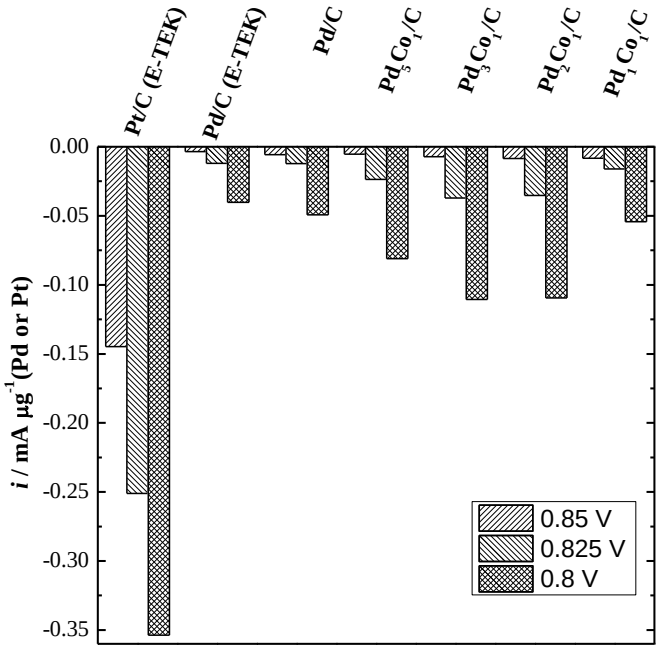

Figure 4.38 Comparison of current densities at various potentials of commercial catalysts (E-TEK) and synthesized Pd and Pd-Co catalyst synthesized by ultrasonic spray reaction method.

Figure 4.39 shows the Tafel plots of the ORR deduced from Fig 10 in the potential ranges of 0.77 to 0.97 V (versus RHE) depending of the electro-catalyst where linear behaviour between Log (*i*) vs *E* is obtained. The deduced values of the Tafel slopes and the exchange current density divided by the active mass of the electro-catalyst (Pt or Pd) are shown in the second and the third columns of Table 4.4. The value of the Tafel slope of Pt obtained here is in agreement of those obtained elsewhere [3, 36, 41, 50]. This indicates that the values of the Tafel slopes obtained here can be used to discuss on the mechanism of the ORR on the palladium alloy.

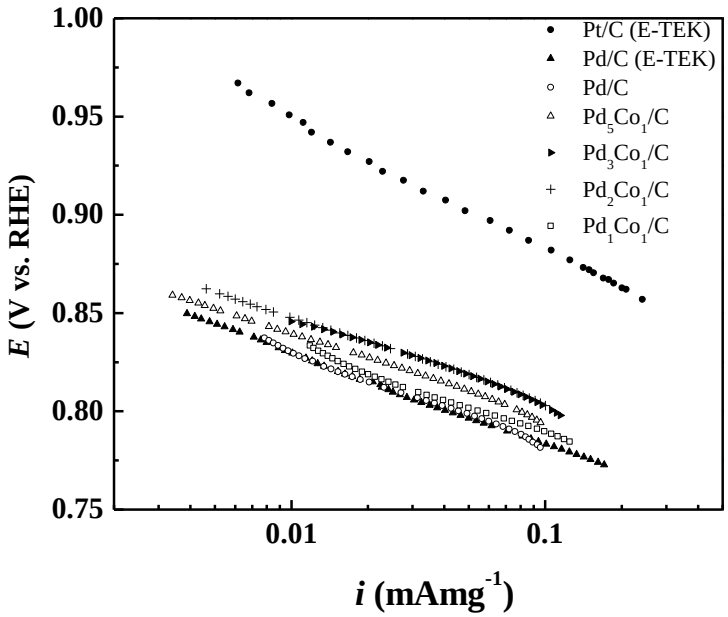

Figure 4.39 Tafel slopes of commercial catalysts (E-TEK) and synthesized Pd and Pd-Co catalyst by ultrasonic spray reaction method in oxygen p urged 0.05 mol dm^{-3} H_2SO_4 at 298K.

Table 4.4 Tafel slopes in low and high currenty density regions and calculated exchange currents densities of Pt, Pd and Pd-Co catalysts fabricated by sputtering method.

Sample	**Tafel slope at low current density mV/decade**	**Tafel slope at high current density mV/decade**	**Exchange current density mA.cm^{-2}**
Pt	69	130	7.94×10^{-6}
Pd	47	80	3.72×10^{-9}
$Pd_{75}Co_{25}$	50	79	1.58×10^{-8}
$Pd_{65}Co_{35}$	48	80	1.10×10^{-8}
$Pd_{50}Co_{50}$	58	82	2.00×10^{-7}
$Pd_{48}Co_{58}$	38	68	3.02×10^{-11}
$Pd_{16}Co_{84}$	34	63	1.35×10^{-12}

It is well known that the Tafel slope value is a kinetic parameter which is useful to propose the type or process involved in the rate determining step (RDS) of the reaction. The first electron transfer step which yields a Tafel slope of 120 mV/decade(at high current density) is known as the rate-determining step of the ORR on platinum electrode in acid medium [128]. Furthermore it was indicated that the ORR kinetics on Pt is different from those on Pd-based electro-catalysts. It was found that the ORR rate-determining step on Pd and Pd-Co catalysts may involve the breaking of the oxygen bond [101]. Another parameter which is very important in the ORR kinetics is the number of electron involved in this reaction. The knowledge of this parameter may help to find a possible expression which will sustain the possible mechanism of the overall process.

The variation of the total experimental current of the ORR at potential of 0.4 V up on the rotating speed of the electrode can be expressed in the form of a Koutecky-Levich plot. These plots are shown in Figure 4.40 for the rotating disk electrode coated with Pt/C, Pd/C and $Pd_{65}Co_{35}$/C. This behaviour is well known and indicates clearly that the total ORR current could be split in two terms, one relative to the kinetic current (i_k) and the other one relative to the diffusion limiting current (i_{lim}) [13, 129] as following:

$$\frac{1}{i} = \frac{1}{i_k} + \frac{1}{i_{lim}}$$

Eq. 4.5

Or

$$\frac{1}{I} = \frac{1}{I_k} + \frac{1}{B\omega^{1/2}}$$

Eq. 4.6

and:

$$i_{lim} = B\omega^{1/2}$$

Eq. 4.7

where I is the total experimental observed current, I_k is the kinetic current, B is equal to $0.62nFAC_{O_2}^{*}\left(D_{O_2}\right)^{\frac{2}{3}} v^{-\frac{1}{6}}$, ω is the rotation speed in rad s^{-1}, F is the Faraday constant 96485 $C.mol^{-1}$, A is the electrode are, $C_{O_2}^{*}$is the concentration of oxygen at bulk (1.2×10^{-6} $mol.cm^{-3}$), $D_{O_2}$is the diffusion coefficient of oxygen (1.4×10^{-5} $cm^2.s^{-1}$) and$v$ is the kinetic viscosity of the electrolyte (0.01 $cm^2.s^{-1}$) [115]. The value of n=4 is used to plot the theoretical lower line in Fig. 16 for the ORR on Pt with a Tafel slope of 60 mV/dec.. As described above, the ORR over Pt electrode surface passes through the four-electron pathway. Since all the plots presented the same slopes with Pt which is *n*=4 pathway, the ORR on Pd-Co/C catalysts also passes through the four-electron pathway. This results show a good agreement with the results described elsewhere [39, 40, 116]. If the ORR is catalysed through four transferred electrons on Pd–Co alloys and Pt, the Tafel slope values are different from measurements made in the same conditions. The values of the Tafel slope we obtained here on Pt (63 mV/dec) is similar to those reported elsewhre and which are in the range of 75–86 mV/dec for Pt and bimetallic Pt alloy prepared by sputtering [36]. This difference is related to the reduction pathway they proposed, for which, the rate determining step is an electron transfer reaction

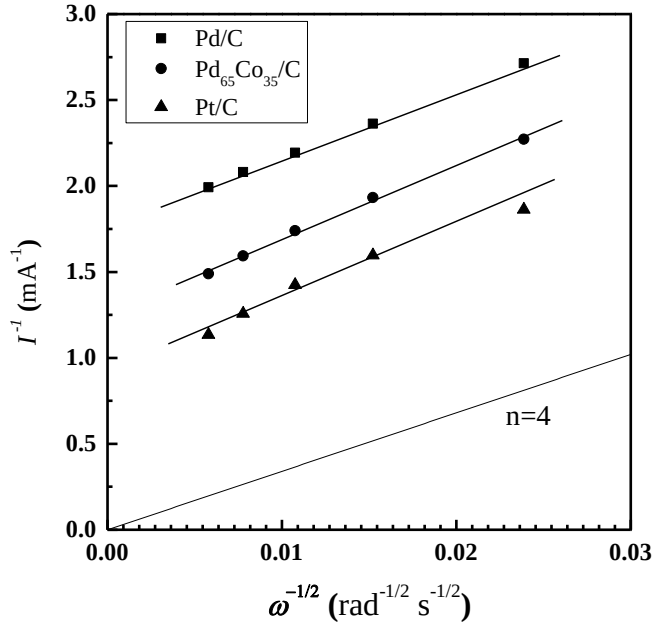

Figure 4.40 Koutecky–Levich plot of Pt/C, Pd/C and $Pd_{65}Co_{35}$/C at 0.4V vs. RHE.

Accordingly, the results obtained here suggest that the ORR on Pd-Co/C catalysts proceed through the four-electron pathway as following if Co of the electro-catalysts contributes to the adsorption of OOHads on Co and then the formation of PdOCoOH according to the following reactions, the rate determining step being reactions (6) [37]:

$$Pd+Co+O_2+H^+ + e^- + \rightarrow PdOCoOH_{ads}$$

Eq. 4.8

$$PdOCoOH_{ads} \rightarrow PdO_{ads} + CoOH_{ads}$$

Eq. 4.9

$$PdO_{ads} + CoOH_{ads} + 3H^+ + 3e^- \rightarrow Pd + Co + 2H_2O$$

Eq. 4.10

This mechanism shows the restitution of the Pd +Co electrode and may explain why significant oxide was detected by XPS analysis.

4.3.4 Conclusion

The Ultrasonic Direct Solution Spray Reaction method with homemade vertical furnace catalyst maker has been developed for carbon supported nano-scale palladium-cobalt binary alloy catalysts. The chemical composition of the alloys can be varied by varying the concentrations of palladium and cobalt precursors in the slurry. These catalysts have fcc structures of substitutional solid solutions replaced by Co atoms. According to the previous work on carbon supported Pd-Co based catalysts, the new technique on this study has very high potential for well defined catalyst particles; narrow distribution range (2.5-6.5 nm) and relatively small particle size (4.0-4.5 nm) in comparison to the classical method which particle size can range from 5 to 90 nanometers. The best electro-catalyst of the ORR on Pd-Co alloys is Pd_3Co. The number of electron involved in the ORR is 4. We conclude that our Ultrasonic Direct Solution Spray Reaction method with homemade vertical furnace catalyst maker has high potential toward low catalyst loading for fuel cell applications.

CHAPTER 5 GENERAL DISCUSSION

Pd-Co thin films in a wide range of chemical compositions (0 to 84 atomic % of Co) were prepared on glassy carbon substrate by the RF sputtering technique. The objectives in this section are to find the optimized chemical composition of Pd-Co alloy for the ORR and to investigate the fundamental electrochemical properties such as the amount of oxide formation/reduction, the amount of hydrogen adsorption and oxide reduction peak position of Pd and Pd-Co alloy catalysts which have never been done before. Their correlations to ORR catalytic activities in acid medium were also examined. Enhancements of catalytic activities for the ORR by Pd-Co binary alloys were confirmed as presented in the previous studies. $Pd_{65}Co_{35}$ alloy gives the highest ORR activity, followed by $Pd_{75}Co_{25}$ and $Pd_{50}Co_{50}$ alloys. No obvious activity enhancements were found for $Pd_{42}Co_{58}$ and $Pd_{16}Co_{84}$, which have higher Co content. There is a linear correlation between the amount of hydrogen adsorption and ORR catalytic activities on Pd-Co alloys. Catalysts having more Co content have lower ORR activities between Pd-Co alloys. With regard to the correlation between the amount of oxide formation/reduction and ORR activities, no linear correlation could be found, but the optimized atomic ratio between Pd and Co for ORR in acid medium was found to be around Pd:Co = 3:1 from these results. This can be considered as an effect of alloying and oxide formation on the electrode surface.

In the second section, the ultrasonic spray reaction method was developed for carbon-supported nano-scale catalysts for PEMFC application. This technique is very new and unique for the application. Carbon supported Pt catalysts were firstly synthesized by using the technique for the optimization of parameters for the catalyst synthesis process. From the TEM images of the synthesized Pt/C catalysts, the mean particle size of the Pt nano-particles increases from 3.4 nm when the catalyst reactor is at 400ºC to 4.7 nm when the reactor is at 700 ºC. The formation of the small Pt nano-particles is obtained at the optimized synthesis temperatures of 400°C. This technique was successfully developed for nano-scale carbon supported catalyst synthesis. In addition, by using carbon paper as a filter of ultrasonic spray reaction method as described in Figure 4.2, carbon supported catalyst are directly deposited onto the carbon paper. It permits to fabricate catalyzed GDE directly. As described in Figure 4.1, fabrication of the GDE includes many steps and each step has to be improved if we want to get an optimized GDE. The classical method for preparing a GDE involves at least seven steps from the slurry preparation process to the synthesized GDE drying process. Firstly, carbon supported catalysts have to be synthesized

by impregnation method or other methods. This step includes so many parameters to be optimized and takes long time, at least 20 hours from the beginning until obtaining the dried carbon supported catalysts. Then the synthesized catalysts was dispersed in an organic solvent and applied onto gas diffusion layer which is normally porous carbon paper or carbon cloth, and then is dried in an oven slowly, because cracks can form in the catalyst layer with fast drying process. The formation of cracks is not desired due to loss of contact area between proton exchange membrane and electrode and cause the loss of performance. This process takes additional 6 hours, so the process of obtaining a catalyzed GDE takes minimum of 26 hours. On the other hand, the catalyzed GDE fabricated by using the ultrasonic spray reaction method , no crack was formed on the surface and the homogeneous catalyst layer are produced as shown in Figure 4.3 and Figure 4.4. This is one of the remarkable advantages of this technique of course, but the most important point of this technique is that the fabrication process time is much shorter than the classical method described above, less than 30 minutes including the catalyst synthesis process and GDE fabrication process. Consequently, when the number of GDE preparation steps and time can be drastically reduced by using this technique for GDE fabrication, the cost of PEMFC is also able to be decreased. The new technique has been successfully developed not only for nano-scale carbon-supported catalyst synthesis but also catalyzed GDE fabrication directly in this section.

In the final section, the developed ultrasonic spray reaction technique for the carbon supported catalysts was applied for carbon supported Pd-Co catalysts synthesis and this is the goal of this study. Fundamental electrochemical properties and optimized composition of Pd-Co electro-catalysts were obtained by using the Pd-Co thin films in the first section of this study. The Pd-Co alloy catalysts of the chemical composition of around Pd:Co=3:1 exhibited the highest ORR activity. In the second section, the new catalyst fabrication process of ultrasonic spray reaction was developed successfully. Fine catalyst particles were well formed on the high surface area carbon support. Optimized operational temperature was defined to be around 400°C to obtain the minimum particle size of the catalysts, and the size was increased with increasing the heat treatment temperature. These two studies were combined in the last section to achieve the goal of this study. Carbon supported Pt, Pd and Pd-Co catalysts were synthesized and characterised for ORR activity. TEM images indicate that this technique is very useful for preparing carbon supported nano-scale catalysts having the dominant particle size of 2.5-4.5 nm. Fine catalyst

particles supported on high surface area carbon powder are essential to apply the catalyst as the PEMFC cathode materials for the commercialization. This is a remarkable result which has never been successfully established in terms of fuel cell technology. XRD showed diffraction peaks which consistent with face-centered cubic (fcc) structure for Pt. XRD of the synthesized Pd and Pd-Co catalysts by ultrasonic spray reaction also indicated fcc crystal system. All diffractograms of the samples are similar to the one of fcc Pd, but the Co-origin peaks cannot be found. The Pd-Co system is substitutional solid solutions, so some Pd atoms are replaced by Co atoms. The solid solution system is considered to be stable in acid media [1]. From the TEM-EELS analysis, Catalytic activity enhancements of the ORR for the synthesized Pd-Co catalysts by ultrasonic spray reaction method are confirmed. The ORR current of Pd_3Co_1/C and Pd_2Co_1/C were almost the same and show the highest current at the all potentials between Pd and Pd-Co catalysts followed by Pd_5Co_1/C, Pd_1Co_1/C and Pd/C. This result has good agreement with the ORR activity enhancement of the thin film synthesized by sputtering technique. From the facts that the optimized compositions obtained from the results of the Pd-Co thin films and carbon supported catalysts are the same, it can be concluded that the catalyst synthesis process by using sputtering method is an effective way as a preliminary work of developing new electro-catalysts for PEMFC. Since the sputtering technique has several advantages, for example, the chemical composition of the multi-element thin film can be easily control regardless of melting point or vapor pressure, any kinds of materials such as metal, ceramics, nitride and oxide can be used as a target, deposition can be made on flat or rounded surface, it makes it possible to find an optimized compositions out within a short time and without big effort. It helps to avoid a time and money consuming.

All Pd based catalysts have around 45mV/dec of tafel slope and Pd mass corrected exchange current around 10^{-11} $mA.mg^{-1}$. It is assumed that the ORR kinetics in this potential region are the same among the Pd and Pd based catalysts and the addition of Co into Pd have small effect on the ORR kinetics. We conclude that ultrasonic spray reaction method with piezoelectric transducer is applicable for Pd-Co binary alloy catalyst synthesis and the activity enhancement effect caused by alloying with Co was confirmed on the synthesized catalyst by this technique.

Table 5.1 summarize the mass activity of commercial Pt and Pd purchased from E-TEK, and the synthesized Pd-Co and Pd catalysts by the ultrasonic spray reaction technique. All the current at various potentials were normalized by using the activity of Pt catalysts. The two compositions of

the catalysts; Pd_3Co_1/C and Pd_2Co_1/C exhibited the highest ORR activities between the Pd-based catalysts. The activities of these two catalysts were about 2.5 times larger than Pd/C catalysts at 0.8 V, but it's about one-third of that of Pt/C. Minimum of 1 $mg.cm^{-2}$ is required for operating PEMFC single cell, the cost of precious metal of Pt/C cathode will be 0.0564 $USD.cm^{-2}$ considering that the price of Pt was about 56.4 $USD.g^{-1}$ as of December 2011. Since the ORR activity of Pd/C catalyst was about one-ninth of Pt/C, minimum of 9 $mg.cm^{-2}$-Pd is required to replace all Pt by Pd and to obtain the same performance of PEMFC. Therefore the cost of precious metal is calculated as 0.191 $USD.cm^{-2}$ considering that the price of Pd is 21.2 $USD.g^{-1}$. In this case, the cost of PEMFC with Pd/C becomes 3.4 times higher than existing technology. On the other hand, only 3 $mg.cm^{-2}$-Pd is required if these Pd-Co alloy catalysts are used as the cathode materials. The cost of precious metal is 0.0636 $USD.cm^{-2}$, so it's still slightly higher than that of Pt/C. However the price of Pt is unstable due to its high demand for environmental applications and economical investments, it's possible that its price will hike up in near future. The depletion of Pt reserve is a problem also. For these reasons, PEMFC technology cannot be solely based on Pt and Pd-Co alloy catalysts can be alternative materials for the PEMFC catalysts.

Table 5.1 Comparison of the ORR mass activity

	0.850V	**0.825V**	**0.800V**
Pt/C (E-TEK)	1	1	1
Pd/C (E-TEK)	0.024	0.048	0.114
Pd/C	0.040	0.048	0.139
Pd_5Co_1/C	0.036	0.094	0.229
Pd_3Co_1/C	0.050	0.148	0.313
Pd_2Co_1/C	0.059	0.140	0.309
Pd_1Co_1/C	0.057	0.064	0.153

Table 5.2 Cost of precious metal for PEMFC cathod

	Cost USD.cm^{-2}
Pt/C	0.0564
Pd/C	0.191
Pd_3Co_1/C	0.0636

CONCLUSION AND RECOMMENDATIONS

We developed a homemade vertical furnace catalyst maker in which the ultrasonic spray device was used for the catalyst preparation. This allows the fabrication of carbon-supported catalysts with smaller particle sizes than those of catalysts made by the classic processes. This new method can be also used for the *in-situ* deposition of the catalyst on a carbon cloth or paper during the same process without altering the catalyst properties. The approach we have just presented opens the way to *in-situ* catalyzed electrode fabrication. This study showed the potential of ultrasonic spray reaction method for direct preparation of the gas diffusion electrode. From micrographic results, we conclude that this method is suitable for the application of catalyzed GDE, and it was shown that the properties of the catalysts changed with synthesis temperature. Interatomic d-spacing was varied by heat-treatment temperatures, and it caused differences in electrocatalytic activity for the oxygen reduction reaction.

Electrochemical properties of Pd-Co alloy catalysts synthesized by physical vapor deposition technique and their correlations to ORR catalytic activities in acid medium were examined in this study. Enhancements of catalytic activities for ORR by Pd-Co binary alloys were confirmed. $Pd_{65}Co_{35}$ alloy gives the highest ORR activity followed by $Pd_{75}Co_{25}$ and $Pd_{50}Co_{50}$ alloys. No obvious activity enhancements were found for $Pd_{42}Co_{58}$ and $Pd_{16}Co_{84}$, which have higher Co content. There is a linear correlation between hydrogen charges and ORR catalytic activities on Pd-Co alloys. Catalysts having more Co content have lower ORR activities. With regard to the correlation between the amount of oxide formation and oxide reduction and ORR activities, no linear correlation could be found. However, the optimized atomic ratio between Pd and Co for ORR in acid medium was found to be around Pd:Co = 3:1 from these results.

We apply the ultrasonic spray reaction technique to the fabrication of carbon-supported nano-scale Pd-Co alloy catalysts. Five different compositions of the catalysts were synthesized; palladium loading of all the samples was in the range of 13.5 to 17.8 wt %, and cobalt loadings were controlled in the range between 0 and 10.3 wt %. From the results of TEM images, catalyst particles were highly dispersed on the carbon support, and agglomerated particles can rarely be found for all synthesized catalysts by the spray method. The dominant particle sizes are between 2.5 and 6.5 nm for all samples. Comparing the synthesized catalysts in this work and in that of other research groups, it can be seen that the synthesized catalysts in this study have a very

narrow range of particle size distribution and small average particle size. It would improve catalyst utilization and specific surface area toward low-catalyst loadings. The crystal structure of the synthesized catalysts were fcc substitutional solid solutions, and this system is considered to be stable in acid medium. The ORR activities of Pd_3Co_1/C and Pd_2Co_1/C were almost the same and show the highest current between Pd and Pd-Co catalysts followed by Pd_5Co_1/C, Pd_1Co_1/C and Pd/C.

This study contributes to the advancement of the knowledge of fundamental properties of Pd-Co alloy catalysts and their correlations to the oxygen reduction reaction activities. In addition, the ultrasonic spray reaction method developed in this study contributes significantly to an industrial fabrication process of catalyzed gas diffusion electrodes for PEMFCs. The synthesis method of small particle size (φ2-4nm) Pd-Co alloy catalysts were not possible to be obtained by using the existing conventional methods, however I have achieved to synthesize the fine particle catalysts supported on carbon supports by using the ultrasonic spray reaction method. These results would be an essential technology for the commercialization of PEMFCs with Pd-Co alloy catalysts in the future.

LIST OF REFERENCES

[1] T. Mallat, *et al.*, "Investigation of Pd + Co alloys by the linear potential sweep method," *Journal of Electroanalytical Chemistry,* vol. 208, pp. 169-173, 1986.

[2] W. R. Grove, "On Voltaic Series and the Combination of Gases by Platinum," *Philosophical Magazine and Journal of Science,* vol. 14, p. 4, 1839.

[3] O. Savadogo, *et al.*, "New palladium alloys catalyst for the oxygen reduction reaction in an acid medium," *Electrochemistry Communications,* vol. 6, pp. 105-109, Feb 2004.

[4] T. Uematsu and S. Shimazu, *Shokubai,* vol. 36, p. 252, 1994.

[5] D. Li, *et al.*, "Catalytic properties of sprayed Ru/Al2O3 and promoter effects of alkali metals in CO2 hydrogenation," *Applied Catalysis A: General,* vol. 172, pp. 351-358, 1998.

[6] D. Li, *et al.*, "Hydrogenation of CO2 over sprayed Ru/TiO2 fine particles and strong metal-support interaction," *Applied Catalysis A: General,* vol. 180, pp. 227-235, 1999.

[7] H. A. Gasteiger, *et al.*, "Activity benchmarks and requirements for Pt, Pt-alloy, and non-Pt oxygen reduction catalysts for PEMFCs," *Applied Catalysis B-Environmental,* vol. 56, pp. 9-35, Mar 10 2005.

[8] B. E. Conway, *et al., Thermodynamic and transport properties of aqueous and molten electrolytes*. New York: Plenum Press, 1983.

[9] J. Lipkowski and P. N. Ross, *Electrocatalysis*. New York: Wiley-VCH, 1998.

[10] D. A. J. Rand and R. Woods, "A study of the dissolution of platinum, palladium, rhodium and gold electrodes in 1 m sulphuric acid by cyclic voltammetry," *Journal of Electroanalytical Chemistry,* vol. 35, pp. 209-218, 1972.

[11] P. Bindra, *et al.*, "Platinum Dissolution in Concentrated Phosphoric Acid," *Journal of the Electrochemical Society,* vol. 126, pp. 1631-1632, 1979.

[12] J. K. Norskov, *et al.*, "Origin of the overpotential for oxygen reduction at a fuel-cell cathode," *Journal of Physical Chemistry B,* vol. 108, pp. 17886-17892, Nov 18 2004.

[13] A. J. Bard and L. R. Faulkner, *Electrochemical methods : fundamentals and applications*, 2nd ed. New York: John Wiley, 2000.

[14] E. Yeager, "Electrocatalysts for O2 reduction," *Electrochimica Acta,* vol. 29, pp. 1527-1537, 1984.

[15] A. Damjanovic, *et al.*, "Distinction between Intermediates Produced in Main and Side Electrodic Reactions," *The Journal of Chemical Physics,* vol. 45, pp. 4057-4059, 1966.

[16] A. Damjanovic and V. Brusic, "Electrode kinetics of oxygen reduction on oxide-free platinum electrodes," *Electrochimica Acta,* vol. 12, pp. 615-628, 1967.

[17] V. S. Bagotskii, *et al.*, *Elektrochimiya,* vol. 8, p. 84, 1972.

[18] H. S. Wroblowa, *et al.*, "Electroreduction of oxygen: A new mechanistic criterion," *Journal of Electroanalytical Chemistry,* vol. 69, pp. 195-201, 1976.

[19] N. A. Anastasijevic, *et al.*, "Determination of the kinetic parameters of the oxygen reduction reaction using the rotating ring-disk electrode : Part I. Theory," *Journal of Electroanalytical Chemistry,* vol. 229, pp. 305-316, 1987.

[20] J. S. Griffith, "On the magnetic properties of some haemoglobin complexes," *Proceedings of the Royal Society of London, Series A (Mathematical and Physical Sciences),* vol. 235, pp. 23-36, 1956.

[21] L. Pauling, "Nature of the Iron–Oxygen Bond in Oxyhæmoglobin," *Nature,* vol. 203, pp. 182-183, 1964.

[22] E. Yeager, "Recent Advances in the Science of Electrocatalysis," *Journal of the Electrochemical Society,* vol. 128, pp. 160C-171C, 1981.

[23] E. Yeager, *et al.*, *The electrolyte factor in O2 reduction electrocatalysis*. Pennington, NJ: Electrochemical Society, 1992.

[24] J. Schmidt, *et al.*, "Oxygen-Adsorption on the Pt(110)(1x2) Surface Studied with Eels," *Surface Science,* vol. 284, pp. 121-128, Mar 10 1993.

[25] A. C. Luntz, *et al.*, "Sequential Precursors in Dissociative Chemisorption - O-2 on Pt(111)," *Physical Review B,* vol. 39, pp. 12903-12906, Jun 15 1989.

[26] B. N. Grgur, *et al.*, "Underpotential deposition of lead on Pt(111) in perchloric acid solution: RRDPt(111)E measurements," *Langmuir,* vol. 13, pp. 6370-6374, Nov 26 1997.

[27] N. M. Markovic, *et al.*, "Surface electrochemistry of CO and H-2/CO mixtures at Pt(100) interface: Electrode kinetics and interfacial structures," *Journal of Physical Chemistry B,* vol. 103, pp. 9616-9623, Nov 4 1999.

[28] H. A. Gasteiger and P. N. Ross, "Oxygen Reduction on Platinum Low-Index Single-Crystal Surfaces in Alkaline Solution: Rotating Ring DiskPt(hkl) Studies," *The Journal of Physical Chemistry,* vol. 100, pp. 6715-6721, 1996.

[29] N. M. Markovi, *et al.*, "Oxygen Reduction Reaction on Pt and Pt Bimetallic Surfaces: A Selective Review," *Fuel Cells,* vol. 1, pp. 105-116, 2001.

[30] A. J. Appleby, "Oxygen reduction at smooth pre-reduced gold and iridium electrodes in 85% orthophosphoric acid," *Journal of Electroanalytical Chemistry* vol. 27, p. 10, 1970.

[31] D. S. Gnanamuthu and J. V. Petrocelli, "A Generalized Expression for the Tafel Slope and the Kinetics of Oxygen Reduction on Noble Metals and Alloys," *Journal of the Electrochemical Society,* vol. 114, p. 6, 1967.

[32] A. J. Appleby, "Oxygen reduction on platinum-ruthenium alloy electrodes in 85% orthophosphoric acid," *Journal of Electroanalytical Chemistry,* vol. 27, p. 8, 1970.

[33] T. Toda, *et al.*, "Enhancement of the electroreduction of oxygen on Pt alloys with Fe, Ni, and Co," *Journal of the Electrochemical Society,* vol. 146, pp. 3750-3756, Oct 1999.

[34] U. A. Paulus, *et al.*, "Oxygen reduction on carbon-supported Pt-Ni and Pt-Co alloy catalysts," *Journal of Physical Chemistry B,* vol. 106, pp. 4181-4191, Apr 25 2002.

[35] U. A. Paulus, *et al.*, "Oxygen reduction on high surface area Pt-based alloy catalysts in comparison to well defined smooth bulk alloy electrodes," *Electrochimica Acta,* vol. 47, pp. 3787-3798, Aug 30 2002.

[36] O. Savadogo, *et al.*, "Investigation of some new palladium alloys catalysts for the oxygen reduction reaction in an acid medium," *Journal of New Materials for Electrochemical Systems,* vol. 7, pp. 77-83, Apr 2004.

[37] J. L. Fernandez, *et al.*, "Pd-Ti and Pd-Co-Au electrocatalysts as a replacement for platinum for oxygen reduction in proton exchange membrane fuel cells," *Journal of the American Chemical Society,* vol. 127, pp. 13100-13101, Sep 28 2005.

[38] V. Raghuveer, *et al.*, "Comparison of Pd-Co-Au electrocatalysts prepared by conventional borohydride and microemulsion methods for oxygen reduction in fuel cells," *Electrochemistry Communications,* vol. 8, pp. 807-814, May 2006.

[39] M. H. Shao, *et al.*, "Palladium monolayer and palladium alloy electrocatalysts for oxygen reduction," *Langmuir,* vol. 22, pp. 10409-10415, Dec 5 2006.

[40] L. Zhang, *et al.*, "The effect of heat treatment on nanoparticle size and ORR activity for carbon-supported Pd-Co alloy electrocatalysts," *Electrochimica Acta,* vol. 52, pp. 3088-3094, Feb 15 2007.

[41] K. Lee, *et al.*, "Methanol-tolerant oxygen reduction electrocatalysts based on Pd-3D transition metal alloys for direct methanol fuel cells," *Journal of the Electrochemical Society,* vol. 153, pp. A20-A24, 2006.

[42] A. Heinzel and V. M. Barragan, "A review of the state-of-the-art of the methanol crossover in direct methanol fuel cells," *Journal of Power Sources,* vol. 84, pp. 70-74, Nov 1999.

[43] M. Neergat, *et al.*, *Handbook of fuel cells : fundamentals, technology, and applications* vol. 4. Chichester, England ; New York: Wiley, 2003.

[44] D. Chu and R. Z. Jiang, "Novel electrocatalysts for direct methanol fuel cells," 2002, pp. 591-599.

[45] W. M. Wang, *et al.*, "Carbon-supported Pd-Co bimetallic nanoparticles as electrocatalysts for the oxygen reduction reaction," *Journal of Power Sources*, vol. 167, pp. 243-249, May 15 2007.

[46] H. Liu and A. Manthiram, "Tuning the electrocatalytic activity and durability of low cost Pd70Co30 nanoalloy for oxygen reduction reaction in fuel cells," *Electrochemistry Communications*, vol. 10, pp. 740-744, May 2008.

[47] L. Zhang, *et al.*, "Effect of synthetic reducing agents on morphology and ORR activity of carbon-supported nano-Pd-Co alloy electrocatalysts," *Electrochimica Acta*, vol. 52, pp. 7964-7971, Nov 1 2007.

[48] J. Mathiyarasu and K. L. N. Phani, "Carbon-supported palladium-cobalt-noble metal (Au, Ag, Pt) nanocatalysts as methanol tolerant oxygen-reduction cathode materials in DMFCs," *Journal of the Electrochemical Society*, vol. 154, pp. B1100-B1105, 2007.

[49] S. Tominaka, *et al.*, "Electrodeposited Pd-Co catalyst for direct methanol fuel cell electrodes: Preparation and characterization," *Electrochimica Acta*, vol. 53, pp. 4679-4686, May 30 2008.

[50] X. W. Li, *et al.*, "Low temperature preparation of carbon-supported Pd-Co alloy electrocatalysts for methanol-tolerant oxygen reduction reaction," *Electrochimica Acta*, vol. 53, pp. 6662-6667, Sep 20 2008.

[51] Y. C. Wei, *et al.*, "The structure-activity relationship of Pd-Co/C electrocatalysts for oxygen reduction reaction," *International Journal of Hydrogen Energy*, vol. 35, pp. 1864-1871, Mar 2010.

[52] S. Zuluaga and S. Stolbov, "Factors controlling the energetics of the oxygen reduction reaction on the Pd-Co electro-catalysts: Insight from first principles," *Journal of Chemical Physics*, vol. 135, Oct 7 2011.

[53] K. Oishi and O. Savadogo, "New Method of Preparation of Catalyzed Gas Diffusion Electrode for Polymer Electrolyte Fuel Cells Based on Ultrasonic Direct Solution Spray Reaction," *Journal of New Materials for Electrochemical Systems*, vol. 11, p. 7, 2008.

[54] S. Iijima, "Helical Microtubules of Graphitic Carbon," *Nature*, vol. 354, pp. 56-58, Nov 7 1991.

[55] T. Yoshitake, *et al.*, "Preparation of fine platinum catalyst supported on single-wall carbon nanohorns for fuel cell application," *Physica B-Condensed Matter*, vol. 323, pp. 124-126, Oct 2002.

[56] X. G. Li and I. M. Hsing, "The effect of the Pt deposition method and the support on Pt dispersion on carbon nanotubes," *Electrochimica Acta,* vol. 51, pp. 5250-5258, Jul 28 2006.

[57] A. Caillard, *et al.*, "Improvement of the sputtered platinum utilization in proton exchange membrane fuel cells using plasma-based carbon nanofibres," *Journal of Physics D-Applied Physics,* vol. 41, pp. -, Sep 21 2008.

[58] A. T. Haug, *et al.*, "Increasing proton exchange membrane fuel cell catalyst effectiveness through sputter deposition," *Journal of the Electrochemical Society,* vol. 149, pp. A280-A287, Mar 2002.

[59] T. R. Ralph and M. P. Hogarth, "Catalysis for Low Temperature Fuel Cells " *Platinum Metals Review,* vol. 46, pp. 117-135, 1 July 2002 2002.

[60] A. J. Appleby, *Cata. Rev.*, vol. 4, 1970.

[61] O. Savadogo and F. J. Rodriguez Varela, "Ethanol-tolerant Oxygen Reduction Reaction (ORR) cathodes for direct ethanol fuel cell applications," in *208th Meeting of the Electrochemical Society, October 16, 2005 - October 21, 2005*, Los Angeles, CA, United states, 2005, pp. 331-338.

[62] O. Savadogo and F. J. Rodriguez Varela, "Palladium-alloy catalysts as ethanol tolerant cathodes for Direct Alcohol Fuel Cell (DEFC) applications," in *208th Meeting of the Electrochemical Society, October 16, 2005 - October 21, 2005*, Los Angeles, CA, United states, 2005, pp. 247-254.

[63] S. Gottesfeld and T. A. Zawodzinski, "Polymer Electrolyte Fuel Cells," in *Advances in Electrochemical Science and Engineering*: Wiley-VCH Verlag GmbH, 2008, pp. 195-301.

[64] B. Hammer and J. K. Norskov, "Theoretical surface science and catalysis - Calculations and concepts," *Advances in Catalysis, Vol 45,* vol. 45, pp. 71-129, 2000.

[65] A. Ruban, *et al.*, "Surface electronic structure and reactivity of transition and noble metals," *Journal of Molecular Catalysis a-Chemical,* vol. 115, pp. 421-429, Feb 7 1997.

[66] A. V. Ruban, *et al.*, "Surface segregation energies in transition-metal alloys," *Physical Review B,* vol. 59, p. 15990, 1999.

[67] B. S. Mun, *et al.*, "A study of electronic structures of Pt3M (M=Ti,V,Cr,Fe,Co,Ni) polycrystalline alloys with valence-band photoemission spectroscopy," *Journal of Chemical Physics,* vol. 123, pp. -, Nov 22 2005.

[68] T. J. Schmidt and H. A. Gasteiger, *Rotating thin-film method for supported catalysts*: John Wiley & Sons, Ltd, 2010.

[69] V. Stamenkovic, *et al.*, "Oxidation of CO and surface properties of well characterized Pt3Sn bimetallic alloy surfaces," *Journal of New Materials for Electrochemical Systems*, vol. 7, pp. 125-132, Apr 2004.

[70] L. Fan, *et al.*, "Characteristics of supported gold catalysts prepared by spray reaction method," in *Studies in Surface Science and Catalysis*. vol. Volume 132, N. O. Yasuhiro Iwasawa and K. Hironobu, Eds.: Elsevier, 2001, pp. 769-772.

[71] T. Uematsu, *et al.*, "New application of spray reaction technique to the preparation of supported gold catalysts for environmental catalysis," *Journal of Molecular Catalysis a-Chemical*, vol. 182, pp. 209-214, May 31 2002.

[72] T. Tsuchiya, *et al.*, "Suspended spray reaction for preparation of Ru/Al2O3 catalyst," *Chemistry Letters*, pp. 652-653, Jun 5 2000.

[73] T. Uematsu, *et al.*, "New Preparation Methods for Active Superfine Catalysts by Spray Reaction," *Studies in Surface Science and Catalysis*, vol. 75, pp. 1809-1812, 1993.

[74] K. Oishi and O. Savadogo, "New Method of Preparation of Catalyzed Gas Diffusion Electrode for Polymer Electrolyte Fuel Cells Based on Ultrasonic Direct Solution Spray Reaction," in *The 7th International Symposium on New Materials and Nanomaterials for Electrochemical Systems*, Montreal, Quebec, Canada, 2008.

[75] H. E. Swanson and United States. National Bureau of Standards, *Standard x-ray diffraction powder patterns*. Washington, DC: U.S. Dept. of Commerce National Bureau of Standards : For sale by the Supt. of Docs. U.S. G.P.O., 1953.

[76] A. Gamez, *et al.*, "Oxygen reduction on well-defined platinum nanoparticles inside recast ionomer," *Electrochimica Acta*, vol. 41, pp. 307-314, Feb 1996.

[77] O. Savadogo, *et al.*, in *The fifth international symposium on New Materials for Electrochemical Systems*, 2003, p. 2003.

[78] O. Savadogo, *et al.*, "OXYGEN REDUCTION CATALYST FOR FUEL CELL," Japan Patent P05P001950, May 26, 2005, 2005.

[79] O. Savadogo and F. Fouda-Onana, "Study of O(2) and OH adsorption energies on Pd-Cu alloys surface with a quantum chemistry approach," *Electrochimica Acta*, vol. 54, pp. 1769-1776, Feb 15 2009.

[80] O. Savadogo, *et al.*, "Palladium-copper alloys as catalysts for the oxygen reduction reaction in an acidic media I: Correlation between the ORR kinetic parameters and intrinsic physical properties of the alloys," *Journal of Electroanalytical Chemistry*, vol. 636, pp. 1-9, Nov 15 2009.

[81] O. Savadogo and F. Fouda-Onana, "presented as a keynote talk (talk K5)," in *5th International Conference on Electrocatalysis*, Kotor, Montenegro, 2006.

[82] F. Fouda-Onana and O. Savadogo, "Study of O(2) and OH adsorption energies on Pd-Cu alloys surface with a quantum chemistry approach," *Electrochimica Acta,* vol. 54, pp. 1769-1776, Feb 15 2009.

[83] V. Raghuveer, *et al.*, "Pd-Co-Mo electrocatalyst for the oxygen reduction reaction in proton exchange membrane fuel cells," *Journal of Physical Chemistry B,* vol. 109, pp. 22909-22912, Dec 8 2005.

[84] M. R. Tarasevich, *et al.*, "Oxygen kinetics and mechanism at electrocatalysts on the base of palladium-iron system," *Electrochimica Acta,* vol. 52, pp. 5108-5118, Apr 20 2007.

[85] S. M. Opalka, *et al.*, "Hydrogen interactions with the PdCu ordered B2 alloy," *Journal of Alloys and Compounds,* vol. 446, pp. 583-587, Oct 31 2007.

[86] H. Liu and A. Manthiram, "Controlled synthesis and characterization of carbon-supported Pd(4)Co nanoalloy electrocatalysts for oxygen reduction reaction in fuel cells," *Energy & Environmental Science,* vol. 2, pp. 124-132, 2009.

[87] B. Li and J. Prakash, "Oxygen reduction reaction on carbon supported Palladium-Nickel alloys in alkaline media," *Electrochemistry Communications,* vol. 11, pp. 1162-1165, Jun 2009.

[88] G. Vazquez and O. Solorza-Feria, "Impedance Study of Ru(x)Se(y) Methanol Tolerant Oxygen Reduction Electrocatalyst," *Journal of New Materials for Electrochemical Systems,* vol. 12, pp. 17-22, Jan 2009.

[89] M. Shao, *et al.*, "Origin of Enhanced Activity in Palladium Alloy Electrocatalysts for Oxygen Reduction Reaction†," *The Journal of Physical Chemistry B,* vol. 111, pp. 6772-6775, 2007/06/01 2007.

[90] J. Zhao, *et al.*, "Synthesis and characterization of Pd-Ni nanoalloy electrocatalysts for oxygen reduction reaction in fuel cells," *Electrochimica Acta,* vol. 55, pp. 1756-1765, Feb 1 2010.

[91] G. Ramos-Sanchez, *et al.*, "PdNi electrocatalyst for oxygen reduction in acid media," *International Journal of Hydrogen Energy,* vol. 33, pp. 3596-3600, Jul 2008.

[92] X. P. Wang, *et al.*, "Bimetallic Palladium-Base Metal Nanoparticle Oxygen Reduction Electrocatalysts," *Proton Exchange Membrane Fuel Cells 8, Pts 1 and 2,* vol. 16, pp. 109-119, 2008.

[93] J. J. Salvador-Pascual, *et al.*, "Kinetics of oxygen reduction reaction on nanosized Pd electrocatalyst in acid media," *Journal of Power Sources,* vol. 172, pp. 229-234, Oct 11 2007.

[94] Z. Y. Bai, *et al.*, "Solvothermal synthesis and characterization of Pd-Rh alloy hollow nanosphere catalysts for formic acid oxidation," *Catalysis Communications,* vol. 11, pp. 919-922, May 11 2010.

[95] X. P. Wang, *et al.*, "Bimetallic Pd-Cu oxygen reduction electrocatalysts," *Journal of the Electrochemical Society,* vol. 155, pp. B602-B609, 2008.

[96] N. N. Kariuki, *et al.*, "Colloidal Synthesis and Characterization of Carbon-Supported Pd-Cu Nanoparticle Oxygen Reduction Electrocatalysts," *Chemistry of Materials,* vol. 22, pp. 4144-4152, Jul 27 2010.

[97] C. X. Xu, *et al.*, "Nanotubular Mesoporous PdCu Bimetallic Electrocatalysts toward Oxygen Reduction Reaction," *Chemistry of Materials,* vol. 21, pp. 3110-3116, Jul 28 2009.

[98] F. Fouda-Onana, *et al.*, "Palladium-copper alloys as catalysts for the oxygen reduction reaction in an acidic media I: Correlation between the ORR kinetic parameters and intrinsic physical properties of the alloys," *Journal of Electroanalytical Chemistry,* vol. 636, pp. 1-9, Nov 15 2009.

[99] O. Savadogo and F. J. R. Varela, "Palladium-alloy catalysts as ethanol tolerant cathodes for direct alcohol fuel cell applications," *Journal of New Materials for Electrochemical Systems,* vol. 11, pp. 69-74, Apr 2008.

[100] F. J. R. Varela, *et al.*, "Synthesis and Evaluation of Highly Tolerant Pd Electrocatalysts as Cathodes in Direct Ethylene Glycol Fuel Cells (DEGFC)," *Energies,* vol. 2, pp. 944-956, Dec 2009.

[101] W. E. Mustain, *et al.*, "CoPdx oxygen reduction electrocatalysts for polymer electrolyte membrane and direct methanol fuel cells," *Electrochimica Acta,* vol. 52, pp. 2102-2108, Jan 1 2007.

[102] T. Osaka, *et al.*, "Electrodeposited Pd-Co catalyst for direct methanol fuel cell electrodes: Preparation and characterization," *Electrochimica Acta,* vol. 53, pp. 4679-4686, May 30 2008.

[103] W. E. Mustain, *et al.*, "Investigations of carbon-supported CoPd3 catalysts as oxygen cathodes in PEM fuel cells," *Electrochemistry Communications,* vol. 8, pp. 406-410, Mar 2006.

[104] E. F. A. Zeid, *et al.*, "Temperature dependence of morphology and oxygen reduction reaction activity for carbon-supported Pd-Co electrocatalysts," *Journal of Applied Electrochemistry,* vol. 40, pp. 1917-1923, Nov 2010.

[105] O. Savadogo and F. J. R. Varela, "Low-temperature direct propane polymer electrolyte membranes fuel cell (DPFC)," *Journal of New Materials for Electrochemical Systems,* vol. 4, pp. 93-97, Apr 2001.

[106] F. J. R. Varela and O. Savadogo, in *VII Congreso de la Sociedad Mexicana del Hidrógeno, III Jornadas Iberoamericanas de Pilas de Combustible e Hidrógeno*, Chihuahua, México, 2007, p. 005.

[107] F. J. R. Varela and O. Savadogo, "The effect of anode catalysts on the behavior of low temperature direct propane polymer electrolyte fuel cells (DPFC)," *Journal of New Materials for Electrochemical Systems*, vol. 9, pp. 127-137, Apr 2006.

[108] J. Prakash, *et al.*, "CoPdx oxygen reduction electrocatalysts for polymer electrolyte membrane and direct methanol fuel cells," *Electrochimica Acta*, vol. 52, pp. 2102-2108, Jan 1 2007.

[109] C. L. Lin, *et al.*, "Methanol tolerance of Pd-Co oxygen reduction reaction electrocatalysts using scanning electrochemical microscopy," *Electrochemical and Solid State Letters*, vol. 11, pp. B136-B139, 2008.

[110] H. Yang, *et al.*, "Low temperature preparation of carbon-supported Pd-Co alloy electrocatalysts for methanol-tolerant oxygen reduction reaction," *Electrochimica Acta*, vol. 53, pp. 6662-6667, Sep 20 2008.

[111] T. Wandlowski, *et al.*, "Electrocatalytic properties of Au(111)-Pd quasi-single-crystal film electrodes as probed by ATR-SEIRAS," *Russian Journal of Electrochemistry*, vol. 42, pp. 1177-1192, Nov 2006.

[112] C. Gabrielli, *et al.*, "Investigation of hydrogen adsorption and absorption in palladium thin films - II. Cyclic voltammetry," *Journal of the Electrochemical Society*, vol. 151, pp. A1937-A1942, 2004.

[113] G. F. Alvarez, *et al.*, "Preparation and characterisation of carbon-supported palladium nanoparticles for oxygen reduction in low temperature PEM fuel cells," *Journal of Applied Electrochemistry*, vol. 41, pp. 925-937, Aug 2011.

[114] K. Kinoshita and Electrochemical Society., *Electrochemical oxygen technology*. New York: Wiley, 1992.

[115] K. L. Hsueh, *et al.*, "Electrolyte effects on oxygen reduction kinetics at platinum: A rotating ring-disc electrode analysis," *Electrochimica Acta*, vol. 28, pp. 691-697, 1983.

[116] W. E. Mustain and J. Prakash, "Kinetics and mechanism for the oxygen reduction reaction on polycrystalline cobalt-palladium electrocatalysts in acid media," *Journal of Power Sources*, vol. 170, pp. 28-37, Jun 30 2007.

[117] T. Ioroi and K. Yasuda, "Platinum-iridium alloys as oxygen reduction electrocatalysts for polymer electrolyte fuel cells," *Journal of the Electrochemical Society*, vol. 152, pp. A1917-A1924, 2005.

[118] J. O. M. Bockris and S. U. M. Khan, *Surface electrochemistry : a molecular level approach*. New York: Plenum, 1993.

[119] S. Tominaka and T. Osaka, "Nanoporous PdCo Catalyst for Microfuel Cells: Electrodeposition and Dealloying," *Advances in Physical Chemistry*, vol. 2011, 2011.

[120] C. Bale, *et al.*, "FactSage thermochemical software and databases," *Calphad-Computer Coupling of Phase Diagrams and Thermochemistry,* vol. 26, pp. 189-228, Jun 2002.

[121] Y. Matsuo, "Ordered alloys in the cobalt-palladium system [single crystal films]," *Journal of the Physical Society of Japan,* vol. 32, pp. 972-8, 1972.

[122] M. P. Seah, *et al.*, "Quantitative XPS I. Analysis of X-ray photoelectron intensities from elemental data in a digital photoelectron database," *Journal of Electron Spectroscopy and Related Phenomena,* vol. 120, pp. 93-111, Oct 2001.

[123] T. Toda, *et al.*, "Enhancement of the electrocatalytic O-2 reduction on Pt-Fe alloys," *Journal of Electroanalytical Chemistry,* vol. 460, pp. 258-262, Jan 18 1999.

[124] T. Toda, *et al.*, "Role of electronic property of Pt and Pt alloys on electrocatalytic reduction of oxygen," *Journal of the Electrochemical Society,* vol. 145, pp. 4185-4188, Dec 1998.

[125] F. L. Williams and D. Nason, "Binary alloy surface compositions from bulk alloy thermodynamic data," *Surface Science,* vol. 45, pp. 377-408, 1974.

[126] L. Guczi, *et al.*, "Bimetallic catalysis: CO hydrogenation over palladium-cobalt catalysts prepared by sol/gel method," *Journal of Molecular Catalysis a-Chemical,* vol. 141, pp. 177-185, May 6 1999.

[127] M. H. Shao, *et al.*, "Electrocatalysis on Platinum Nanoparticles: Particle Size Effect on Oxygen Reduction Reaction Activity," *Nano Letters,* vol. 11, pp. 3714-3719, Sep 2011.

[128] J. X. Wang, *et al.*, "Kinetic analysis of oxygen reduction on Pt(111) in acid solutions: Intrinsic kinetic parameters and anion adsorption effects," *Journal of Physical Chemistry B,* vol. 108, pp. 4127-4133, Apr 1 2004.

[129] O. Savadogo and A. Essalik, "2-Percent Platinum-H2wo4 Based Electrocatalysts for Phosphoric-Acid Fuel-Cell Cathode," *Journal of the Electrochemical Society,* vol. 141, pp. L92-L94, Aug 1994.